Pharmacological Research 107 (2016) 249–275

Contents lists available at ScienceDirect

Pharmacological Research

journal homepage: www.elsevier.com/locate/yphrs

Invited review

Cyclin-dependent protein kinase inhibitors including palbociclib as anticancer drugs

Robert Roskoski Jr.

Blue Ridge Institute for Medical Research, 3754 Brevard Road, Suite 116, Box 19 Horse Shoe, NC 28742-8814, United States

ARTICLE INFO

Article history:
Received 10 March 2016
Accepted 11 March 2016
Available online 16 March 2016

Chemical compounds studied in this article:
7-Hydroxystaurosporine (PubMed CID: 72271)
Abemaciclib (PubMed CID: 46220502)
Alvocidib (PubMed CID: 5287969)
AT7519 (PubMed CID: 11338033)
BMS-387032 (PubMed CID: 3025986)
Dinaciclib (PubMed CID: 46926350)
Palbociclib (PubMed CID: 5330286)
Ribociclib (PubMed CID: 44631912)
Riviciclib (PubMed CID: 23643976)
Seliciclib (PubMed CID: 160355)

Keywords:
ATP-binding site
Breast cancer
Catalytic spine
K/E/D/D
Protein kinase structure
Regulatory spine

ABSTRACT

Cyclins and cyclin-dependent protein kinases (CDKs) are important regulatory components that are required for cell cycle progression. The levels of the cell cycle CDKs are generally constant and their activities are controlled by cyclins, proteins whose levels oscillate during each cell cycle. Additional CDK family members were subsequently discovered that play significant roles in a wide range of activities including the control of gene transcription, metabolism, and neuronal function. In response to mitogenic stimuli, cells in the G1 phase of the cell cycle produce cyclins of the D type that activate CDK4/6. These activated enzymes catalyze the monophosphorylation of the retinoblastoma protein. Then CDK2-cyclin E catalyzes the hyperphosphorylation of Rb that promotes the release and activation of the E2F transcription factors, which in turn lead to the generation of several proteins required for cell cycle progression. As a result, cells pass through the G1-restriction point and are committed to complete cell division. CDK2-cyclin A, CDK1-cyclin A, and CDK1-cyclin B are required for S, G2, and M-phase progression. Increased cyclin or CDK expression or decreased levels of endogenous CDK inhibitors such as INK4 or CIP/KIP have been observed in various cancers. In contrast to the mutational activation of EGFR, Kit, or B-Raf in the pathogenesis of malignancies, mutations in the CDKs that cause cancers are rare. Owing to their role in cell proliferation, CDKs represent natural targets for anticancer therapies. Abemaciclib (LY2835219), ribociclib (Lee011), and palbociclib (Ibrance® or PD0332991) target CDK4/6 with IC_{50} values in the low nanomolar range. Palbociclib and other CDK inhibitors bind in the cleft between the small and large lobes of the CDKs and inhibit the binding of ATP. Like ATP, palbociclib forms hydrogen bonds with residues in the hinge segment of the cleft. Like the adenine base of ATP, palbociclib interacts with catalytic spine residues CS6 and CS7. CDK antagonists are in clinical trials for the treatment of a variety of malignancies. Significantly, palbociclib has been approved by the FDA for the treatment of hormone-receptor positive/human epidermal growth factor receptor-2 negative breast cancer in conjunction with letrozole as a first-line therapy and with fulvestrant as a second-line treatment. As inhibitors of the cell cycle, it is not surprising that one of their most common toxicities is myelosuppression with decreased neutrophil production.

Contents

Abbreviations: AS, activation segment; CDK, cyclin-dependent protein kinase; CIP/KIP, CDK interacting protein/kinase inhibitor protein; CS or C-spine, catalytic spine; CL, catalytic loop; ER^+, estrogen receptor positive; GRL, glycine-rich loop; $HER^{+/-}$, human epidermal growth factor receptor positive or negative; HR^+, hormone receptor positive with either or both estrogen and progesterone receptors; HΦ or Φ, hydrophobic; INK4, inhibiting CDK4; NSCLC, non-small cell lung cancer; pCDK4/6, phosphorylated cyclin-dependent protein kinases 4 and 6; PI3-kinase, phosphoinositide 3-kinase; PKA, protein kinase A; PKC, protein kinase C; PR, progesterone receptor; Rb, retinoblastoma protein; RS or R-spine, regulatory spine; Sh1, shell residue 1; WAF1, wild type p53-activated fragment.

E-mail address: rrj@brimr.org

http://dx.doi.org/10.1016/j.phrs.2016.03.012
1043-6618/

1. Introduction to the somatic mitotic cell cycle

1.1. Overview of cyclin-dependent protein kinases and their regulatory cyclins

The replication of each cell in every tissue and organ is exactingly controlled during development and throughout the life of the individual. In a normal adult, cells divide only when and where they are needed. Moreover, the contents of a cell including each chromosome must be accurately replicated. The cell cycle consists of G1 (presynthetic growth, or gap 1), S (DNA synthesis), G2 (premitotic growth, or gap 2), and M (mitotic) phases (Fig. 1A) [1]. During G1 cells are preparing for DNA synthesis and during G2 cells perform surveillance to establish the integrity of newly synthesized DNA before commencing mitosis. The chromosomal DNA is replicated during the S-phase and all of the cellular components are partitioned between two identical daughter cells during mitosis or the M-phase. When cells cease proliferation owing to the absence of mitogenic signaling or to the presence of specific antimitogenic signaling, they exit the cycle and enter a nondividing quiescent state known as G0. In contrast, senescence is an irreversible state of G1 cell cycle arrest in which cells are refractory to growth factor stimulation.

Cells within the hematopoietic system or cells that line the gut epithelium actively proliferate and cycle continuously [2]. Most cells in adult animals are mostly in a quiescent or G0 phase, but they can reenter the cell cycle. In contrast, terminally differentiated cells such as neurons and cardiac myocytes have lost the capacity to proliferate and are locked permanently in the G0 phase. Loss of the normal controls of cellular replication is a fundamental defect in cancer. Thus, understanding the mechanisms that control cell division represents an essential component of one strategy toward the development of therapeutic modalities for cancer treatment. The dilemma is to target and inhibit cancerous growth while not blocking the physiological proliferation of needed cells.

Cyclins and cyclin-dependent protein kinases (CDKs) are important components required for passage through the cell division cycle [3]. Human cells possess 20 CDKs (1–20) and 29 cyclins. The CDKs are protein-serine/threonine kinases that belong to the CMGC family (Cyclin-dependent protein kinases, Mitogen-activated protein kinases, Glycogen synthase kinases, and CDK-like kinases) [4]. As their name implies, CDKs interact with cyclins as a first step in producing enzyme activity. After the formation of a CDK-cyclin complex, the CDK activation segment undergoes phosphorylation at a conserved threonine residue as catalyzed by CDK7 for the full expression of CDK-cyclin enzyme activity. In much of the literature, the CDK activation segment is called the T-loop in reference to its conserved threonine. This class of enzymes was initially discovered as proteins that participate in the normal transit through the cell cycle (CDK1/2/3/4/6/7/8/10). Subsequently, the CDKs were found to play important regulatory roles in many diverse functions including the control of gene transcription (CDK7/8/9/10/12), neuronal activity (CDK5/16), metabolism (CDK5/8), hematopoiesis, angiogenesis, proteolysis, and DNA damage and repair (CDK1/3/9/12), epigenetics (CDK1/2/4), and spermatogenesis (CDK16) [5].

The levels of the CDKs are generally constant throughout the cell cycle. The activities of the cell cycle group of CDKs are controlled by cyclins, proteins whose levels oscillate during the cell cycle (Fig. 1B) [6]. The oscillation of cyclins accounts for their names as they oscillate or cycle up and down during the cell cycle. CDKs are regulated by a mechanism involving the synthesis (which increases protein kinase activity) and degradation (which decreases enzyme activity) of their cognate cyclins. Most of the CDKs possess about 300 amino

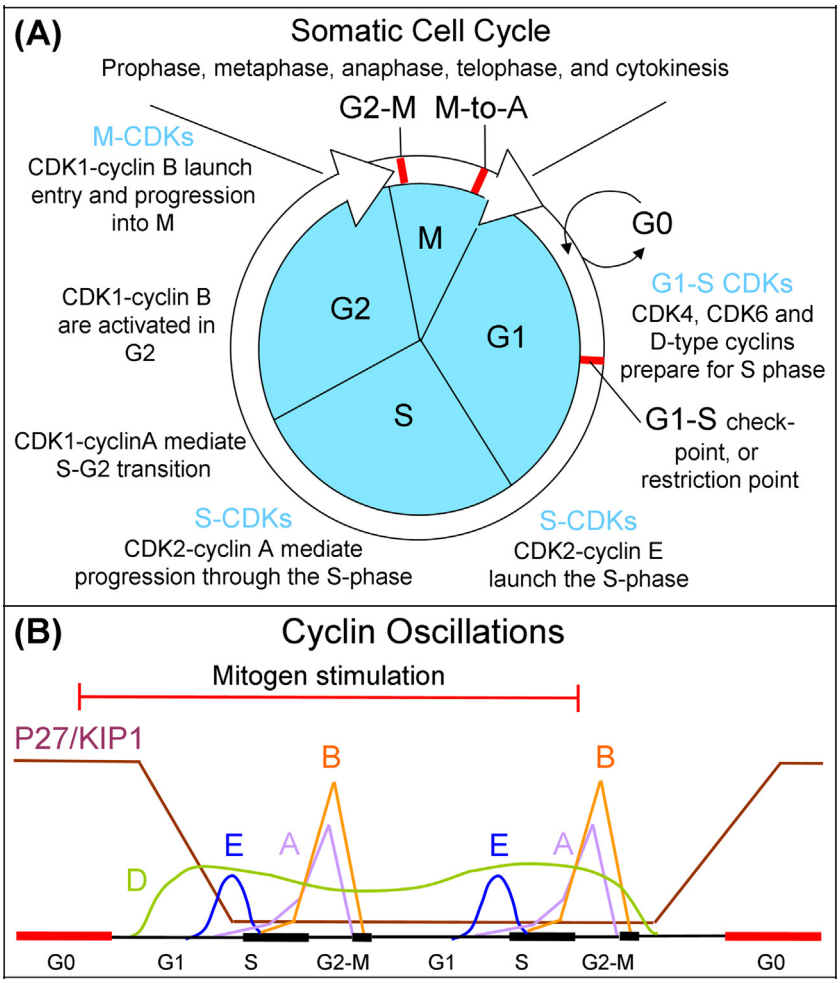

Fig. 1. (A) Overview of the cell division cycle. (B) Cellular content of cyclins D, E, A, and B in response to mitogenic stimulation; adapted from Ref. [6] with permission of AAAS.

acid residues with a molecular weight of about 35 kDa. Two of them (CDK12 and CDK13) are much larger with about 1500 residues and a molecular weight of about 165 kDa with modular components besides the 250 amino-acid-residue protein kinase domain.

Using human HeLa cells, Arooz et al. reported that the peak levels of cyclin A2 and cyclin E1, at the G2 phase and G1 phase, respectively, were only about 1/8th that of their partner CDK2 [7]. Consequently, the CDKs are generally present in excess and are not maximally stimulated by their regulatory subunits. This observation suggests that enhanced CDK activity in cancer is more likely the result of increased cyclin levels than increased CDK expression.

The cyclins are a large family of about 29 proteins in humans with molecular weights ranging from 35 to 90 kDa [3]. Cyclins are expressed in discrete portions of the cell cycle and are then degraded by an intricately regulated process involving interactions with ubiquitin ligases (E3s) and proteasomes [8]. This periodic expression is mediated by the cell cycle-dependent activation of the E2F and FOXM1 transcription factors [9]. The proteolysis of cyclins results from the actions of the Skp1-Cul1-F-box protein (SCF), which operates from late G1 to early M-phase, and the anaphase-promoting complex/cyclosome (APC/C), which acts during anaphase until the end of G1 [10]. The cyclin family consists of three major groups. Group I or the cyclin B group consists of A, B, D, E, F, G, J, I and O; group II corresponds to cyclin Y; and group III or the cyclin C group consists of cyclins C, H, K, L, and T (which are major partners with the transcriptional CDKs) [3]. These proteins contain a 100 amino-acid-residue domain of five α-helices called the cyclin box. The A, B, D, E, F, J, and O type cyclins contain two cyclin boxes while the rest contain a single cyclin box. The structures and interactions of cyclins and their cognate CDKs are described later.

In order to ensure proper progression through the cell cycle, cells rely on a series of checkpoints that prevent them from progressing into a new phase inappropriately or prematurely before they have successfully completed their current phase. As a result, cell-cycle progression can be blocked at these checkpoints when such transit may be deleterious to the cell. The first is the G1-S checkpoint (also called start, restriction point, or R-point) where G1-S and S-phase CDK-cyclin complexes are activated during G1 (Fig. 1A) [11]. After passing the restriction point, cell proliferation is independent of mitogens and growth factors and the cell is committed to complete cell division. The G1-S enzymes include CDK4 and CDK6 and the D-type cyclins (D1/2/3), the various forms of which are expressed in a tissue-specific fashion. CDK2-cyclin E is required for the transition to the S-phase. G2-M constitutes a second checkpoint where M-phase CDK1-cyclin A/B are activated thereby bringing the cell to metaphase during mitosis. The third checkpoint is the metaphase-to-anaphase transition, which leads to sister-chromatid segregation, completion of mitosis, and cytokinesis at which time the cytoplasm of a single cell is divided to form two identical daughter cells. Progression occurs when M-phase cyclin-CDK complexes stimulate an enzyme called the anaphase-promoting complex, which causes the proteolytic destruction of proteins that hold the sister chromatids together.

Table 1
Selected proteins that participate in the regulation of the cell cycle.[a]

Cyclin-dependent protein kinases and their cyclin partners

Enzyme	Cyclin	Selected functions
CDK1	A/B	Triggers S-G2 and G2 → M transitions and G2 progression; cyclin A is synthesized in late G1, S, and G2 and is destroyed during prometaphase; B-type cyclins are synthesized in S/G2 and destroyed following chromosome attachment to the spindle
CDK2	E	Triggers G1 → S transition; induces histone biosynthesis and centrosome duplication
	A	Progression through S phase
CDK3	C	Triggers reentry from G0 to G1 through phosphorylation of Rb; DNA repair
CDK4/6	D1/2/3	Mediates the phosphorylation of Rb in G1; stimulates cyclin E synthesis; synthesis of D-type cyclins is controlled by extracellular mitogens
CDK5	p35, G	Neuronal function; epigenetic regulation; glycogen synthesis; insulin secretion
CDK 7 or CAK[b]	H	Mediates the activation of CDKs by catalyzing the phosphorylation of a Threonine residue within the T-loop or activation segment; forms part of the TFIIH complex that is important for the regulation of RNA polymerase II transcription and DNA repair
CDK8	C	Regulation of RNA polymerase II transcription; inhibition of lipogenesis; Wnt/β-catenin signaling
CDK9	T	Regulation of RNA polymerase II transcription
	K	DNA repair
CDK10	M	G2-M transition

Polypeptide inhibitors/modulators of cyclin-dependent protein kinases

Inhibitor (*Gene*)	Targets	Function
p16/INK4A *(CDKN2A)*	CDK4/6	Cell cycle arrest in senescence and aging; decreased expression in many cancers
p15/INK4B *(CDKN2B)*	CDK4/6	Cell cycle arrest in response to transforming growth factor-β
p18/INK4C *(CDKN2C)*	CDK4/6	Cell cycle arrest
p19/INK4D *(CDKN2D)*	CDK4/6	Cell cycle arrest with maximal physiological expression during S phase
p21/CIP/WAF1 (*CDKN1A)*	Most CDK-cyclin complexes	Cell cycle arrest in G1; induced by p53 tumor suppressor; cell cycle arrest after DNA damage, senescence, and terminal differentiation; decreased expression in many cancers
p27/KIP1 (*CDKN1B*)	Most CDK-cyclin complexes	Cell cycle arrest in G1 in response to growth suppressors, contact inhibition, and differentiation; decreased expression in many cancers
p57/KIP2 (*CDKN1C*)	Most CDK-cyclin complexes except CDK4/6	High expression in G0 and G1; cell cycle arrest in G1; decreased expression in many cancers

Other components

Enzyme	Substrates	Function
Wee1 kinase	CDK1 Y15	Nuclear kinase; inhibits CDK1-cyclin B in G2
Myt kinase	CDK1 T14, Y15	Cytoplasmic kinase; inhibits CDK1-cyclinB in G2
Cdc25C phosphatase	CDK1 pT14, pY15	Promotes G2 → M transition; catalyzes the dephosphorylation of CDK1-cyclinA or CDK1-cyclin B pT14 and pY15

[a] Adapted from Ref. [5].
[b] CAK: CDK-activating protein kinase.

Cell cycle progression may be deleterious to the cell after DNA is damaged by oxidation, alkylation, or hydrolysis of the bases by endogenous processes or as a result of irradiation or treatment with cytotoxic drugs such as cisplatin or doxorubicin; cell cycle checkpoints are activated following such insults [12]. Checkpoint activation retards cell cycle transit, which allows cells to repair the damage before continuing to divide. DNA damage checkpoints occur at the G1/S, G2/M boundaries and within the S phase. All DNA damage responses require either ATM, ATR, or both protein kinases, which have the ability to bind to the chromosomes at the site of DNA damage together with accessory proteins that are platforms on which DNA damage response components and DNA repair complexes are assembled. As part of this response ATR catalyzes the phosphorylation of Chk1 (checkpoint kinase-1) at Ser317 and Ser395 resulting in its activation; these two residues are downstream from the protein kinase domain. ATM catalyzes the phosphorylation of Chk1 at Thr68 resulting in its activation; this residue occurs upstream from the protein kinase domain. The cyclin-dependent kinase inhibitor p21/CIP/WAF1 is induced by various mechanisms downstream from ATM or ATR and can arrest the cell cycle at checkpoints by deactivating CDK-cyclin complexes.

Following mitogenic stimulation, one or more cyclin D members are expressed leading to the activation of CDK4/6, which are key regulators of the G1-S transition. Cyclin D forms a complex with CDK4/6, which results in protein kinase activation as described later. The CDK4/6-cyclin D complex catalyzes the phosphorylation of the retinoblastoma (Rb) protein at one and only one site distributed among all 14 potential phosphorylation sites to yield monophosphorylated Rb that exists for several hours in G1 [13]. The expression of cyclin E activates CDK2 later in G1 thereby leading to the hyperphosphorylation of Rb at all 14 sites thereby inactivating it. The CDK2-cyclin E complex is processive in nature; it catalyzes consecutive reactions without releasing its substrate. The mechanism for promoting cyclin E expression late in G1 is unclear. (See Ref. [13] for a discussion of previous formulations of Rb phosphorylation and inactivation that involve various hypophosphorylated Rb forms). Hyperphosphorylated Rb releases its bound E2F transcription factor, which leads to the generation of several proteins required for cell cycle progression through G1 and S including cyclin A, Rb itself, and enzymes required for deoxyribonucleotide biosynthesis [14].

CDK4 and CDK6 are protein kinases with narrow substrate specificity; they catalyze the phosphorylation of Rb (RB1) and two other Rb-like family proteins (RBL2 or p130 and RBL1 or p107), but not many other proteins [1,15]. The expression of cyclin D proteins is followed by the expression of cyclin E, cyclin A, and cyclin B along with the activation of their cognate CDKs. The relative levels of cyclin expression are depicted in Fig. 1B, which is an idealized version owing to the differences that exist among various cell types under different conditions. In contrast to CDK4 and CDK6, CDK1 and CDK2 are broad specificity protein kinases that catalyze the phosphorylation of dozens of proteins [1]. The duration of the cell

cycle also varies considerably, lasting on the order of a day in rapidly proliferating cells with mitosis taking about an hour.

Human CDK7 is a subunit of the TFIIH transcription factor; CDK7 is involved in transcription initiation by mediating the phosphorylation of a serine residue of the RNA polymerase II C-terminal domain. CDK7 also catalyzes the phosphorylation and activation of other CDKs, thus functioning as a CDK-activating kinase (CAK). Unlike cyclins for cell-cycle-related protein kinases, the cyclin subunits of the transcriptional CDKs fail to show significant oscillations in protein levels during the cell cycle; their activities are regulated by intricate protein–protein interactions and other mechanisms. CDK5 participates in the regulation of insulin secretion, glycogen synthesis, and neuronal functions [5]. CDK8 and CDK14 are involved in Wnt/β-catenin signaling and CDK16 plays a role in neuronal function and in spermatogenesis. Like other CMGC protein kinases such as ERK, most CDKs are proline-directed protein kinases that catalyze the phosphorylation of serine or threonine immediately before a proline residue. CDK7 can also catalyze the phosphorylation of residues in the absence of a target proline residue.

1.2. Endogenous CDK polypeptide inhibitors/modulators

In addition to regulation by the cyclin activators, CDKs are subject to inhibition by two families of polypeptide inhibitors: CIP/KIP and INK4. These inhibitors can halt cell cycle passage under unfavorable conditions [16,17]. The CIP/KIP family of three proteins was identified as cell cycle regulators that interact with and inhibit the CDKs. The three members of the family include p21/CIP/WAF1, p27/KIP1, and p57/KIP2. The highest levels of p21/CIP/WAF1 are found during G1 and G2. The level of this protein is increased in response to DNA damage in a process that involves the p53 tumor suppressor protein and its expression is required for physiological DNA damage responses. p27/KIP1 accumulates when the cell enters the G0 phase of the cycle and it is degraded following Thr187 and Ser10 phosphorylation catalyzed by CDK2 followed by E3 ubiquitin ligase-mediated degradation as the cell re-enters G1. p57/KIP2 is a negative regulator of cell proliferation and is required for embryonic development. The CIP/KIP family of proteins also participates in apoptosis, cytoskeletal rearrangement, and transcriptional regulation. Their structure and interaction with CDKs will be considered later.

The INK4 family of CDK antagonists consists of four members: p16/INK4A, p15/INK4B, p18/INK4C, and p19/INK4D [18]. Each of these proteins binds to CDK4 and CDK6 and prevents the binding and activation by the D-type cyclins. Moreover, each of these CDK inhibitors controls cell cycle G1 progression. p16/INK4A is named after its molecular weight (in kDa) and its role in inhibiting CDK4 (INK4). p16/INK4A decelerates the passage from the G1 to S phase when it would be deleterious to the cell; it therefore acts as a tumor suppressor and is implicated in the prevention of melanoma and cervical, esophageal, and oropharyngeal squamous cell carcinomas [2]. Studies in p18/INK4C knockout mice suggested a role for this gene in (i) regulating spermatogenesis and (ii) suppressing tumorigenesis. The abundance of the transcript of the p19/INK4D gene was found to oscillate in a cell-cycle dependent manner with the lowest expression at mid G1 and a maximal expression during the S phase. Like p18/INK4C, p19/INK4D also plays a role in regulating spermatogenesis [19]. Moreover, p19/INK4D and p27/KIP1 actively repress neuronal proliferation in postmitotic brain cells in mice [20].

One aspect of the behavior of p21/CIP1 and p27/KIP1 is paradoxical [21]. As these polypeptides inhibit the actions of CDK2-cyclin E and CDK2-cyclin A, they stimulate and stabilize the formation of CDK4/6-cyclin D complexes. Furthermore, once a ternary complex has formed between CDK4/6-cyclin D and either p21/CIP1 or p27/KIP2, the CDK-cyclin-inhibitor ternary complex can still catalyze the phosphorylation of its physiological substrates. Although p21/CIP1 or p27/KIP1 inhibits the action of most CDK-cyclin complexes, they do not inhibit the catalytic activity of CDK4/6-cyclin D. Such formation of ternary complexes serves to remove these inhibitors from CDK2 in a process known as CDK inhibitor reshuffling. This process allows for the activation of S-phase CDK activity. Table 1 provides a summary of the actions of selected proteins that participate in the regulation of the somatic mitotic cycle.

2. Cell cycle dysregulation and cancer

2.1. Cyclins

The uncontrolled proliferation of several human cancers is associated with the dysregulation of CDKs [22]. Dysregulation may involve cyclins, endogenous CDK inhibitors/modulators, or CDKs. Consequently, cyclin gene amplification and protein overexpression, untimely cyclin expression, or cellular mislocalization can produce inappropriate activation of CDKs [5]. Cyclin D1 amplification occurs in 15–40% of all cancers [23] including breast, lung, and oral carcinomas and melanomas [24]. Schwaederlé et al. found that 50/392 tumor samples harbored cyclin D1, D2, D3, and E1 amplifications most commonly associated with gastrointestinal (10/91 tumor samples), breast (22/81), gynecologic (2/33), head and neck (5/39), lung (5/26), nonsolid tumors (2/30), brain (0/56) and other neoplasms (2/16) [25]. Increased cyclin D mRNA occurs in most multiple myeloma cells, and Bergsagel et al. suggested that dysregulation of cyclin D genes is a unifying oncogenic event in multiple myeloma [26].

Increased cyclin D1 protein expression as determined by immunohistochemical staining has been reported in colorectal, pancreatic, endometrial, and head and neck squamous cell carcinomas, and NSCLC (Table 2). The expression of cyclin D activates CDK4 and CDK6 leading to G1-S progression. Cyclin E1 gene amplification is associated with ovarian carcinomas [41,42] and uterine serous carcinomas [43]. Cyclin E protein expression levels are correlated with increased malignant behavior of colorectal, pancreatic, ovarian carcinomas, chronic lymphoblastic leukemia, and a variety of lymphomas (Table 2). Cyclin E interacts with CDK2 and leads to the induction of the S-phase of the cell cycle (Fig. 1A).

Cyclin A expression levels are correlated with poorer outcomes in esophageal, hepatocellular, endometrial, and thyroid tumors, and soft tissue sarcomas (Table 2). Cyclin A interacts with CKD2 to mediate passage through the S-phase and it interacts with CDK1 to promote entry into the M-phase of the cell cycle. Cyclin B expression levels are correlated with poorer outcomes in breast, lung, stomach, and esophageal carcinomas (Table 2). Cyclin B interacts with CDK1 and leads to the progression through G2 and entry into mitosis.

2.2. Loss of endogenous CDK inhibitors/modulators

The INK4 family of CDK antagonists acts on CDK4 and 6 to block passage through the G1 phase of the cell cycle. The CIP/KIP family can block the action of most CDKs, while promoting the activity of CDK4/6-cyclin D. p16/INK4A expression is decreased in acute lymphoblastic leukemia as a result of the deletion of its gene [56]. Little or no expression of p16/INK4A protein has been reported in Hodgkin lymphomas, NSCLC, melanoma, retinoblastoma, and osteosarcoma (Table 3). In most of these cases, no or low protein expression is correlated with poorer survival.

No or low protein expression of p21/CIP/WAF1 has been reported in breast, stomach, colon, and endometrial carcinomas and in Hodgkin lymphomas (Table 3). In most cases this is correlated with metastasis and diminished survival. The highest levels

Table 2
Cyclin expression in various malignancies.

Cyclin	Parameter	Cancer[a]	No. affected/total; comments	References
D	Protein overexpression	Advanced colorectal carcinoma	26/45; correlates with CDK4 overexpression	[27]
D1	Gene amplification	Post-menopausal ER^+ patients	100/1155; poor clinical outcome	[28]
D1	Protein expression	Primary colorectal carcinoma	7/8; greater expression than in adjacent normal mucosa	[29]
D1	Protein expression	Primary/recurrent colorectal carcinoma	5 of 11/9 of 11; decreases apoptosis in recurrent tumors	[30]
D1	Protein expression	Stage II and III colon cancer	211/386; correlates with increased recurrence	[31]
D1	Protein expression	Pancreatic carcinoma	36/53; not correlated with tumor size nor metastasis	[32]
D1	Protein expression	NSCLC	52/104; correlation of CDK4-cyclin D1 levels and apoptosis	[33]
D1b	mRNA expression	NSCLC	n = 102; correlates with tumor grade, metastasis, and tumor stage	[34]
D1	Protein expression	Endometrial carcinoma	n = 65; D1 expression unlinked to *PTEN*, *KRAS*, or β-catenin mutations	[35]
D1	Protein expression	Head and neck squamous cell carcinoma	23/98; correlates with poorer survival	[36]
D1	Protein overexpression	Head and neck squamous cell carcinoma	56/115; correlates with poor prognosis	[37]
D1	11q13 amplification	Head and neck squamous cell carcinoma	22/56; correlates with reduced survival	[37]
D1/2/3	mRNA expression	Multiple myeloma	256/261; correlates with early oncogenic events	[26]
E	Protein expression	Breast carcinoma	61/183; chiefly nuclear labeling	[38]
E	Protein expression	Colorectal carcinoma	35/38 showed elevation compared with normal mucosa	[39]
E	Protein expression	Pancreatic carcinoma	22/32; correlates with lymph node metastasis	[40]
E1	Gene amplification	Ovarian carcinoma	18/88; correlates with poorer survival	[41]
E1	Protein overexpression	Ovarian carcinoma	44/88; no correlation with malignant phenotype	[41]
E1	Gene amplification	Ovarian carcinoma	106/489; correlates with reduced survival	[42]
E1	Gene amplification	Uterine serous carcinoma	20/44; correlates with early tumor progression	[43]
E	Protein expression	Chronic lymphoblastic leukemia	19/24; no cyclin A or B; 23/24 CDK4 positive	[44]
E	Protein expression	Various malignant lymphomas	98/98; greater expression correlates with diminished survival	[45]
A	Protein expression	Esophageal squamous cell carcinoma	49/124; correlates with poorer survival rate	[46]
A	Protein overexpression	Hepatocellular carcinoma	12/31; correlates with reduced survival rate	[47]
A	Protein overexpression	Benign/malignant thyroid tumors	33 of 104/33 of 64; no correlation with tumor size or metastasis	[48]
A	Protein expression	Endometrial adenocarcinoma	207/208; correlates with tumor grade	[49]
A	Protein expression	Soft tissue sarcomas	n = 126; correlates with poorer survival rate	[50]
B	Protein expression	Breast carcinoma	Correlates with tumor size and grade	[51]
B1	Nuclear expression	Breast carcinoma	17/109; correlates with tumor size and lymph node metastasis	[52]
B	Protein overexpression	NSCLC	17/77; correlates with reduced survival rate	[53]
B	Protein expression	Gastric carcinoma	262/379; correlates with metastasis and poor prognosis	[54]
B	Protein expression	Esophageal carcinoma	n = 87; correlates with tumor grade	[55]

[a] NSCLC: non-small cell lung cancer.

of this protein occur during progression through G1 and G2. As a result, p21/CIP/WAF1 retards entry into the S- and M-phase of the cell cycle. No or low expression of p27/KIP1 has been reported in breast, stomach, esophageal, colon, and prostate carcinomas (Table 3). Decreased levels are correlated with tumor recurrence and poorer survival. No or low expression of p57/KIP2 protein has been reported in bladder, colorectal, liver, pancreatic, and ovarian carcinomas. Aberrations in P57/KIP2 expression have also been reported in both childhood and adult acute lymphoblastic leukemias.

2.3. Cyclin-dependent protein kinases

CDK1 protein overexpression has been reported in melanoma and in diffuse large B-cell lymphoma (Table 4). CDK2, CDK4, or CDK8 overexpression occurs in colorectal carcinoma. Additionally, CDK4 gene amplification occurs in osteosarcoma, liposarcoma, rhabdomyosarcoma, and cancer of the uterine cervix. Over expression of CDK4 protein has been reported in colorectal carcinoma, NSCLC, uterine cervical carcinoma, and melanoma. CDK6 gene amplification and overexpression have been demonstrated in lymphomas, leukemias, and gliomas. Moreover, CDK6 is overexpressed in medulloblastoma, which is the most common brain tumor in children, and this overexpression may serve to link the p53 and Rb tumor suppressor pathways [118]. Additional CDK aberrations associated with cancer are given in Table 4.

A large number of mutations of the CDKs have been described in the catalogue of Cosmic Mutations in Cancer (www.sanger.ac.uk/genetics/CGP/cosmic). The incidence of these mutations is quite low and only in a few, if any, cases have there been any follow up studies demonstrating that the mutations result in increased protein kinase catalytic activity. The low expression in p16/INK4A (a CDK4 inhibitor), the high expression of the D cyclins (CDK4 activators), and the overexpression of CDK4 itself, indicates that CDK4 is a potentially useful drug target for breast, cervical, colorectal, esophageal, kidney, liver, lung, pancreatic, and prostate carcinomas, NSCLC, acute lymphoblastic lymphoma, mantle cell lymphoma, liposarcoma, melanoma, medulloblastoma, and multiple myeloma [119].

3. Structures of the cyclin-dependent protein kinases

3.1. Primary structures of the CDKs

The cyclin-dependent protein kinases catalyze the phosphorylation of a protein-serine or threonine residue that occurs immediately before a proline residue thereby classifying them as proline-directed protein kinases. The related ERK/MAP kinases constitute another group of proline-directed kinases [120]. CDK2-cyclin A uses a dual protein substrate recognition mechanism in which the sequence flanking the phosphoryl acceptor site (S/TPXR/K) is recognized by the enzyme while the cyclin A component of the complex binds to a downstream R/KXL substrate recruitment motif, where S or T are the phosphorylatable residues and X is any amino acid [121]. CDK2-cyclin E is more selective than CDK2-cyclin A and these complexes share just a few of the substrates such as Rb and p27/KIP1 [121]. CDK1-cyclin B uses a similar strategy for substrate recognition but is less stringent about its requirement for the basic amino acid three residues removed (P + 3) from the phosphorylatable serine/threonine [122]. This dual protein substrate recognition mechanism of the CDKs differs from that of PKA, which contains a substrate recognition motif that is entirely within the enzyme [123]. CDK 4 and 6 exhibit narrow substrate specificity while CDK1 and 2 exhibit broad substrate specificity

Table 3
Expression of endogenous polypeptide modulators/inhibitors of CDKs in various malignancies.

Inhibitor	Parameter	Cancer[a]	No. affected/total; comments	References
P15/INK4B	Gene deletion	Acute lymphoblastic leukemia	310/973; modest correlation with disease progression	[56]
P16/INK4A	Gene deletion	Acute lymphoblastic leukemia	592/1917; modest correlation with disease progression	[56]
P16/INK4A	No protein expression	Hodgkin lymphomas	70/147; correlates with relapse or not responding to initial therapy	[57]
P16/INK4A	No protein expression	NSCLC	31/115; correlates with reduced survival	[58,59]
P16/INK4A	No protein expression	Early stage NSCLC	49/100; correlates with reduced survival	[60]
P16/INK4A	Low protein expression	Malignant pleural mesothelioma	45/88; correlates with reduced survival	[61]
P16/INK4A	Weak protein expression	Melanoma	8/90; correlates with reduced survival	[62]
P16/INK4A	Protein expression	Retinoblastoma	36/38; correlates with high grade tumors	[63]
P16/INK4A	Low protein expression	Osteosarcoma	143/354; correlates with reduced survival	[64]
P21/CIP/WAF1	No protein expression	Breast carcinoma	53/104; correlates with reduced survival	[59]
P21/CIP/WAF1	Low protein expression	Breast carcinoma	73/106; correlates with reduced survival	[65]
P21/CIP/WAF1	No protein expression	Gastric carcinoma	92/133; correlates with reduced survival	[66]
P21/CIP/WAF1	No protein expression	Gastric carcinoma	63/93; correlates with reduced survival	[67]
P21/CIP/WAF1	Low protein expression	Gastric carcinoma	55/71; correlates with reduced survival	[68]
P21/CIP/WAF1	Low protein expression	Colon carcinoma	197/294; correlates with reduced survival	[69]
P21/CIP/WAF1	Low protein expression	Colon carcinoma	51/211; correlates with metastasis	[70]
P21/CIP/WAF1	Low protein expression	Colon carcinoma	89/93; correlates with metastasis and reduced survival	[71]
P21/CIP/WAF1	Low protein expression	Stage II and III colon cancer	219/383; correlates with increased recurrence	[31]
P21/CIP/WAF1	No protein expression	Endometrial carcinoma	46/95; no correlation with survival	[72]
P21/CIP/WAF1	No protein expression	Endometrial carcinoma	28/75; correlates with poorer prognosis	[73]
P21/CIP/WAF1	No protein expression	Hodgkin lymphomas	71/147; correlates with relapse/not responding to initial therapy	[57]
P27/KIP1	Low protein expression	Breast carcinoma in young women (20–44 years)	173/274; correlates with increased mortality	[74]
P27/KIP1	Low protein expression	Breast carcinoma (Median age of 62 yrs.)	94/168; correlates with tumor grade and poor outcome	[75]
P27/KIP1	Low protein expression	Breast carcinoma	n = 6463; 20-meta analyses; correlates with reduced survival	[76]
P27/KIP1	Low protein expression	Gastric carcinoma	86/138; correlates with decreased 5-year survival	[77]
P27/KIP1	Low protein expression	Barrett esophageal carcinomas	45/54; correlates with decreased survival	[78]
P27/KIP1	No protein expression	Stage II colon cancer	18/152; correlates with increased mortality	[75]
P27/KIP1	Low protein expression	Stage II and III colon cancer	101/383; correlates with increased recurrence	[31]
P27/KIP1	Low or no protein expression	Prostate carcinoma	40/50; correlates with increased tumor grade	[79]
P27/KIP1	Low protein expression	Prostate carcinoma	22/113; correlates with treatment failure	[80]
P27/KIP1	Low protein expression	Prostate carcinoma	14/86; correlates with adverse prognosis	[81]
P27/KIP1	Low protein expression	Prostate carcinoma	62/129; correlates with decreased recurrence-free survival	[82]
P27/KIP1	Low protein expression	Recurring/non-recurring prostate carcinoma	50 of 202/50 of 202; correlates with recurrence following prostatectomy	[83]
P27/KIP1	No protein expression	Gastroenteropancreatic neuroendocrine tumors	61/327; correlates with reduced survival	[84]
P57/KIP2	Low mRNA expression	Bladder carcinoma	9/24; more common than decreased IGF2 or H19 expression	[85]
P57/KIP2	Low protein expression	Colorectal carcinoma	66/110; correlates with large tumor size but not with prognosis	[86]
P57/KIP2	No protein expression	Hepatocellular carcinoma	25/47; correlates with decreased survival	[87]
P57/KIP2	Low protein expression	Pancreatic carcinoma	23/25; correlates with stage IV disease	[88]
P57/KIP2	Low protein expression	Ovarian carcinoma	12/33; correlates with reduced survival	[89]
P57/KIP2	Low protein expression	Advanced ovarian carcinoma	130/171; no correlation with prognosis	[90]
P57/KIP2	No mRNA expression	Childhood acute lymphoblastic leukemia	39/74; no correlation with promoter methylation	[91]
P57/KIP2	DNA methylation of promoter	Adult acute lymphoblastic leukemia	36/72; inversely correlates with mRNA expression	[92]

[a] NSCLC: non-small cell lung cancer.

[1]. The chief substrates of CDK4/6 are limited to Rb and its p107 and p130 relatives while the many dozens of substrates of CDK1/2 are required for progression through G2 and the M-phases of the mitotic cycle [1]. The mechanisms responsible for the differences between narrow and broad substrate specificity of the CDKs are not entirely clear. The stoichiometry of the protein kinase reaction is given by the following chemical equation:

$$MgATP^{1-} + protein - O:H \rightarrow protein - O:PO_3{}^{2-} + MgADP + H^+$$

Note that the phosphoryl group ($PO_3{}^{2-}$) and not the phosphate ($OPO_3{}^{2-}$) group is transferred from ATP to the protein substrate.

Hanks et al. and Hanks and Hunter analyzed the sequences of some five dozen protein-serine/threonine and protein-tyrosine kinases and divided the primary structures into 12 domains (I-VIA,VIB-XI) [124,125]. Protein kinase catalytic domains contain 250–300 amino acid residues. Domain I is G-rich and contains a GxGxΦG signature (^{11}GEGTYG^{16} of CDK2), where Φ refers to a hydrophobic residue, and in the case of the CDKs the hydrophobic residue is tyrosine. The Gly-rich loop overlays bound ATP/ADP and occurs between the β1- and β2-strands (Fig. 2A). This is the most flexible part of the lobe as it accommodates the binding of ATP and release of ADP. Domain II of protein kinases contains a conserved Ala-Xxx-Lys (^{31}ALK^{33}) sequence in the β3-strand and domain III contains a conserved glutamate (E51) residue in the αC-helix that form a salt bridge with the conserved lysine in active protein kinases (K33 of CDK2). Domain III of the CDK1 and 2 contain the sequence PSTAIRE within the αC-helix, which interacts with activating cyclins. Domain VIB contains a conserved HRD sequence, which forms part of the catalytic loop (^{125}HRDLKPQN^{132} in CDK2). Domain VII contains a ^{145}DFG^{147} signature and domain VIII contains

Table 4
CDK anomalies associated with cancer[a].

Enzyme	Parameter	Cancer[b]	No. affected/total	References
CDK1	Protein overexpression	Melanoma	All (n = 5)	[93]
CDK1	Gene amplification and protein overexpression	Diffuse large B-cell lymphoma	Nearly all (n = 38)	[94]
CDK2	Protein overexpression	Primary colorectal carcinoma	7/8	[29]
CDK2	Protein overexpression	Melanoma	All (n = 5)	[93]
CDK2	Protein overexpression	Melanoma	23/49	[95]
CDK3	Protein overexpression	Glioblastoma	20/35[c]	[96]
CDK4	Protein overexpression	Primary colorectal carcinoma	6/8	[29]
CDK4	Protein overexpression	Advanced colorectal carcinoma	39/45	[27]
CDK4	Protein overexpression	NSCLC	52/104	[33]
CDK4	Gene amplification	Uterine cervix	29/112	[97]
CDK4	Protein overexpression	Uterine cervix	45/62	[97]
CDK4	Protein overexpression	Melanoma lacking *NRAS* and *BRAF* mutations	Unknown	[98]
CDK4	Gene amplification	Glioblastoma/anaplastic astrocytoma	7 of 14/3 of 11	[99]
CDK4	Gene amplification	Osteosarcoma	6/67	[100]
CDK4	Gene amplification	Osteosarcoma	7/24	[101]
CDK4	Gene amplification	Liposarcoma	44/48	[102]
CDK4	Gene amplification	Rhabdomyosarcoma (adult)	1/1	[103]
CDK5	Protein overexpression	Breast carcinoma	96/324	[104]
CDK5	Protein overexpression	Primary pancreatic carcinoma	22/24	[105]
CDK5	mRNA upregulation	Colorectal/head and neck/breast, lung ovary, prostate, and bladder carcinomas, sarcoma, myeloma	Unknown	[106]
CDK6	Gene amplification	Glioma	2/37	[107]
CDK6	Protein overexpression	Medulloblastoma	50/169	[108]
CDK6	Protein overexpression	T-cell lymphoma/leukemia	25/25	[109]
CDK8	Protein expression	Early/advanced gastric carcinoma	23 of 24/24 of 24	[110]
CDK8	Protein overexpression	Primary/metastatic colon carcinoma	6 of 10/6 of 9	[111]
CDK8	Gene amplification	Colorectal carcinoma	31/50	[112]
CDK8	Protein expression	Colorectal carcinoma	329/470	[113]
CDK8	Protein expression	Colorectal carcinoma	96/127	[114]
CDK9	Protein overexpression	PNET/neuroblastoma	7 of 18/2 of 7	[115]
CDK11	Protein expression	Osteosarcoma	4/6	[116]
CDK14	Protein expression	Esophageal carcinoma	115/223	[117]

[a] Adapted from Ref. [5].
[b] NSCLC: non-small cell lung cancer; PNET, primary neuroectodermal tumors.
[c] Estimate.

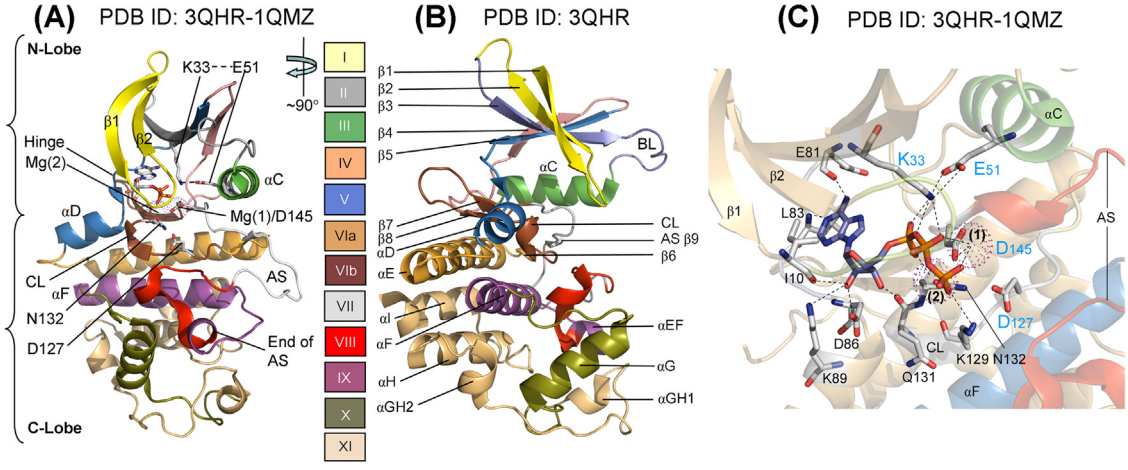

Fig. 2. (A) Overall structure of the active form of the catalytic subunit of pCDK2 containing bound ATP, which is located beneath the Gly-rich loop and shown in a stick format. The activation segment (AS) is in its active open conformation. (B) Secondary structure of pCDK2. The locations of the 12 domains described by Hanks and Hunter [125] in A and B are indicated by the color code. (C) ATP-binding site. The PDB files used to prepare each figure are shown above each illustration. The superposition of 1QMZ with 3QHR was used to illustrate the location of the two Mg^{2+} ions, which are depicted as spherical dots and labeled (1) and (2). BL, αC-β4 back loop; CL, catalytic loop. Figures adapted from PDB files were prepared with the PyMOL Molecular Graphics System Version 1.5.0.4 Schrödinger, LLC.

a conserved ^{170}APE^{172} sequence (CDK2), which together represent the beginning and end of the protein kinase activation segment. The remaining domains make up the αF, αG, αH, and αI helices.

The elucidation of the X-ray structure of PKA provided an initial framework for understanding the role of the various domains on protein kinase function, which is considered next.

3.2. The K/E/D/D motif and the secondary and tertiary structures

Knighton et al. determined the X-ray crystal structure of the catalytic subunit of PKA bound to a polypeptide protein kinase antagonist that mimics a peptide substrate (PDB ID: 2CPK) [126,127]. This structure has served as a prototype for all protein kinase catalytic domains including those of the CDK family. All protein kinases including the CDKs have a small N-terminal lobe and large C-terminal lobe [128]. The small lobe contains five conserved β-strands and a regulatory αC-helix and the large lobe contains seven conserved helices (αD–αI and αEF) and four short strands (β6–β9). The N-lobe and C-lobe form a cleft that serves as a docking site for ATP. The locations of the 12 Hanks domains are illustrated in Fig. 2A and B. Of the many hundreds of protein kinase domain structures in the protein data bank, all of them have this fundamental protein kinase fold first described for PKA [126,127].

Nearly all active protein kinases contain a K/E/D/D (Lys/Glu/Asp/Asp) signature motif that plays important structural and catalytic roles [129]. The first two residues occur within the small lobe and the second two residues occur within the large lobe. Although both lobes contribute to nucleotide binding, most of the interaction involves the N-lobe. K33 (the K of K/E/D/D) of the β3-strand of CDK2 holds the α- and β-phosphates in position (Fig. 2C). The carboxylate group of E51 (the E of K/E/D/D) of the αC- or PSTAIRE-helix forms a salt bridge with the ε-amino group of K33 and serves to stabilize its interactions with these phosphates. The presence of a salt bridge between the β3-lysine and the αC-glutamate is a prerequisite for the formation of active protein kinases. This salt bridge is very important and is a central structural theme in the protein kinase literature [129].

The C-lobe participates in nucleotide binding and it makes a major contribution to protein/peptide substrate binding. Two Mg^{2+} ions participate in the protein kinase catalytic cycle of CDK2 [130] and several other protein kinases [131]. CDK2 D145 (the D of DFG and the first D of K/E/D/D) binds to $Mg^{2+}(1)$ (Fig. 2C), which in turn will coordinate with the β- and γ-phosphates of ATP. CDK2 N132 of the catalytic loop binds $Mg^{2+}(2)$, which in turn will coordinate with the α- and γ-phosphates of ATP. The γ-phosphate interacts with a lysine (K129 of CDK2) within the catalytic loop, a residue that is conserved within the protein-serine/threonine kinase family. The 2′- hydroxyl group of the ATP ribose forms a hydrogen bond with the carbonyl group of I10 (before the G-rich loop), another with the side chain of D86 within the hinge, and a third with K89 following the hinge. The 3′-hydroxyl hydrogen bonds to the carbonyl group of Q131 following the catalytic loop. A31 of the catalytic spine (CS8), L83 in the hinge, and L134 after the catalytic loop (CS6) make hydrophobic contacts with the adenine base of ATP (not shown). Most small molecule protein kinase inhibitors make contact with many of the residues of the ATP-binding pocket that are homologous to these residues.

3.3. CDK substrate-binding sites and cyclin substrate-recruitment sites

The activation segment of the C-lobe of CDKs and other protein kinases occurs with an extended open conformation in active enzymes and a compact closed conformation in dormant enzymes. The activation segment forms a platform for the peptide/protein substrates. Brown et al. determined the crystal structure of a peptide substrate bound to both the CDK2 substrate-binding site and the cyclin A substrate-recruitment site [121]. The segment connecting the two portions of the peptide was not observed and is depicted by the dashed line (Fig. 3A). The CDK2 substrate-binding site involves the activation segment and the catalytic loop. Brown et al. determined the crystal structure of an optimal peptide substrate with an HHASPRK sequence bound to CDK2-cyclin A that was phosphorylated at T160 within the activation segment, which is the fully activated enzyme form [121]. The phosphorylatable S residue is labeled P+0 (where P refers to phosphate), the next residue, a proline, is labeled P+1, and the following R residue is labeled P+2. V164 of the activation segment has an unusual left-handed conformation that results in the carbonyl oxygen atom being directed away from the peptide substrate where it makes hydrogen bonds with R169 just before the APE of the activation segment (Fig. 3B). Binding of any residue except proline at the P+1 site of the enzyme is precluded. In unphosphorylated CDK2-cyclin A, CDK2 V163 blocks the P+1 site. As a consequence, the unphosphorylated enzyme is inactive while the arginine at the P+2 site is directed toward the solvent and does not interact with the protein. The P+3 lysine of the substrate forms a hydrogen bond with the phosphate on T160 and to the main-chain oxygen of residue I270 of cyclin A, which accounts for the requirement for a basic residue at this position.

Brown et al. determined the crystal structure of a peptide substrate bound to the substrate recruitment site of the pCDK2-cyclin A complex [121]. The R/KXL recruitment site occurs on the surface of cyclin A. L92 of RXL^{92}, which is defined as the P+0 site [132], docks into a hydrophobic pocket located in the cyclin A α1 and α3 helices. Moreover, the N—H group of the substrate peptide L92 residue forms a hydrogen bond with the carbonyl group of Q254 of cyclin A (Fig. 3C). The side chain of the important R90 of the ^{90}RXL (P-2) motif forms salt bridges with the cyclin A E220 side chain, the N—H group of R90 forms a hydrogen bond with the cyclin A I281 carbonyl group, and the R90 carbonyl group forms a hydrogen bond with the cyclin A Q254 N—H group. N96 (P+4) and F94 (P+2) of the peptide substrate make polar contacts with the side chain of R250 of cyclin A. There are numerous hydrophobic and van der Waals contacts between the cyclin A peptide recruitment site and the substrate peptide. The peptide substrate-recruitment sites in cyclin A and E that interact with the K/RXL within the substrate consists of a conserved MRAIL motif (^{210}MRAIL^{214} in cyclin A2).

Most protein kinases including the CDKs exist in active and inactive conformations as described later. The first step in CDK activation results from binding its cyclin partner and the second step, which is required for full activation, involves the phosphorylation of a threonine residue within the activation segment (T160 for CDK2) as catalyzed by a CDK-activating kinase (CAK), which corresponds to CDK7 [5]. The activation segment of the CDKs is sometimes called the T-loop, referring to this threonine residue. The glutamate residue at the end of the activation segment (APE) of all protein kinases forms a salt bridge with an arginine residue in the αHI loop; this salt bridge consists of Glu172 and Arg274in CDK2 (not shown).

3.4. Mechanism of the CDK2 reaction

Hengge considered two reaction mechanisms for the transfer of the phosphoryl group from ATP to substrates as catalyzed by protein kinases; these are associative or dissociative [133]. The differences between these mechanisms involve (i) the respective groups that accept the hydrogen atom from the protein substrate and (ii) the transition states. The transition state of a chemical reaction is an unstable intermediate that occurs midway between the reactants and products [134,135]. The transition state is a complex where chemical bonds are being made and broken. The energized transition state has a fleeting existence ($\approx 10^{-12}$ s – 10^{-13} s), which is the time of a single bond vibration. The transition state in an associative process occurs when bond formation with the protein substrate begins before the bond between the β- and γ-phosphates is broken. The proton on the hydroxyl group of the protein substrate is accepted by the transferring phosphate. In contrast, the dissociative mechanism involves a complete break of the phos-

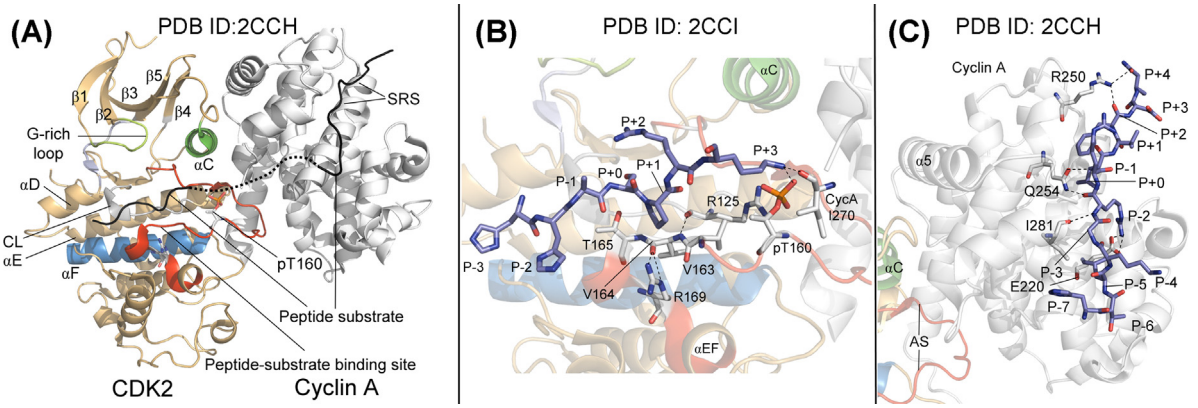

Fig. 3. (A) Overview of pCDK2-cyclin A interacting with a peptide substrate (black) at both the enzyme peptide substrate binding site and the cyclin substrate recruitment site (SRS). The chain connecting the two bound peptide segments was disordered and is represented by the dashed line. Cyclin A is the gray structure. (B) Protein-substrate binding site of pCDK2-cyclin A. The substrate is shown in a stick format with carbon atoms in blue. Enzyme and cyclin carbon atoms are gray. (C) Peptide binding to the pCDK2-cyclin A substrate recruitment site. The carbon atoms of the substrate are in blue and those from cyclin A are gray. AS, activation segment; CL, catalytic loop site.

phoryl leaving group yielding a metaphosphate with a minus one charge. The HRD aspartate (D127 of CDK2) acts as a catalytic base that accepts the proton from the substrate residue. In the dissociative transition state, bond breaking between the phosphorus center and the leaving group (ADP) is more advanced than bond making with the incoming oxygen of serine/threonine. Although there is data that supports each of these mechanisms, the preponderance of results favors a dissociative process [136,137].

Bao et al. determined the structure of the transition state of CDK2 using ADP, Mg^{2+}, a peptide substrate, and MgF_3^- [138]. MgF_3^- mimics the γ-phosphate in the transition state of ATP-requiring reactions. Cook et al. determined the structure of the transition state substituting nitrate (NO_3^-) for MgF_3^- [139]. Pauling proposed that the large rate acceleration of enzymes is caused by the high specificity of the protein catalyst for binding, not the substrate, but rather the transition state [140,141]. Pauling thought that this idea could be tested by studying inhibitors that have a greater affinity for the enzyme than the substrates themselves. Thus, transition state analogues are inhibitors that take advantage of the special interactions that distinguish the substrate in the transition state from the substrate in the ground state. The development of transition state analogues for enzymatic reactions that act as tight-binding inhibitors provides support for this notion [134,135]. Despite structural studies on the CDK2 transition state, there has been little, if any, development, of CDK transition-state analogue inhibitors.

CDK2 catalyzes the nucleophilic in-line attack of the protein-serine/threonine substrate onto the γ-phosphorus atom of Mg_2ATP (Fig. 4). The ATP and peptide substrates are bound as described earlier. HRD-D127, the catalytic base within the catalytic loop abstracts a proton from the seryl substrate as formulated in the dissociative reaction mechanism. In this transition state, the *meta*-phosphate has dissociated from the ADP leaving group and has not yet formed a bond with the seryl group. The αC-E51 has formed a salt bridge with the β3-K33 and the latter interacts with the α- and β-phosphates of ATP. The two Mg^{2+} ions counter the negative charge of the *meta*-phosphate and the oxygen atoms of ATP.

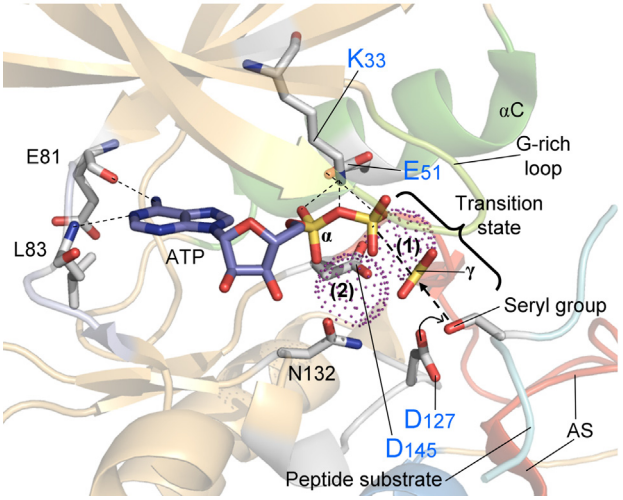

Fig. 4. Mechanism of the CDK2 reaction of ATP with a peptide substrate with HRD-D127 abstracting a proton from the peptide —OH group. AS, activation segment. Prepared from PDB ID: 1GY3 with the superposition of 3QHR to depict the location of two Mg^{2+} ions (shown as dotted spheres).

4. Structure of the CDK hydrophobic skeletons

4.1. The regulatory and catalytic spines

Kornev et al. [142,143] compared the structures of about two dozen active and inactive protein kinases using a spatial alignment algorithm. They used this data to establish the presence of protein kinase (i) regulatory and (ii) catalytic spines. In contrast to protein kinase amino acid signatures such as APE, DFG, or HRD, the residues that form the spines were not identified by examination of the primary structures. Rather, the spines were identified by their location as determined by their X-ray crystal structures. The spatial alignment analysis revealed a skeleton of four nonconsecutive hydrophobic residues that make up a regulatory or R-spine and eight hydrophobic residues that constitute a catalytic or C-spine.

The R-spine interacts with a conserved aspartate (D185 of CDK2) in the αF-helix. Going from the aspartate of the αF-helix up to the top residue in the β4-strand, Meharena et al. labeled the regulatory spine residues RS0, RS1, RS2, RS3, and RS4 [144]. We have labeled the catalytic spine residues CS1–CS8 (Fig. 5A) [145]. As noted later, there are three conserved "shell" residues that interact with the R-spine. Altogether each protein kinase contains 16 amino acid residues that comprise this protein kinase skeletal composite. Each spine contains residues from both the N- and C-lobes. The regulatory spine contains residues from the αC-helix and the activation segment, whose spatial arrangements are important in producing active and inactive states. The catalytic spine facilitates ATP binding while the regulatory spine facilitates the positioning of the pro-

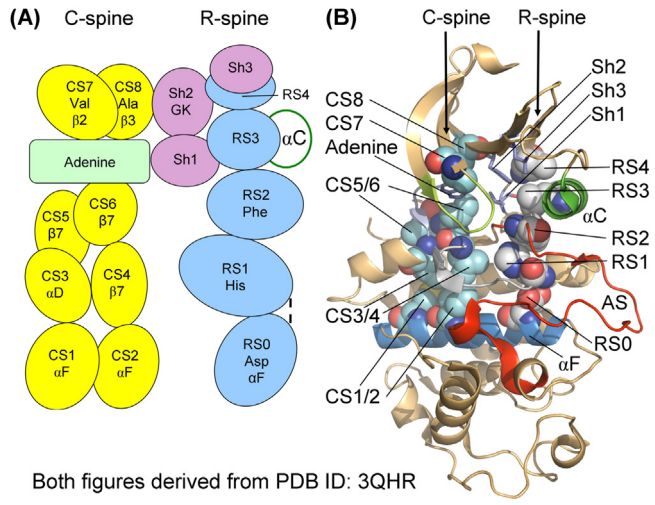

Fig. 5. (A) Diagram of a frontal projection of the classical view of protein kinases depicting the location of the C-spine, R-spine, and shell residues of the active conformation of pCDK2. The dashed line represents a hydrogen bond. (B) Depiction of the C-spine and R-spine residues of pCDK2 shown as spheres. The carbon atoms of the C-spine are sky blue while those of the R-spine are gray; the shell residues are shown in a stick format with carbon atoms in dark blue. AS, activation segment.

tein substrate to promote catalysis. The accurate alignment of the spines is necessary for the formation of an active protein kinase conformation.

The CDK2 regulatory spine consists of a residue from the beginning of the β4-strand (Leu66, RS4), another that is four residues after the αC-E51 (Leu55, RS3), the phenylalanine of the activation segment DFG (Phe145, RS2), along with the HRD-histidine (H125, RS1) of the catalytic loop. The backbone of His125 is anchored to the αF-helix by a hydrogen bond to a conserved aspartate residue (Asp185, RS0). Residues that make up the protein-substrate positioning segment, the activation segment, the αHI-loop, and the catalytic spine of protein kinase domains form hydrophobic contacts with the αF-helix [142]. The αF helix thus serves as a foundation for the key structural elements of protein kinases.

The protein kinase catalytic spine contains residues from the N- and C-lobes and is completed by the adenine portion of ATP [143]. The two residues of the small lobe of CDK2 that bind to the adenine group of ATP include Val18 (CS7) near the beginning of the β2-strand and Ala31 (CS8) from the conserved Ala-Xxx-Lys of the β3-strand. Furthermore, Leu134 (CS6) from the middle of the large lobe β7-strand binds to the adenine base in the active enzyme. Leu133 (CS4) and Ile135 (CS5), hydrophobic residues that flank Leu173, bind to Leu87 (CS3) at the beginning of the αD-helix. The αD-helix Leu87 makes hydrophobic contacts with Ile192 (CS2) and Met196 (CS1) in the αF-helix (Fig. 5B). Note that both the R-spine and C-spine are anchored to the αF-helix, which is a very hydrophobic component of the enzyme that traverses the entire large lobe. Table 5 lists the residues of the spines of CDK1/2/4/6/9.

4.2. Shell residues stabilizing the R-spine

Using site-directed mutagenesis, Meharena et al. identified three residues in murine PKA that stabilize the R-spine, which they labeled Sh1, Sh2, and Sh3, where Sh refers to shell [144]. The Sh1 Val104Gly mutant exhibited 5% of the catalytic activity of wild type PKA while the Sh2 Met120Gly and Sh3 Met118Gly double mutant was kinase dead. These results indicate that the shell residues contribute to an active protein kinase conformation. The Sh1 residue of protein kinases occurs in the αC-β4 back loop (Fig. 2B). The Sh2 or gatekeeper occurs at the end of the β5-strand immediately before the hinge, and Sh3 is two residues upstream from the gatekeeper in the β5-strand.

Sh1 (Val64 of CDK2) interacts with RS3 (Leu55) and Sh2 (Phe80) while Sh3 (Leu78) interacts with RS4 (Leu66) (Fig. 5A and B). Sh2 is the classical gatekeeper residue, which interacts with Sh1 (Val64) below it and with RS4 (Leu66) next to it. The name gatekeeper indicates the role that this residue plays in controlling access to a hydrophobic pocket adjacent to the adenine binding site [146,147] that is occupied by components of many small molecule antagonists as described later. Based upon the local spatial pattern alignment data [142], only three of 14 amino acid residues in PKA surrounding RS3 and RS4 are conserved. These shell residues stabilize the protein kinase regulatory spine [144].

5. The two-step activation of CDK2

Schulze-Gahmen et al. determined the X-ray crystal structure of CDK2 in its inactive state in the absence of cyclin [148]. They showed that CDK2 occurred with a compact closed activation segment with the αC-helix lateral to the β4-stand and αC-E51 displaced from β3-K33 by an αAS helix within the activation segment. Moreover, the R-spine is not linear, but displays a kink with a displaced RS3 (Fig. 6A). Jeffrey et al. determined the structure of unphosphorylated CDK2 with cyclin A (Fig. 6C) [149]. The activation segment occurs in an open conformation extending from the center of the enzyme, the αC-helix is inward, and αC-E51 forms a salt bridge with β3-K33. Moreover, the R-spine is linear (Fig. 6D). Russo et al. determined the structure of CDK2-cyclin A in the active form with phosphorylated T160, which occurs within the activation segment or T-loop (Fig. 6E) [150]. The structure of the phosphorylated activation segment is very similar to that of unphosphorylated CDK2-cyclin A.

Russo et al. found that the phosphate on T160 forms salt bridges with R50 of the αC-helix, R126 from the catalytic loop (HRD), and R150 in the activation segment (Fig. 6F) [150]. In unphosphorylated CDK2-cyclin A, the three basic residues are near each other but do not interact with T160 (Fig. 6D). The threonine —OH group in the free CDK2 enzyme is 18 Å from the catalytic loop arginine, 24 Å from the activation segment arginine, and 30 Å from the αC-helix arginine (Fig. 6B). Moreover, the T160 —OH group of the uncomplexed CDK2 is buried and not amenable for phosphorylation while that of the unphosphorylated CDK2-cyclin A complex is exposed to solvent making it available for phosphorylation by the CDK-activating enzyme (CDK7) [151]. The charge cluster observed in phosphorylated CDK-cyclin A accounts in part for the interaction of the activation segment to other regulatory components of the enzyme. Even though the disposition of the αC-helix and activation segment in the unphosphorylated CDK2-cyclin A complex is close to that of the unphosphorylated complex, the enzymatic activity of the latter is only 0.3% that of the phosphorylated complex [152].

The displacement of the αC-helix and the compact conformation of the activation segment in inactive CDK2 in contrast to active CDK2 is clearly depicted in Fig. 6G. The aliphatic side chain of inactive CDK2 RS3 is displaced when compared with that of active CDK2 (Fig. 6H). Also CS7, CS8, Sh2, and Sh3 of the inactive enzyme are displaced when compared with those of the active enzyme. Furthermore, the phenyl group of RS2 in the inactive enzyme is tilted when compared with that of the active protein.

6. Interaction of KIP/CIP and INK4 with CDKs

6.1. p27/KIP1 and CDK2-cyclin A

The KIP/CIP family of inhibitors, which consist of p27/KIP1, p21/CIP1, and P57/KIP2, bind to and inhibit CDK-cyclin complexes

Table 5
Human CDK1/2/4/6/9 regulatory spine, shell, and catalytic spine residues.

	Symbol	CDK1	CDK2	CDK4	CDK6	CDK9
Regulatory spine						
β4-strand (N-lobe)	RS4	Leu66	Leu66	Leu74	Leu79	Leu81
αC-helix (N-lobe)	RS3	Leu55	Leu55	Leu60	Leu65	Leu70
Activation loop DFG-Phe (C-lobe)	RS2	Phe147	Phe145	Phe159	Phe164	Phe168
Catalytic loop HRD-His (C-lobe)	RS1	His126	His125	His138	His143	His147
αF-helix (C-lobe)	RS0	Asp186	Asp185	Asp196	Asp201	Asp211
Shell						
Two residues upstream from the gatekeeper	Sh3	Leu78	Leu78	Leu91	Leu96	Leu101
Gatekeeper, end of the β5-strand	Sh2	Phe80	Phe80	Phe93	Phe98	Phe103
αC-β4 back loop	Sh1	Val64	Val64	Val72	Val77	Val79
Catalytic spine						
β3-strand AxK-Ala (N-lobe)	CS8	Ala31	Ala31	Ala33	Ala41	Ala46
β2-strand Val (N-lobe)	CS7	Val18	Val18	Val20	Val27	Val33
β7-strand (C-lobe)	CS6	Leu135	Leu134	Leu147	Leu152	Leu156
β7-strand (C-lobe)	CS5	Ile136	Ile135	Val148	Val153	Ile157
β7-strand (C-lobe)	CS4	Leu134	Leu133	Ile146	Leu151	Val155
αD-helix (C-lobe)	CS3	Leu87	Leu87	Leu100	Leu105	Leu110
αF-helix (C-lobe)	CS2	Ile193	Ile192	Ile203	Ile208	Ile218
αF-helix (C-lobe)	CS1	Leu197	Met196	Met207	Met212	Met222

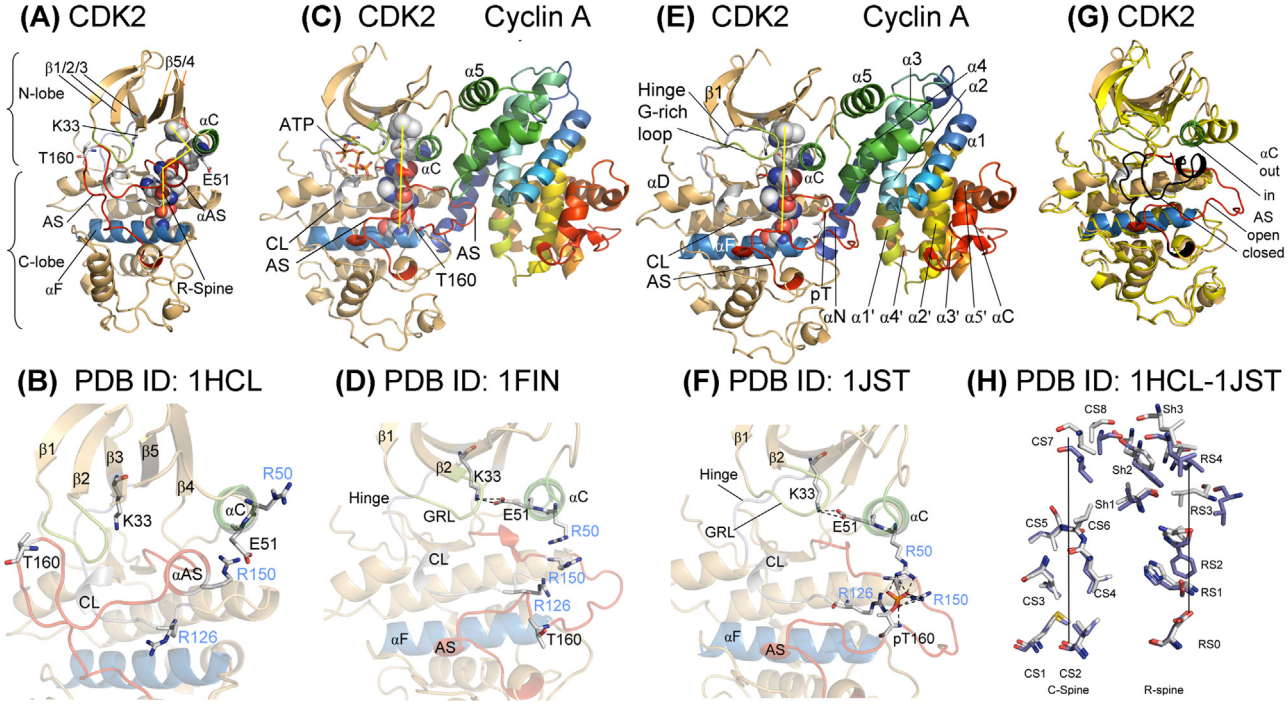

Fig. 6. (A) Inactive non-phosphorylated CDK2 free from cyclin A. The R-spine residues are shown as spheres with a yellow line indicating their trajectory. (B) Location of the important arginine (R) residues in inactive CDK2: R50, R126, R150. (C) Semi-active non-phosphorylated CDK2-cyclin A. Bound ATP is shown in a stick format. (D) Location of important arginine residues in semi-active CDK2-cyclin A. (E) Active pCDK2-cyclin A. (F) Interaction of pT160 of active CDK2-cyclin A with R50, R126, and R150. (G) Superposition of active and inactive CDK2. The open activation segment (AS) of active CDK2 is red and the closed activation segment of inactive CDK2 is black. (H) Superposition of active (gray carbon atoms) and inactive (dark blue carbon atoms) CDK2 R-spine, C-spine, and shell residues. AS, activation segment, CL, catalytic loop, GRL, glycine-rich loop. The PDB IDs refer to the structures shown above and below them.

[153]. These proteins can bind to cyclin and CDKs independently, but they have much higher affinity for CDK-cyclin complexes, which are their preferred targets. These proteins contain a 65-residue segment at their amino-termini that can bind to and inhibit their target enzymes. Their carboxyterminal regions are of different sizes with divergent sequences. Russo et al. determined the X-ray crystal structure of the 69-amino acid N-terminal domain of p17/KIP1 bound to the phosphorylated CDK2-cyclin A complex [153]. The inhibitor binds to a peptide-binding groove in cyclin A that corresponds to the substrate-recruitment site (SRS) (Fig. 7A). p27/KIP1 courses over the small lobe of CDK2 and inserts itself into the catalytic cleft where ATP normally binds.

From the N-terminus to the C-terminus, p27/KIP1 consists of the coil in contact with cyclin A, an amphipathic α-helix, an amphipathic β-hairpin, a β-strand, a 3_{10}-helix, and a coil (Fig. 7A). The buried surface area as a result of the p27/KIP1 interaction with the enzyme-cyclin complex amounts to 5750 Å^2 (60% with CDK2 and 40% with cyclin A), which is larger than the buried surface area of the CDK2-cyclin A complex of 3550 Å^2 [153]. Cyclin A contains two cyclin boxes, but only the first box interacts with the protein inhibitor. The most distinct interactions of cyclin A with the ^{32}LFG^{34} motif of p27/KIP1 involve hydrophobic contacts with M210, I213, and L214 of the ^{210}MRAIL^{214} motif that was described earlier as the substrate-recruitment site (Section 3.3). The LFG motif occurs

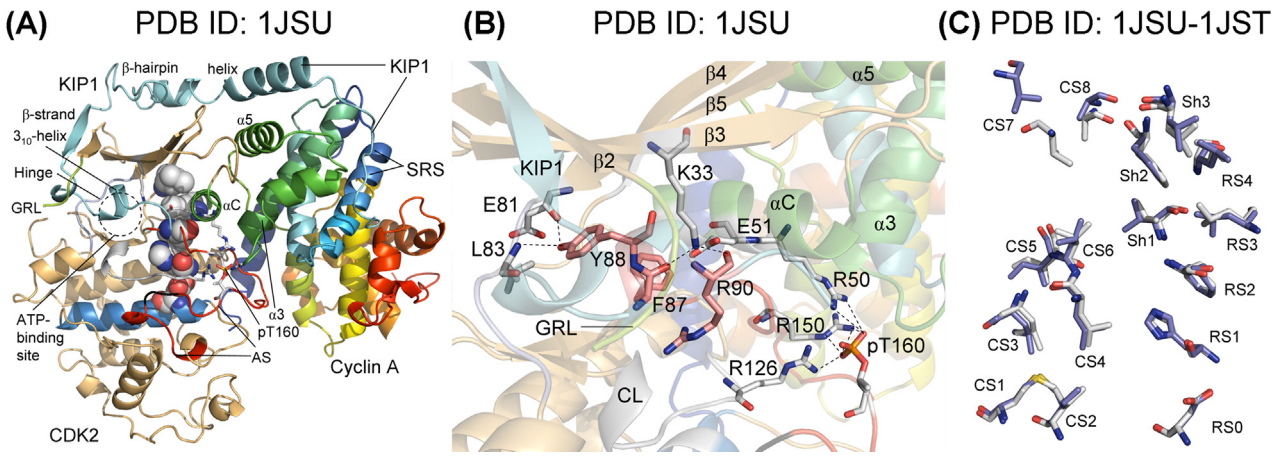

Fig. 7. (A) Binding of KIP1 to pCDK2-cyclin A. AS, activation segment; GRL, Gly-rich loop; SRS, substrate recruitment site. (B) Hydrogen bonds between KIP1 and pCDK2. The carbon atoms of pCDK2 are gray and those of KIP1 are orange. The dashed lines represent polar contacts. (C) Superposition of the C-spine, R-spine, and shell residues of pCDK2-cyclinA-KIP1 and pCKD2-cyclin A. The carbon atoms of the spine and shell residues of pCDK2-cyclin A are colored gray and those from the pCDK2-cyclin A-KIP1 ternary complex are colored dark blue.

in the three members of the CIP/KIP family and the MRAIL motif is conserved in cyclins D, E, A, and B.

p27/KIP1 makes hydrophobic contacts with residues in the β2 (A21), β3 (V30, L32), β4 (I70), and β5 (Y77, V79) strands of CDK2 [153]. The inhibitor also hydrogen bonds to the outer aspect of the CDK2 small lobe. The 3_{10}-helix (residues 85–90) fills most of the space of the catalytic cleft and occupies the ATP-binding pocket (Fig. 7A). The Y88 —OH group makes hydrogen bonds with E81 and L83 of the hinge that mimic those made by ATP (Fig. 7B), and its aromatic ring makes hydrophobic contacts with F80 (Sh2), F82, and L134 (CS6). K33 of the β3-strand of CDK2 forms hydrogen bonds with F87 and R90 of p27/KIP1. A comparison of the superposition of the C- and R-spines of pCDK2-cyclin A bound to the inhibitor with active pCDK2-cyclin A shows that the greatest differences involve CS7 and CS8 (Fig. 7C), which occur within the N-lobe.

Russo et al. hypothesize that the LFG motif of p27/KIP1 serves as an initial anchor in complex formation because this can occur in the absence of any structural rearrangements [153]. This is in contrast to the binding of the inhibitor to CDK2 where major structural changes occur. As a result, binding of the antagonist to cyclin may facilitate its subsequent binding to CDK2. The LFG motif of p27/KIP1 and MRAIL of cyclins D, E, A, and B explains, in part, the specificity of these inhibitors for complexes containing these cyclins. In contrast, cyclin H (a partner of CDK7) and p35 (a partner of CDK5) lack the motifs that bind to p27/KIP1 and are thereby not inhibited by it. The inhibition constants of the KIP/CIP antagonists for different CDK-cyclin complexes vary considerably [154]. For example, CDK1-cyclin B is poorly inhibited by the p21/CIP1 (K_i value ≈ 400 nM vs. 0.5–15 nM for CDK2/3/4/6) and this lower affinity may be due to the 35-amino acid insertion at the N-terminus of CDK1. Moreover, the amino acids of CDK2 that interact with p27/KIP1 are conserved in CDK4/5/6, targets of KIP/CIP, but not in the nontarget CDK1.

6.2. INK4 inhibitors and CDK6

CDK4 and 6 are the preferred targets of the INK family of inhibitors (p16/INK4A, p15/INK4B, p18/INK4C, and p19/INK4D) [3]. These inhibitors are induced by a variety of antiproliferative signals such as transforming growth factor-β (p15/INK4B), senescence (p16/INK4A), and terminal differentiation (p18INK4C and p19/INK4D) [155]. These antagonists can bind to monomeric CDK4/6, which interferes with the subsequent binding and activation by cyclin D. Moreover, the INK4 proteins can bind and inhibit the CDK4/6-cyclin D complexes without dissociating cyclin. Consequently, the INK4 family has a narrower CDK preference than that of the KIP/CIP family.

Russo et al. reported that the INK4 family binds to the side of the small and large lobes opposite to the cyclin binding site of their target CDK4/6 protein kinases and distorts the R-spine so that the enzyme assumes an inactive conformation (Fig. 8A) [156]. p16/INK4A contains four ankyrin repeats, each of about 33 amino acid residues that consist of paired α-helices separated by loops (Fig. 8B) [157]. Ankyrin repeats occur in a large number of proteins where they participate in protein–protein interactions. The surface of p16/INK4A binds to the small lobe and the tips of the repeats interact with the large lobe. These interactions are mediated mostly by hydrogen-bonding networks involving the second and third ankyrin repeats [156]. Like inactive free CDK2, p16/INK4A bound to unphosphorylated CDK6 lacks activating changes. Moreover, the complex with p16/INK4A possesses structural distortions that are further removed from the active structure than that of uncomplexed CDK6 so that cyclin binding is compromised and the movement of the αC-helix into its active state is blocked. The activation segment is in a closed and inactive conformation (Fig. 8A).

Although p19/INK4D contains five ankyrin repeats, Russo et al. found that its binding to unphosphorylated CDK6 closely resembles that of p16/INK4A (Fig. 8C and D) [156]. The first and second ankyrin repeats interact with the N-lobe and the third repeat interacts with both lobes while the last two repeats fail to contact the enzyme. The R-spine is distorted and the β3-strand K43 fails to interact with the αC-E61. As a result, interactions with ATP phosphates would be impaired. The hinge residues (99–102) that ordinarily form hydrogen bonds with the adenine base of ATP are displaced by an average of 2.5 Å, thus prohibiting normal contact with the nucleotide substrate. The activation segment of the p19/INK4D-CDK6 complex is in a closed and inactive conformation that differs from that of the p16/INK4A-CDK6 complex as it contains an additional helix (residues 172–176).

Jeffrey et al. determined the crystal structure of p18/INK4C bound to a complex of unphosphorylated CDK6 with a D-type cyclin (cyclin K) [155]. They found that p18/INK4C and cyclin bind on opposite sides of the enzyme and do not interact with each other (Fig. 8E). The p18/INK4C interface with CDK6 is similar in size when compared with p16/INK4A and p19/INK4D, but the CDK6-cyclin K interface is much less than that of the active unphosphorylated CDK2-cyclin A complex (2500 Å^2 vs. 3540 Å^2). This decreased interface may weaken complex formation and promote cyclin dissociation. The first three ankyrin repeats interact with the N-lobe

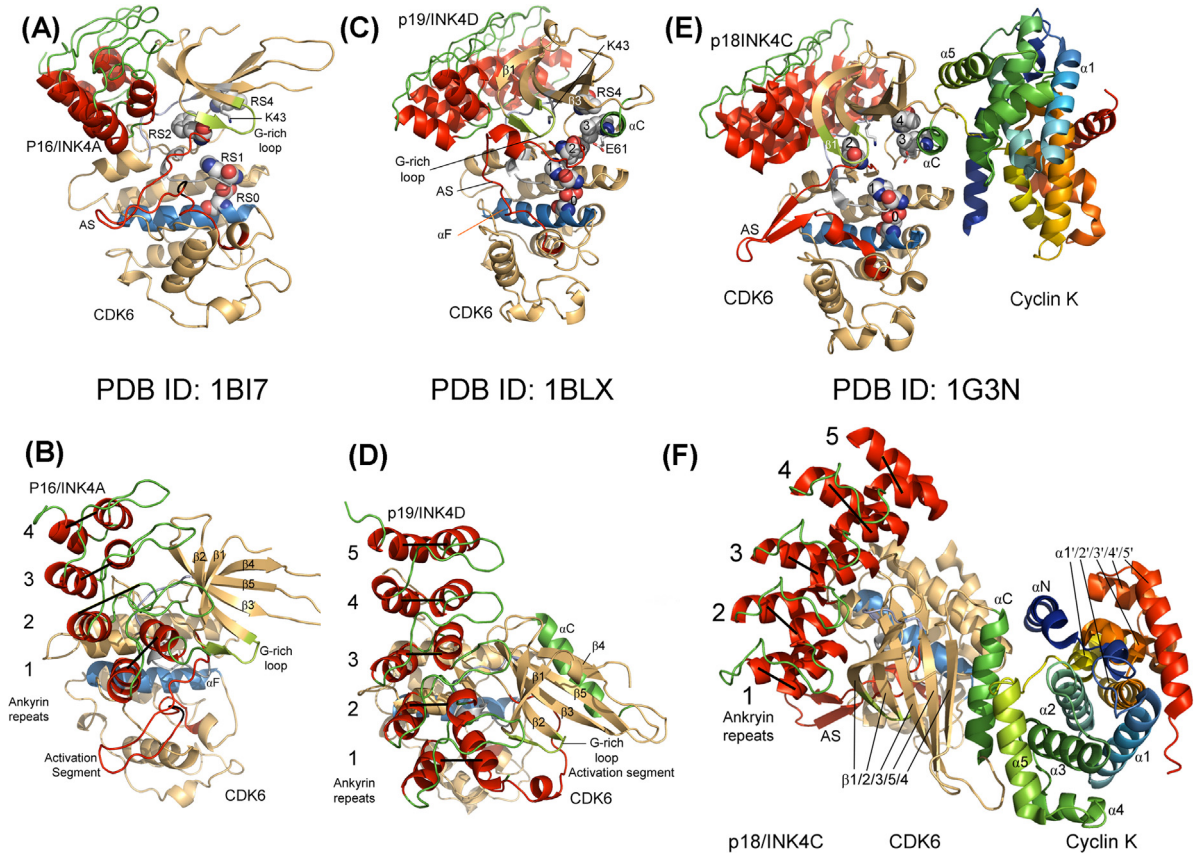

Fig. 8. (A) p16/INK4A bound to inactive CDK6. The helices of p16/INK4A are red and the loops are green. The residues that make up the non-linear R-spine (RS0/1/2/4) are shown as spheres; RS3 is missing. AS, activation segment. (B) The p16/INK4A-CDK6 complex viewed from above the protein kinase as it is classically depicted. Black bars connect each of the two helices that constitute the ankyrin repeats. (C) p19/INK4D bound to inactive CDK6. The R-spine residues are labeled 0, 1, 2, 3 and RS4. (D) The p19/INK4D-CDK6 complex viewed from above. Black bars connect the two helices of each ankyrin repeat. (E) p18/INK4C bound to CDK6-cyclin K. The R-spine residues are labeled 0, 1, 2, 3, and 4. (F) The p18/INK4 C-CDK6-cyclin K complex viewed from above.

of CDK2 while the forth and fifth repeats are not in contact with the enzyme (Fig. 8F). The hydroxyl group of S155 near the catalytic loop of the large lobe forms a hydrogen bond with the G81 carbonyl group of the third repeat (not shown). The relative arrangement of p18/INK4C and CDK6-cyclin K are very similar to those observed in the p16/INK4A and p19/INK4D complexes indicating that cyclin fails to influence the inhibitor-enzyme interface significantly. p18/INK4C displaces the αC-helix so that the β3-strand K43 fails to interact with the αC-E61. Moreover, the inhibitor breaks the R-spine and markedly displaces RS2. The activation segment is in an inactive closed conformation and contains an antiparallel β-sheet (residues 169–172 and 177–180). The inactive activation segments of CDK6 bound to INK4A/D/C differ from one another and from the activation segment from active enzyme conformations thereby illustrating the flexibility or plasticity of this enzyme component.

7. Selected CDK inhibitors in clinical trials

7.1. First-generation drugs

7.1.1. Alvocidib or flavopiridol

Alvocidib is a flavonoid alkaloid that was the first CDK antagonist that entered clinical trials. The 2-chlorophenyl-chromen-4-one core represents the flavonoid and the 1-methylpiperadine portion is the alkaloid entity (Fig. 9A). This drug inhibits CDK1/2/4/6 with IC_{50} values less than 200 nM (klifs.vu-compmedchem.nl/). However, its IC_{50} for CDK9 is 3 nM and inhibition of this enzyme is most likely responsible for its pharmacologic actions. CDK9 catalyzes the phosphorylation of the C-terminal domain of RNA polymerase II that is required for RNA elongation (Table 1). CDK9 forms part of PTEFb (Positive Transcription Elongation Factor-b) along with cyclins T1, T2a, T2b, or K. PTEFb is associated with a large protein complex forming an overall super elongation complex [158]. Thus, alvocidib inhibits the participation of PTEFb in G1 progression [159].

Initial clinical studies with alvocidib were associated with tumor lysis syndrome, a potentially fatal complication that results in the breakdown of large numbers of cells. Tumor lysis syndrome is characterized by hyperkalemia (elevated serum K^+), hyperphosphatemia, hypocalcemia, hyperuricemia, and elevated lactate dehydrogenase and blood urea nitrogen. More recent studies have been designed to minimize this syndrome as reported in a phase I clinical trial for the treatment of acute leukemias [160]. Phase I trials involve small numbers of patients and are used to determine safe dosage ranges and to begin determining side effects. Karp et al. used a drug regiment consisting of alvocidib, cytosine arabinoside (a DNA synthesis inhibitor), and mitoxantrone (a type II DNA topoisomerase inhibitor); they reported that using a 30-min bolus injection of alvocidib followed by a four-hour infusion was more effective in treating the disease than a 1-hour bolus, while minimizing the incidence of the syndrome [160]. Moreover, Zeidner et al. found in a phase II clinical trial that the same drug regimen was effective in the treatment of newly diagnosed acute myelogenous leukemia with plans to enter into a phase III trial [161]. Phase II trials are used to determine whether a drug or drug combination is effective against a specific disease, to further evaluate safety, and to identify additional side effects. Phase III trials are used to confirm

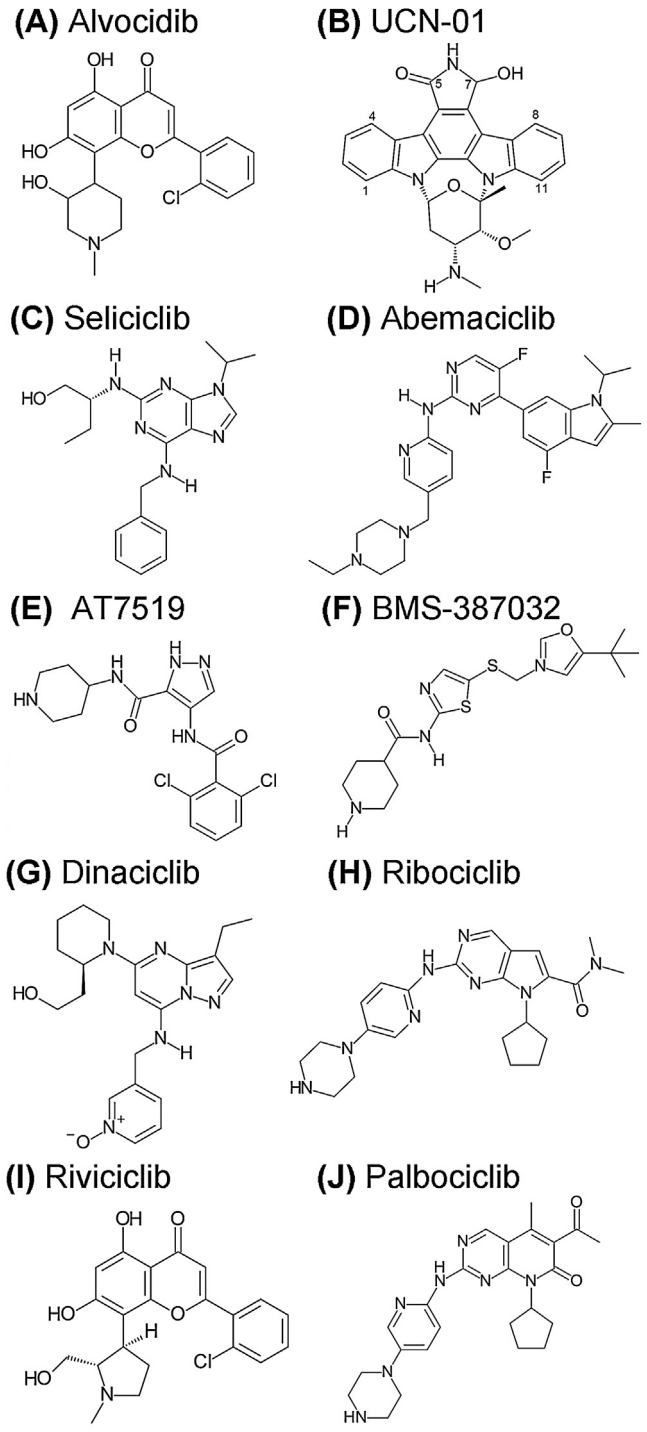

Fig. 9. Structures of selected CDK inhibitors in clinical trials.

the effectiveness of a drug regimen, to monitor side effects, and compare such regimens with one or more standard or approved treatment modalities.

The efficacy of alvocidib given intravenously as a single agent in the treatment of various leukemias, mantle cell lymphoma, multiple myeloma, non-Hodgkin lymphomas, kidney or head and neck cancers has been studied (ClinicalTrials.gov). Christian et al. reported that 19 of 42 patients with refractory chronic lymphocytic leukemia responded to alvocidib as a single agent [162] and Lin et al. reported that 34 of 64 patients with the illness responded to the drug [163]. Owing to its limited effectiveness as a single agent, more studies with alvocidib in combination with other agents are underway.

The combination of alvocidib with (i) gemcitabine – an inhibitor of DNA repair – or docetaxel – a blocker of microtubule dynamics during mitosis – in pancreatic cancer, (ii) cisplatin – a DNA crosslinker – in ovarian carcinoma, (iii) doxorubicin – producing DNA double strand breaks – in sarcomas, (iv) irinotecan – a DNA topoisomerase I inhibitor – in gastric cancer, (v) imatinib – an Abl protein kinase antagonist – in leukemia, and (vi) paclitaxel – a blocker of microtubule dynamics – in esophageal cancers have also been studied in clinical trials (Table 6). George et al. found that eight of 18 patients with NSCLC responded to a combination of paclitaxel, carboplatin – a DNA crosslinker- and alvocidib [164]. Commonly occurring side effects include diarrhea, fatigue, and hematological toxicities [165]. The drug has been in clinical trials for a relatively long time, and whether it ever becomes approved is a matter for conjecture.

X-ray crystallographic studies indicate that alvocidib is situated in the CDK9 cleft occurring between the small and large lobes within the ATP-binding site beneath the G-rich loop that occurs between the small lobe β1- and β2-strands (Fig. 10A). The ketone group of the flavonoid hydrogen bonds with the N—H group of C106 and the 3-hydroxy group of the piperidine segment forms a hydrogen bond with the carboxylate group of the DFG-D167. Alvocidib makes hydrophobic contacts with I25 before the G-rich loop, the C-spine (CS7) V33, CS8 A46, the aliphatic arm of K48, Sh1 V79 of the αC-β4 loop, F105 of the hinge, A153 and N154 of the catalytic loop, and CS6 L156 (not shown). The drug occupies the front pocket and FP-I as described by van Linden et al. [166]. Because alvocidib binds to the active conformation (DFG-D in, αC-helix inward, open activation segment, and linear R-spine), the drug is classified as a type I inhibitor [145].

7.1.2. UCN-01 or 7-Hydroxystaurosporine

UCN-01 is a bis-indole derivative (Fig. 9B) that is given intravenously and targets CDK2 (IC_{50} value of 30 nM). The drug also inhibits Chk1 (IC_{50} value of 10 nM), Chk2 (10 nM), PKA (42 nM), and PKC (62 nM) (www.ebi.ac.uk/chembl/compound/inspect/). There are no apparent data on its inhibitory power on other members of the CDK family, but the drug inhibits the growth of numerous cancer cell lines with IC_{50} values less than 20 nM. The parent staurosporine binds to dozens of protein kinases (it has low selectivity) with high affinity [167]. In combination with irinotecan, a DNA topoisomerase I inhibitor, UCN-01 has antitumor effects as demonstrated in patients with resistant solid tumor malignancies [168]. When combined with DNA-damaging agents, UCN-01 is capable of overriding S- and G2-checkpoints. This is thought to be due to the ability of UCN-01 to inhibit the Chk1 protein kinase, critical for the regulation of the S- and G2-checkpoints. In such cells lacking S- and G2-checkpoints as a result of Chk1 inhibition, cancer cells lacking p53 undergo mitotic catastrophe and eventually apoptosis.

UCN-01 has been studied in patients with advanced solid tumors as well as breast, pancreatic, and small cell lung cancers (ClinicalTrials.gov). Studies have also been performed on patients with acute myelogenous leukemia, chronic lymphoblastic leukemia, and T-cell lymphomas. Moreover, Kortmansky et al. conducted a phase I trial consisting of a combination of UNC-01 and 5-fluorouracil – an inhibitor of thymidylate synthase and DNA synthesis – for patients with advanced colon carcinomas and other tumors [169]. In this trial 5-fluorouracil was given weekly during a 24-hour infusion; UCN-01 was given once every four weeks immediately after the 5-fluoruracil infusion was completed. They found that this regimen prevented disease progression in a quarter (8/32) of the patients with a duration of 3–7 months. Hotte et al. performed a phase I clinical trial using the topoisomerase inhibitor topotecan and UCN-01 in patients with advanced solid malignancies [170]. They found that

Table 6
Selected CDK inhibitors in clinical trials.

Name, code	Drug targets	Diseases; comments[a]	Sponsor	CDK inhibitor class[b]
First generation				
Alvocidib, HMR-1275 or flavopiridol	CDK9/1/2/4/6	Advanced solid tumors, ALL, AML, CLL, CML, mantle cell lymphoma, multiple myeloma, non-Hodgkin and other lymphomas, advanced sarcomas, breast, esophageal, head and neck, kidney, ovarian, pancreatic, gastric carcinomas, NSCLC	Tolero Pharmaceuticals, NCI	I
UCN-01, 7-Hydroxystaurosporine	CDK2 and most likely other CDKs	Advanced solid tumors, ALL, AML, CLL, T-cell and other lymphomas, breast, kidney, ovarian, pancreatic, small cell lung cancers, melanoma, myelodysplastic syndrome	NCI	I
Seliciclib, roscovitine or CYC202	CDK1/2/5/7/9	Advanced solid tumors, breast, hepatocellular, nasopharyngeal carcinomas, NSCLC	Cyclacel	I/I½B
Second generation				
Abemaciclib, LY2835219	CDK4/6	Advanced solid tumors, HR^+-$HER2^-$ breast cancer, NSCLC, mantle cell lymphoma, melanoma	Eli Lilly and Co.	Unknown
AT7519	CDK1/2/4/6/7/9	Advanced solid tumors, CLL, mantle cell lymphoma, multiple myeloma, non-Hodgkin lymphomas, colorectal, pancreatic carcinomas, NSCLC	NCI-Canada clinical trials group	I½B
BMS-387032, SNS-032	CDK2/7/9	CLL, multiple myeloma, advanced and refractory solid malignancies; additional clinical trials unlikely	Sunesis Pharmaceuticals	I½B
Dinaciclib	CDK1/2/5/9	ALL, AML, CLL, mantle cell lymphoma, multiple myeloma, melanoma, NSCLC, breast and pancreatic cancers	NCI	I½B
Ribociclib, Lee011	Cdk4/6	Advanced solid malignancies, breast, endometrial, ovarian, and prostate carcinomas, glioblastoma, liposarcoma, lymphomas, melanoma, NSCLC, myelofibrosis	Novartis	Unknown
Riviciclib, P276-00	CDK9/4/1	Head and neck cancers, melanoma, mantle cell lymphoma, multiple myeloma, pancreatic carcinomas	Piramal Enterprises Ltd.	Unknown
Palbociclib, PD0332991	CDK4/6	ALL, colon, hepatocellular, ovarian, and prostate carcinomas, glioma, melanoma, mantle cell lymphoma, multiple myeloma, neuroblastoma; the FDA approved palbociclib with letrozole for the first line treatment of ER^+-$HER2^-$ breast cancer and palbociclib with fulvestrant for the second-line treatment of this cancer	Pfizer Inc.	I

[a] ALL: acute lymphoblastic leukemia; AML: acute myelogenous leukemia; CLL: chronic lymphocytic leukemia, CML: chronic myelogenous leukemia; ER^+: estrogen receptor positive; $HER2^-$: human epidermal growth factor receptor-2 negative; HR^+: hormone receptor positive; NSCLC: non-small cell lung cancer.
[b] See Ref. [145].

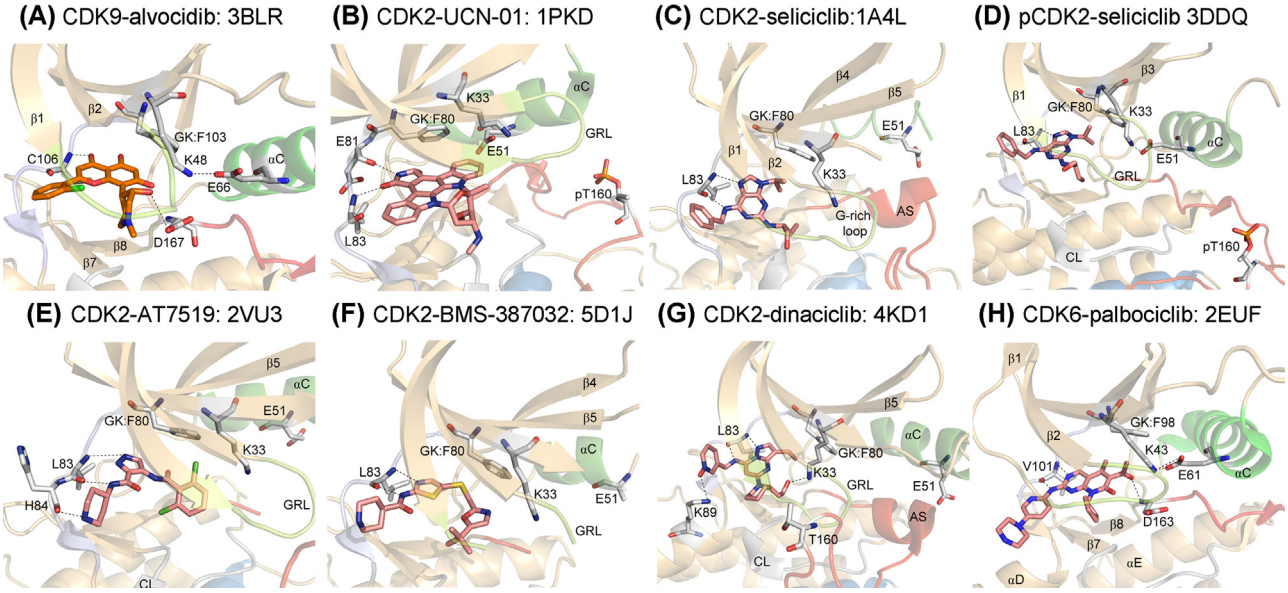

Fig. 10. The protein kinase and corresponding PDB ID of the drug-enzyme complexes are given. The drug carbon atoms are orange and those of the enzyme are gray. The dashed lines represent polar bonds.

this combination produced stable disease with a median duration of four months. Side effects included fatigue, constipation, nausea, hyperglycemia, vomiting, hypotension, anorexia, and headaches, but these were reported to be well tolerated. Fracasso et al. reported similar results in a phase I trial in patients with advanced solid tumors using a combination of irinotecan and UCN-01 [168]. Gojo et al. performed a phase I study on 13 patients with acute myelogenous leukemia or acute lymphoblastic leukemia using UCN-01 in

combination with perifosine (an orally available alkylphospholipid) [171]. This combination of drugs inhibits the PKB/Akt protein kinase *in vitro*. Although they reported that this combination can be safely administered, it was clinically ineffective using their dosing regimen, perhaps owing to a failure to inhibit PKB/Akt activity *in vivo*. Clearly more work is required to establish appropriate combination drug regimens targeting specific illnesses before the clinical effectiveness of UCN-01 can be determined.

UCN-01 binds within the ATP-binding site of the active phosphorylated form of CDK2. The N—H group of the drug forms a hydrogen bond with the carbonyl group of E81 and the 5-oxo group forms a hydrogen bond with the N—H group of L83, both hinge residues (Fig. 10B). UCN-01 makes hydrophobic contacts with I10 before the G-rich loop, C-spine (CS7) V18, CS8 A31, the aliphatic portion of the β3-strand K33, shell residue V64 (Sh1) in the αC-β4 back loop, the gatekeeper F80, and the aliphatic portion of DFG-D146. The drug occupies the front pocket of CDK2 [166]. Because UCN-01 binds to the active conformation of CDK2 (DFG-D in, αC-helix inward, open activation segment, and linear R-spine), the drug is classified as a type I inhibitor [145]. The binding of UCN-01 to the active conformation of CDK2 is nearly identical to the binding of staurosporine to the CDK2 inactive conformation (PDB ID: 4ERW). Consequently, it is difficult to assign a specific role to the 7-hydroxyl group (a modification that converts staurosporine to UCN-01) that increases protein kinase selectivity.

7.1.3. Seliciclib or roscovitine

Seliciclib is an orally effective tri-substituted purine (Fig. 9C) that targets CDK1/2/5 with rather high IC_{50} values ranging from 100 to 200 nM (http://klifs.vu-compmedchem.nl/); the drug most likely inhibits CDK7/9 as described next. Whittaker et al. reported that treatment of human HT29 and KM12 colon carcinoma cell lines with seliciclib decreased retinoblastoma protein (Rb) phosphorylation and total Rb and cyclin D1 protein levels [172]. Seliciclib produced a reduction of cells in G1 while it produced an increase in cells in the G2-M phase. These investigators observed that seliciclib reduced cyclin D1, A, and B1 mRNAs. This was accompanied by a loss of RNA polymerase II phosphorylation and total RNA polymerase II protein, suggesting that seliciclib was inhibiting transcription, possibly via inhibition of CDK7 and CDK9 complexes. Seliciclib has the potential to inhibit CDK4/6 and CDK1/2 activities in cancer cells through the down-regulation of cyclins D, A, and B. This provides a possible mechanism by which seliciclib can cause a reduction in Rb phosphorylation and cell cycle arrest in the G2-M phase.

Hsieh et al. reported that monotherapy with seliciclib in patients with undifferentiated nasopharyngeal carcinomas was effective in reducing cervical lymph node size in half of the patients (7/14) [173]. Furthermore, all 14 patients had stable disease. Analysis of pre- and post-treatment tissue samples showed a reduction in cyclin D1 expression. Tolerable side effects included nausea and vomiting and elevation of alanine aminotransferase (most likely related to liver cell toxicity). These investigators also examined the RNA expression profile and found that seliciclib decreased the transcription of 136 genes in post-treatment samples; many of these genes are important for tumor growth and cell survival. Le Tourneau et al. summarized the results of a phase I clinical trial involving 56 patients with advanced solid malignancies that received oral seliciclib [174]. Six patients had stable disease lasting more than four months and one partial response was observed in a patient with hepatocellular carcinoma. Chief side effects included weakness, nausea and vomiting, elevation of liver enzymes, hypokalemia, and skin rash. The patients could not tolerate daily administration and various interrupted dosing schedules were used, e.g., 1600 mg twice daily for three days every two weeks.

Seliciclib binds within the ATP-binding site of inactive CDK2; the αC-E51 and β3-K33 are not in contact, the activation segment is in its closed conformation bearing an additional AS helix, and the R-spine is non-linear with RS3 displaced. N7 of the purine base forms a hydrogen bond with the N—H group of L83 in the hinge and the N—H group linked to *C*3 of the purine base forms a hydrogen bond with the carbonyl group of L83 (Fig. 10C). Seliciclib makes hydrophobic contacts with I10 before the G-rich loop, CS7 V18, CS8 A31, the aliphatic portion of the β3-stand K33, the F80 gatekeeper (Sh2), F82 of the hinge, N132 of the catalytic loop, CS6 L134, and A144 just before the DFG-D145 sequence. Seliciclib also binds within the ATP-binding site of active pCDK2 (the αC-E51 and β3-K33 form a salt bridge, the activation segment is in its open conformation bearing pT160, and the R-spine is linear). The drug forms the same hydrogen bonds in the active and inactive enzyme conformations and it makes the same hydrophobic contacts with the exception of K33 and A144, lacking in the active enzyme (Fig. 10D). Seliciclib occupies the front pocket in each case [166]. The drug is a class I inhibitor (binding to the active conformation of CDK2) and I ½ inhibitor (binding to an inactive DFG-D in conformation) [145]. Because seliciclib must be given intermittently owing to its toxicity and in the absence of significant antitumor responses, it appears unlikely that it will gain FDA approval unless a better drug regimen can be developed.

7.2. Second-generation drugs

7.2.1. Abemaciclib or LY2835219

Abemaciclib is a 2-anilino-2,4-pyrimidine-[5-benzimidazole] derivative (Fig. 9D) that selectively inhibits CDK4-cyclin D1 (IC_{50} value of 2 nM) and CDK6-cyclin D1 (10 nM); its IC_{50} values for CDK1-cyclin B1, CDK2-cyclin E, and CDK7-cyclin H exceed 1000 nM [175]. As noted above, transition through the G1-S restriction point is controlled by the Rb pathway (CDK4/6-cyclin D-Rb-p16/INK4A). Gelbert et al. reported that low nanomolar concentrations of abemaciclib inhibited Rb phosphorylation in a variety of tumor cell lines including human colon carcinoma colo-205 and myelomonocytic leukemia MV-4-11 cells resulting in G1 arrest [175]. The drug inhibited the expression of Rb/E2F-regulated dihydrofolate reductase and ribonucleoside diphosphate reductase large and small subunits (RRM1/RRM2) in colo-205 cells. Low concentrations of the drug also induced arrest in Rb-proficient MDA-MB-231 breast cancer cells, but failed to produce G1 arrest in Rb-deficient MDA-MB-468 breast cancer cells at concentrations up to 2500 nM. Oral administration of abemaciclib also inhibited the growth of colo-205, MV-4-11, U87 MG glioblastoma, H460 lung, and Jeko-1 mantle cell lymphoma human xenografts in mice.

The effectiveness of oral abemaciclib monotherapy is under study in patients with HR^+-$HER2^-$ breast cancer, advanced breast cancers, NSCLC, and mantle cell lymphoma, and advanced solid tumors (ClinicalTrials.gov). Abemaciclib is also under study in combination with necitumumab (a monoclonal antibody directed toward EGFR/ErbB1/HER1) for NSCLC and with fulvestrant (an estrogen receptor antagonist) for HR^+-$HER2^-$ breast cancer. Another trial is studying the combination of abemaciclib with tamoxifen (an estrogen-receptor modulator), or one of three aromatase antagonists (letrozole, anastrozole, or exemestane), or exemestane with everolimus (an mTOR inhibitor) in patients with HR^+-breast cancer. Note that aromatase antagonists block the conversion of the A ring of steroids to an aromatic moiety as is found in estradiol. Further studies are addressing the efficacy of anastrozole or letrozole in combination with abemaciclib or placebo in postmenopausal women with HR^+-$HER2^-$ breast cancer as first-line therapy, i.e., an initial therapy after diagnosis. These clinical studies indicate that abemaciclib can be administered continuously without interruption [176]. In a phase I trial of 47 patients

with metastatic breast cancer with disease progression, abemaciclib produced clinical benefit in 23 and partial responses in nine. The benefits were greater in those patients with HR^+ disease (22/36 experienced clinical benefit and 9/36 achieved a partial response). The addition of fulvestrant increased the clinical benefit in 13 of 18 patients. Side effects included diarrhea, nausea, vomiting, anorexia, and fatigue. Neutropenia was also a common side effect, which was generally not severe and rarely led to infection and fever. Unfortunately, the X-ray crystal structure of this promising drug with CDK4 or 6 has not been reported.

7.2.2. AT7519

AT7519 is a dichlorobenzoyl-pyrazole derivative (Fig. 9E) that inhibits CDK9-cyclin T (IC_{50} value less than 10 nM), CDK5-p35 (13 nM), and CDK2-cyclin A (47 nM) [177]. It is a less potent inhibitor of CDK3-cyclin E (360 nM), CDK4-cyclin D1 (100 nM), CDK6-cyclin D3 (170 nM), and CDK7-cyclin H (2400 nM). Santo et al. reported that 500 nM AT7519, which is a high concentration, inhibited RNA polymerase II phosphorylation and RNA synthesis in multiple myeloma cells in culture. The drug decreased RNA pol II C-terminal domain phosphorylation at Ser2 and Ser5 within one hour. AT7519 decreased cyclin D1, cyclin A, and cyclin B1 protein levels within two hours. These cells showed an increase in cells in G0-G1 and G2-M phase as early as six hours while drug-induced apoptosis was evident by 12 h. AT7519 also decreased multiple myeloma cell growth in mouse xenografts.

AT7519 has been studied in clinical trials in patients with multiple myeloma, non-Hodgkin lymphomas, mantle cell lymphoma, and chronic lymphoblastic leukemia (ClinicalTrials.gov). In a phase I clinical trial, Mahadevan et al. administered the drug by intravenous infusion for one hour daily for five days, which was repeated every three weeks, to 28 patients with refractory solid tumors including colorectal cancer (6 patients), NSCLC (5), and pancreatic cancer (4) [178]. Four patients exhibited stable disease lasting more than six months and one had a prolonged partial response. Dose-limiting toxicities included fatigue and electrocardiographic prolongation of the corrected QT interval. Nausea, vomiting, anorexia, constipation, peripheral edema, pyrexia, and hypotension occurred in 25–50% of the patients. In another phase I clinical trial, Chen et al. administered AT7519 as a one-hour intravenous infusion on days 1, 4, 8, and 11 every three weeks to 34 patients with a variety of advanced solid malignancies or non-Hodgkin lymphomas [179]. Ten patients had stable disease as the best response with a median duration of 3.3 months. No complete or partial responses were observed. The most common adverse events included fatigue (53%), mucositis (53%), vomiting (34%) and nausea (32%); however, these were generally of low grade and easily manageable. Anemia and lymphopenia were the most common hematological toxicities and the drug regimen was such that no patients exhibited prolongation of the corrected QT interval.

AT7519 binds within the ATP-binding pocket of inactive CDK2 (the αC-E51 and β3-K33 are not in contact, the activation segment is in its closed conformation, and RS 3/4 is displaced upward). The pyrazole *N*2 group of the drug forms a hydrogen bond with the N—H group of the hinge L83 and the 5-carboxamide N—H group forms a hydrogen bond with the carbonyl oxygen of the same residue; the piperidinyl N—H forms a hydrogen bond with the carbonyl group of H84 (Fig. 10E). The 2,6-dichlorophenyl group of AT7519 makes hydrophobic contacts with CS7 V18, the aliphatic chain of the β3-strand K33, the gatekeeper F80, N132 of the catalytic loop, CS6 L134, A144 before the activation segment, and DFG-D145. Additional hydrophobic contacts include I10 before the G-rich loop, CS8 A31, Sh1 V64 in the αC-β4 back loop, and F82 of the hinge. AT7519 binds to the front pocket of CDK2 [166]. The drug is a type I½ inhibitor (binding to an inactive DFG-D in conformation) [145]. It is unlikely that AT7519 will gain FDA approval unless better clinical outcomes are observed.

7.2.3. BMS-387032 or SNS-032

BMS-387032 is a thiazole-oxazole derivative (Fig. 9F) that inhibits CDK2 (K_i value of 40 nM), CDK5 (50 nM), CDK7 (125 nM), and CDK9 (10 nM) (klifs.vu-compmedchem.nl/). It is a weaker inhibitor of CDK1 (500 nM) and CDK4 (1000 nM). During the development of BMS-387032, Misra et al. found that it was ineffective in inhibiting PKC, Chk1, Lck, FAK, or EGFR1/2, with IC_{50} values greater than 25 μM [180]. These investigators found that BMS-387032 was effective in inhibiting tumor formation in P388 murine leukemias and following subcutaneous injection of A2780 human ovarian carcinoma cells into mice [180].

Heath et al. performed a phase I clinical trial with BMS-387032 in patients with refractory metastatic solid tumors [181]. They administered the drug intravenously over a one-hour period three times weekly. Of 21 patients, three experienced a best response of stable disease. Fatigue and nausea were the most common side effects. They found that oral bioavailability ranged from 4 to 33%. In another clinical trial, Tong et al. administered BMS-387032 by a six-hour weekly infusion for three weeks out of each four-week course to 19 patients with chronic lymphoblastic leukemia and 18 patients with multiple myeloma [182]. These investigators reported that one patient with chronic lymphoblastic leukemia experienced a short-lived decrease in measurable disease and another had stable disease of four months duration. One patient with multiple myeloma had stable disease for three months and the splenomegaly of another patient normalized. Tumor lysis syndrome was the dose-limiting toxicity in patients with chronic lymphoblastic leukemia while patients with chronic lymphoblastic leukemia or multiple myeloma experienced myelosupression (neutropenia, thrombocytopenia, and anemia). Tong et al. reported that adverse gastrointestinal events included nausea, vomiting, diarrhea, and constipation [182]. Note that these first three adverse events commonly occur during the treatment with many anticancer agents.

X-ray crystallographic studies show that BMS-387032 binds within the ATP-binding site of inactive CDK2 (Fig. 10F). The *N*3 nitrogen of the oxazole component forms a hydrogen bond with the N—H group of L83 of the hinge while the carboxamide N—H group forms a hydrogen bond with the carbonyl group of L83. BMS-387032 makes hydrophobic contacts with I10 before the G-rich loop, CS7 V16, CS8 A31, the F80 gatekeeper, the aliphatic component of hinge residues Q85 and D86, CS6 L134, and A144, and DFG-D145. BMS-387032 occupies the front pocket [166] of an inactive enzyme conformation and is thus a type I ½ inhibitor [145]. Whether the drug will achieve clinical status is unclear.

7.2.4. Dinaciclib

Dinaciclib is a pyrazolopyrimidine derivative (Fig. 9G) that inhibits CDK1 (IC_{50} value of 3 nM), CDK2 (1 nM), CDK5 (1 nM), and CDK9 (1 nM) [183]. The drug was initially developed as a CDK2 antagonist [184]. Parry et al. reported that 100 nM of dinaciclib inhibited Ser807 and Ser809 phosphorylation of Rb in human ovarian A2780 cancer cells in culture during a two-hour exposure, which is consistent with CDK4/6 inhibition [183]. This suppression of phosphorylation correlated with the onset of apoptosis. Diminished phosphorylation was observed four hours after the drug was removed. Additional experiments showed that short exposures could produce effects lasting up to 24 h suggesting that continuous exposure may not be required for sustained activity *in vivo*. These investigators determined the effectiveness of dinaciclib in inducing apoptosis in 47 diverse tumor cell lines and found that the IC_{50} values ranged from 6 to 17 nM. Moreover, Parry et al. found that

dinaciclib was effective in blocking the growth of subcutaneously injected human ovarian A2780 carcinoma cells in mice [183].

The effectiveness of oral dinaciclib monotherapy is under study in patients with acute lymphoblastic leukemia, acute myelogenous leukemia, chronic lymphoblastic leukemia, mantle cell lymphoma, multiple myeloma, melanoma, breast and lung cancers (Table 6). The combination of dinaciclib with other drugs is also under study including the addition of the PKB/Akt inhibitor MK2206 for pancreatic cancer, the PARP inhibitor veliparib for advanced solid malignancies, the proteosome inhibitor bortezomib and dexamethasone for relapsed multiple myeloma, the DNA-targeted epirubicin for metastatic triple-negative breast cancer (ER^-, PR^-, $HER2^-$), the CD20-directed antibody of ofatumumab for relapsed or refractory chronic lymphoblastic leukemia or small lymphocytic lymphoma, and the CD20-directed antibody rituximab for chronic lymphoblastic leukemia and small lymphocytic lymphoma. CD20 is a glycosylated membrane protein that participates in B-cell activation and proliferation.

In a phase I clinical trial, Nemunaitis et al. administered dinaciclib during a two-hour infusion on days 1, 8, and 15 of a 28-day cycle to 48 patients with advanced solid tumors [185]. They reported that 10 subjects achieved stable disease for at least four months. The most common adverse effects were anorexia, anemia, fatigue, and nausea. In a phase II clinical trial, Stephenson et al. reported that intravenous dinaciclib monotherapy was ineffective in the treatment of NSCLC [186]. They reported that common severe (grade 3 or 4) drug-related adverse effects included neutropenia, leukopenia, vomiting, and diarrhea. In another phase II trial, Mita et al. reported that dinaciclib produced antitumor activity in 2 of 7 patients with ER^+-$HER2^-$ metastatic breast cancer [187]. They found that grade 3 or 4 treatment-related adverse events were common and included neutropenia, leukopenia, increased serum aspartate aminotransferase (an indicator of liver toxicity), and febrile neutropenia. They concluded that although dinaciclib monotherapy demonstrated some antitumor activity and was generally well tolerated, efficacy was not superior to capecitabine, a precursor of cytotoxic 5-fluorouracil.

In a phase I/II clinical trial in patients with relapsed and refractory chronic lymphoblastic leukemia, Flynn et al. reported that 28 of 52 patients responded to therapy [188]. Dinaciclib was given by infusion on days 1, 8, and 15 of a 28-day cycle. Common toxicities included anemia, neutropenia, thrombocytopenia, diarrhea, fatigue, and nausea. Three patients experienced tumor lysis syndrome. These authors concluded that dinaciclib is better tolerated than alvocidib (flavopiridol), justifying its further development. Mitri et al. performed a phase I study with dinaciclib in combination with epirubicin (an anthracene derivative that intercalates with DNA and triggers cleavage by DNA topoisomerase II) for the treatment of triple-negative breast cancer [189]. No treatment responses were noted, median time to progression was 5.5 weeks (range 3–12 weeks), and the study was terminated owing to toxicity of the drug combination regimen.

Dinaciclib binds within the ATP-binding pocket of inactive CDK2 (Fig. 10G). A nitrogen from the pyrazole ring forms a hydrogen bond with the N—H group of the hinge L83 and the amino group of the drug hydrogen bonds with the carbonyl group of L83. The oxide forms a salt bridge with the ε-amino group of K89 while the 2-hydroxyl group hydrogen bonds with the ε-amino group of the β3-strand K33. Dinaciclib makes hydrophobic contacts with I10 before the G-rich loop, CS7 V18, CS8 A31, the aliphatic portion of K33, Sh1 V64, the gatekeeper F80, F82 and ^{84}HQD^{86} of the hinge, Q131 in the catalytic loop, CS6 L134, and A144. Dinaciclib occupies the front pocket [166] of an inactive enzyme conformation and is thus a type I ½ inhibitor [145]. The results of numerous clinical trials that are planned or underway will determine whether dinaciclib will enter the clinic as an approved drug.

7.2.5. Ribociclib

The scaffold of ribociclib consists of a pyrrolo[2,3*d*]pyrimidine core (Fig. 9H); this orally effective drug inhibits CDK4 (IC_{50} value 10 nM) and CDK6 (39 nM) [190]. The inhibitor potency against CDK1 and CDK2 is much less (>50 μM). Rader et al. reported that ribociclib significantly reduced proliferation in 12 of 17 human neuroblastoma-derived cell lines by inducing cytostasis at nanomolar concentrations (mean IC_{50} of 307 nM in sensitive lines) [191]. The drug produced cell-cycle arrest and cellular senescence that these investigators attributed to dose-dependent decreases in phosphorylated Rb and FOXM1, respectively. FOXM1 (forkhead box protein M1) is a transcription factor that plays a key role in cell cycle transit. Additionally, these investigators found that subcutaneous neuroblast xenograft growth delay produced by ribociclib *in vivo* was directly correlated with its IC_{50} values *in vitro*.

The effectiveness of oral ribociclib monotherapy is being investigated in subjects with breast cancer, glioblastoma, and liposarcoma (ClinicalTrials.gov). The combination of ribociclib with other drugs is also under study. Examples include ribociclib with letrozole for treatment of postmenopausal women with HR^+-$HER2^-$ advanced breast cancer or with relapsed ER^+-ovarian, fallopian tube, primary peritoneal or endometrial cancer or with fulvestrant and BLY719 or BKM120 (PI3-kinase antagonists) in patients with advanced breast cancer. Other combinations involve ribociclib and HDM201 (an E3 ubiquitin-protein ligase inhibitor) in patients with liposarcoma, ribociclib and MEK162 (a MEK antagonist) in patients with *NRAS* mutant melanoma, ribociclib and ceritinib (an ALK inhibitor) in patients with ALK^+-NSCLC. Other studies underway include ribociclib with buparlisib (a PI3-kinase antagonist) and letrozole (an aromatase inhibitor) in HR^+-$HER2^-$ post-menopausal women with advanced breast cancer and ribociclib and everolimus (an mTOR antagonist) plus exemestane (an aromatase inhibitor) in the treatment of HR^+-$HER2^-$ advanced breast cancer. Additional clinical trials are examining the efficacy of ribociclib and encorafenib (a B-Raf antagonist) in patients with *BRAF* mutant melanoma, ribociclib and ruxolitinib (a Janus kinase inhibitor) in patients with myelofibrosis, and ribociclib, encorafenib, and MEK162 in advanced *BRAF* mutant melanoma. Other potential therapies include ribociclib and tamoxifen (an estrogen-receptor modulator) in advanced ER^+-$HER2^-$ breast cancer, ribociclib and paclitaxel (a blocker of microtubule dynamics) in patients with Rb^+-advanced breast cancer, and ribociclib and trastuzumab (a monoclonal antibody directed toward EGFR2/HER2) or T-DM1 (trastuzumab conjugated with the tubulin inhibitor DM1) for advanced/metastatic $HER2^+$ breast cancer. Further clinical trials are underway to test the therapeutic efficacy of the combination of ribociclib with gemcitabine (an inhibitor of DNA repair) in patients with advanced solid malignancies or lymphoma, with docetaxel (a blocker of microtubule dynamics during mitosis) and prednisone in metastatic castration resistant prostate cancer, and with enzalutamide (an androgen-receptor antagonist) with or without ribociclib for metastatic, castrate-resistant, chemotherapy-naive prostate cancer that retains Rb expression.

In a phase I clinical trial, 70 subjects with advanced lymphomas or solid malignancies were treated with oral ribociclib [176]. Vidula and Rugo reported that 10 of 70 patients had stable disease and a partial response was observed in one patient with HR^+-breast cancer [176]. The chief toxicities were myelosuppression, diarrhea, nausea, and asymptomatic corrected electrocardiographic QT prolongation. In a phase II trial involving five patients with HR^+-$HER2^-$ breast cancer receiving ribociclib, exemestane, and everolimus, these investigators reported that this drug combination regimen was well tolerated with mild to moderate bone

marrow toxicity. In another phase II trial with HR^+-$HER2^-$ breast cancer patients receiving various combinations of ribociclib, letrozole, and BLY719 (a PI3-kinase antagonist), the most common adverse events included neutropenia, nausea, hyperglycemia, diarrhea, and anorexia [176]. Preliminary results suggest that letrozole and ribociclib are effective in the treatment of this illness. Unfortunately, the X-ray crystal structure of this promising drug with CDK4 or 6 has not been reported.

7.2.6. Riviciclib

Riviciclib is a flavonoid derivative with a 5,7-dihydroxychromen-4-one core (Fig. 9I) that inhibits CDK9-cyclin T1 (IC_{50} value of 20 nM), CDK4-cyclin D1 (63 nM), and CDK1-cyclin B (79 nM). The drug also inhibits CDK2-cyclin A (224 nM), CDK2-cyclin E (2500 nM), CDK6-cyclin D3 (396 nM), and CDK9-cyclin H (2900 nM) [192]. Joshi et al. reported that riviciclib is a steady-state competitive inhibitor with respect to ATP indicating that the drug binds within the ATP-binding pocket [192]. They found that the compound is selective with respect to the CDKs and its inhibitory potency against PKA, PKC, Src, MAPK1, and MAPK2 is two or more orders of magnitude greater than that for CDK4. These investigators examined the potency of riviciclib against a panel of 12 tumor cell lines and found that it inhibited DNA synthesis (^{3}H-thymidine incorporation into DNA) with IC_{50} values ranging from 300 to 800 nM. In contrast, the IC_{50} values for normal human lung fibroblast WI-38 cells and MRC-5 cells were 16,500 nM and 11,500 nM, respectively. Following incubation of H-460 human NSCLC or human MCF-7 breast cancer cells in culture with riviciclib, these investigators found reduced CDK4 activity after six hours, which was followed by a subsequent reduction in cellular cyclin D1, CDK4, and Rb levels as determined by Western blot analysis. Decreased Rb phosphorylation was observed after three hours. They demonstrated that loss of CDK4 activity precedes cyclin D1 and CDK4 depletion. Riviciclib also induced apoptosis in human promyelocytic leukemia HL-60 cells as demonstrated by increased caspase-3 activity and DNA fragmentation. They ascribed these effects to CDK4 inhibition, but acknowledged that inhibition of transcription mediated by CDK9-cyclin T1 might also play a role. Inhibition of the latter enzyme affects the transcription of mRNAs with short half lives including proteins encoding growth and apoptosis regulators. In support of the latter hypothesis, Manohar et al. reported that riviciclib causes multiple myeloma cell death in culture by disrupting the balance between cell survival and apoptosis through inhibition of transcription and down regulation of Mcl-1 (a member of the Bcl-2 family that inhibits apoptosis) [193].

In another study, Joshi et al. studied the effects of riviciclib on an asynchronous population of human prostate carcinoma (PC-3) and human promyelocytic leukemia (HL-60) cells [194]. They reported that the drug arrested slow-growing PC-3 cells in G2-M with no significant apoptosis. In contrast, they observed significant apoptosis in fast-growing HL-60 cells. However, synchronized human NSCLC (H-460) cells and human normal lung fibroblast (WI-38) cells showed G1 arrest. Based on the role of CDK4 and CDK1 in cell cycle transit, an inhibitor of these two enzymes would be predicted to produce a G1 or a G2 arrest. Consistent with this expectation, asynchronous population of cells treated with riviciclib arrested the cells in both G1 and G2. Furthermore, cells synchronized in the G0 phase by serum starvation maintained a G1 block in response to drug treatment. Prolonged exposure to the compound resulted in apoptosis in cancer cells, whereas in the normal fibroblast cell line, no apoptosis was seen even after prolong exposure. These investigators suggested that the selective killing effect of riviciclib against cells that are actively proliferating could be exploited in developing this compound as a potential anticancer agent. The authors found that riviciclib inhibited the growth of human colon carcinoma HCT-116 cells and human NSCLC H-460 cells in mouse xenografts.

Cassaday et al. examined the role of intravenous riviciclib in the treatment of 13 patients with relapsed or refractory mantle cell lymphoma [195]. Only two patients experienced stable disease with a duration of about 60 days. Owing to the lack of a positive outcome, these investigators suggested that given the results observed in their study, if evaluation of CDK inhibition in mantle cell lymphoma continues, riviciclib should be used earlier in the course of the disease or as a part of a combination of drugs for relapsed or refractory disease. The X-ray structures of this drug complexed to any of its CDK targets are not available. All clinical trials with P276-00 (riviciclib) are completed; in the absence of any new studies it is unlikely that this drug will meet approval.

7.2.7. Palbociclib (Ibrance®) or PD0332991

Palbociclib is a CDK4/6 antagonist that in combination with the aromatase antagonist letrozole is FDA-approved for the treatment of post-menopausal women with ER^+-$HER2^-$ advanced breast cancer as an initial, or first-line, endocrine-based therapy for metastatic disease (www.brimr.org/PKI/PKIs.htm). The scaffold of palbociclib consists of a pyrido[2,3-*d*]pyrimidinone core (Fig. 9J); this orally effective drug inhibits CDK4-cyclin D1 (IC_{50} value 11 nM), CDK4-cyclin D3 (9 nM), and CDK6-cyclin D2 (15 nM) [196]. It is ineffective against CDK2-cyclin E2, CDK2-cyclin A, CDK1-cyclin B, and CDK5-p25 with IC_{50} values exceeding 10 μM. During the development of this compound, VanderWel et al. found that the addition of a cyclopentyl group at *N*8 of the pyrido[2,3-*d*]pyrimidinone core provided an excellent combination of selectivity and potency for CDK4/6 [197]. Moreover, the inclusion of a methyl group at the *C*5 position decreased CDK1/2 inhibition by these congeners while they remained effective against CDK4/6. Toogood et al. from the same laboratory reported that including a 2-aminopyridine at the *C*2-position of the core increased selectivity for CDK4/6 *in vitro* [198]. Moreover, addition of the acetyl group at *C*6 maintained the selectivity toward CDK4/6.

The only known substrates of CDK4/6 are members of the Rb-like family including p110/Rb, p107/RBL1 and p130/RBL2 [1]. Ser780 and Ser795 are CDK4/6 monophosphorylation sites that can be used to monitor the effectiveness of their inhibition. Fry et al. found that the IC_{50} for the reduction of Ser780 phosphorylation in MDA-MB-435 tumor cells was 66 nM while that for Ser795 was 63 nM [196]. Similar results were found using Colo-205 human colon cancer cells. The reduction in phosphorylation occurred at four hours and reached a maximum at 16 h. This is a reversible process and dephosphorylation of these residues occurred within two hours after drug removal and was complete by 16 h. These investigators found that palbociclib inhibited thymidine incorporation into DNA in Rb^+ human colon and lung carcinoma cells as well as human leukemia cells with IC_{50} values ranging from 40 to 170 nM. The drug was ineffective against Rb^- cells at concentrations as high as 3000 nM. These results are consistent with the notion that palbociclib exerts its effects by inhibiting CDK4/6.

Finn et al. examined the effects of palbociclib in 47 human breast cancer cell lines, alone and in combination with tamoxifen or trastuzumab [199]. They found that ER^+ cell lines were most sensitive to growth inhibition by the drug. They also found that the sensitive cell lines showed G0-G1 arrest and decreased Rb phosphorylation in response to the drug. Also of importance, they found that palbociclib and tamoxifen were synergistic in ER^+ cells lines while palbociclib and trastuzumab were synergistic in HER2-amplified cell lines. Furthermore, Miller et al. identified a role for the unliganded estrogen receptor and the CDK4/6-Rb-E2F pathway that participates in the hormone-independent growth of breast cancer cells in culture [200]. These studies provide a basis for understanding the effectiveness of treating ER^+ breast cancers

with a combination of receptor antagonists or aromatase inhibitors and CDK4/6 inhibitors as described later.

Fry et al. found that 40 nM palbociclib treatment for 24 h increased the percentage of MDA-MG-453 cells in the G1 phase. G1 arrest was still observed at concentrations as high as 10,000 nM suggesting that the drug is not appreciably inhibiting any of the other CDKs [196]. These investigators found that palbociclib produced tumor regression in several mouse xenografts including those of breast, colon, glioblastoma, prostate, and lung. The authors found that Colo-205 tumors reappeared after palbociclib treatment was discontinued. Cells from these tumors were then were re-implanted into mice and after growth to 100–150 mg, the animals were treated with palbociclib. These authors found that the tumors responded with equal sensitivity indicating that no resistance had developed during the initial treatment. This study demonstrated that the drug is cytostatic for cells in culture causing G1 arrest, but it induces apoptosis and tumor regression in animal xenografts. The mechanism for the induction of tumor apoptosis in animals *in vivo* is unclear except to confirm that drug-induced apoptosis is an intricate process. Furthermore, the arrest of cells in G1 in response to CDK4/6 inhibition may antagonize cell killing by agents that are effective in S-phase or during mitosis such as DNA-damaging agents. Consequently, the choice of drug combinations with CDK4/6 antagonists such as palbociclib will have to be made accordingly.

Phosphorylated Rb fails to suppress the transcription of genes controlled by the E2F transcription factors [13]. Fry et al. monitored the expression of four E2F-regulated genes in Colo-205 tumors in mice treated with palbociclib [196] These genes encoded CDK1, cyclin E2, thymidine kinase, and topoisomerase 2A. These investigators observed that all four gene products were down-regulated in a dose-dependent fashion and paralleled the regressive response of the tumor. Moreover, VanderWel et al. found that palbociclib inhibited the growth of MDA-MB-435 tumor xenografts, which were originally thought to be derived from a human breast cancer [197], but are now considered to be derived from a melanoma (www.ATCC.org).

The effectiveness of oral palbociclib monotherapy is under study in patients with liposarcoma, oligodendroglioma, oligoastrocytoma, mantle cell lymphoma, urothelial carcinoma, NSCLC, and numerous primary childhood brain tumors (ClinicalTrials.gov). There are several clinical trials underway examining the effectiveness of palbociclib with a variety of hormone antagonists in breast cancer such as tamoxifen and the aromatase inhibitors. Other combination studies include palbociclib with cetuximab (a monoclonal antibody directed toward EGFR/HER1/ErbB1) for the treatment of head and neck cancers, with AZD2014 (an mTOR inhibitor) for the treatment of ER^+ breast cancer, and with PD-0325901 (a MEK antagonist) for the treatment of NSCLC and other solid malignancies. Additional clinical trials are underway to determine the effectiveness of palbociclib, lenalidomide (an analogue of thalidomide with immunomodulatory, antiangiogenic, and antineoplastic properties), and dexamethasone for multiple myeloma and a combination of palbociclib and ibrutinib for the treatment of mantle cell lymphoma (ibrutinib is an antagonist of Bruton protein-tyrosine kinase approved for the treatment of mantle cell lymphoma).

Finn et al. studied the responses of 84 postmenopausal women with ER^+-$HER2^-$ breast cancer to palbociclib plus letrozole and compared them to a cohort receiving letrozole alone [201]. These investigators reported that median progression-free survival was 10.2 months (range, 5.7–12.6) for the letrozole group and 20.2 months (13.8–27.5) for the palbociclib plus letrozole group. In one cohort (n = 66), median progression-free survival was 5.7 months (range, 2.6–10.5) for the letrozole group and 26.1 months (11.2–not estimable) for the palbociclib plus letrozole group. In another cohort (n = 99), median progression-free survival was 11.1 months (7.1–16.4) for the letrozole group and 18.1 months (13.1–27.5) for the palbociclib plus letrozole group. These authors reported that grade 3–4 neutropenia occurred in 45 (54%) of 83 patients in the palbociclib plus letrozole group versus one (1%) of 77 patients in the letrozole group while leukopenia was observed in 16 (19%) in the combination group versus none in the letrozole group, and fatigue was reported in four (4%) of the combination group versus one (1%) in the letrozole group. Serious adverse events that occurred in more than one patient in the palbociclib plus letrozole group were pulmonary embolism (three, 4% of patients), back pain (two, 2%), and diarrhea (two, 2% of patients). No cases of febrile neutropenia or neutropenia-related infections were reported during the study. They indicated that 11 (13%) patients in the palbociclib plus letrozole group and two (2%) in the letrozole group discontinued the study because of adverse events. These studies prompted FDA approval of the combination of palbociclib with letrozole for the initial treatment of HR^+-$HER2^-$ breast cancer in 2015 (www.brimr.org/PKI/PKIs.htm).

Turner et al. summarized a phase III clinical trial that involved 521 patients with advanced HR^+-$HER2^-$ breast cancer that had relapsed or progressed during prior first-line endocrine therapy [202]. They randomly assigned patients in a 2:1 ratio to receive palbociclib and fulvestrant or placebo and fulvestrant. Fulvestrant is an estrogen-receptor antagonist that leads to the acceleration of proteosomal degradation of the receptor, a drug that is given intramuscularly. The median progression-free survival was 9.2 months with palbociclib–fulvestrant and 3.8 months with placebo–fulvestrant. The most common grade 3 or 4 adverse events in the palbociclib–fulvestrant group were neutropenia (62%, vs. 0.6% in the placebo–fulvestrant group), leukopenia (25% vs. 0.6%), anemia (2.6% vs. 1.7%), thrombocytopenia (2.3% vs. 0%), and fatigue (2.0% vs. 1.2%). Febrile neutropenia was reported in 0.6% of palbociclib-treated patients and 0.6% of placebo-treated patients. The rate of discontinuation due to adverse events was 2.6% with palbociclib and 1.7% with placebo. These results indicated that palbociclib combined with fulvestrant resulted in longer progression-free survival than fulvestrant alone. These results led to the approval of this drug combination as a second-line treatment for HR^+-$HER2^-$ breast cancer following an initial first-line treatment (www.brimr.org/PKI/PKIs.htm).

The X-ray crystal structure of palbociclib bound to the complex of CDK6-cyclin V shows that a hydrogen bond forms between the carbonyl group of V101 of the hinge of the enzyme and the 2-amino group attached to the pyridopyrimidine core (Fig. 10H). Cyclin V or cyclin K is a gene product of Kaposi sarcoma herpes virus that activates CDK6. A second hydrogen bond forms between the *N*3 nitrogen of the core of palbociclib and the N—H group of V101 while a third hydrogen bond forms between the DFG-D163 N—H group and the 6-acetyl carbonyl group. The 5-methyl and 6-acetyl groups occupy hydrophobic pocket BP-I-A in the gate area [145,166] while the *C*2 piperazinylpyridinylamino group faces the solvent. Palbociclib makes numerous hydrophobic contacts with the enzyme including interactions with the β1-strand I19, CS7 V27, the aliphatic arm of β3-K43, Sh1 V77 within the αC-β4 loop, the F98 gatekeeper, Q103 of the hinge, CS6 L152, and A162, which occurs just before DFG-D163 of the activation segment. The *N*8 cyclopentyl group occupies the space where the ribose of ATP binds. The drug binds to an active conformation of the CDK6-cyclin V complex (αC-helix in, open activation segment, linear R-spine) and is thus a type I inhibitor [145]. As noted above, palbociclib is in clinical trials for diseases other than breast cancer and it is possible that its approval for additional clinical indications may be forthcoming as part of a therapeutic regimen.

8. Protein-protein interaction inhibitors

There are three general targets for protein–protein interaction inhibitors in the CDK family [5]. Inhibition can result from the blockade at the activation-segment protein-substrate platform of the enzyme, blockade at the substrate-recruitment site of the cyclin, or blockade at the interface of CDKs with their cognate cyclins. Targeting such interactions with compounds of molecular weight of less than 500 Da is challenging owing to the flat and usually featureless contact areas [203]. The lack of a cavity in flat interaction domains limits the site of contact to only one side of a small molecule and such contacts exhibit lower binding affinities than those involving multiple sites in deeper clefts [204]. Using peptides *per se* is problematic owing to their breakdown as catalyzed by proteases and their inability to traverse cell membranes; as a consequence various derivatives that mimic peptides are employed.

Arkin et al. have reviewed about one dozen small molecule inhibitors of protein–protein interactions that have progressed to clinical trials [205]. They cite examples of drugs that bind to specific primary, secondary, or tertiary protein structures. Specific targets include inhibitors of apoptosis proteins (IAPs), HIV integrase, the Von-Hippel Lindau tumor suppressor protein, the Bcl apoptotic regulatory proteins, the MDM2 ubiquitin E3 ligase responsible for degradation of the p53 tumor suppressor, and the PDK1 phosphoinositide-dependent protein kinase that activates PKB/Akt, an enzyme that participates in cell proliferation and survival. These investigators reported that ABT-199 (venetoclax) binds to Bcl-2 and blocks its inhibitory interactions with the pro-apoptotic proteins BAD and BAK. As a consequence of this blockade, cells undergo apoptosis. Based upon early clinical trials, Arkin et al. indicated that the results of treating CLL patients with oral ABT-199 (MW of 866) are promising. The importance of optimizing ligand efficiency (LE) and lipophilic ligand efficiency (LLE) in improving the drug-like qualities of the protein–protein interaction inhibitors (PPIs) [205] as well as other drugs [206] is a recurring theme in medicinal chemistry.

Mendoza et al. studied an RXL peptide that binds to the substrate-recruitment sites of cyclins (Section 3.3) with the sequence PVKRRLDL and inhibits CDK2-cyclin A activity [207]. They synthesized PEN (RQIKIWFQNRRMKWKK)-PVKRRLDL and PEN-PVKRRLDG peptides where PEN is a 16-amino acid sequence found in the *Drosophila* antennapedia sequence that interacts with the APC (Amino Acid-Polyamine-Organocation) family of transport proteins that contains twelve α-helices that span the plasma membrane and mediate cellular uptake of peptides. They observed that PEN-PVKRRLDL and PEN-PVKRRLDG promoted apoptosis in USO2 cells with wild type p53 (human osteosarcoma), MDA-MB-435 cells with mutant p53 (human myeloma cells) and SVT2 simian virus-transformed mouse cells with inactivated p53 and Rb, but not wild-type early passage mouse embryo fibroblasts. They found that these peptides promoted apoptosis in a concentration-dependent fashion in cells derived from four mammary tumors from MMTV-HER2 transgenic mice. Additionally, they found that PEN-PVKRRLDL injection into and around SVT2 cell xenografts resulted in a dose-dependent inhibition of tumor growth. They also reported that PEN-PVKRRLDG inhibited tumor growth in trastuzumab-resistant HER2 transgenic mice.

Mendoza et al. suggested that inhibition of CDK2-cyclin A phosphorylation of substrates such as E2F indicates that cell killing *in vitro* and inhibition of tumor growth *in vivo* could be driven by E2F-mediated apoptosis [207]. Their observations of RXL peptide-mediated cell killing *in vitro* and *in vivo* occur in both p53 wild-type and mutant backgrounds, suggesting that apoptosis occurs through an E2F-mediated mechanism. Because p53 is mutated in approximately half of all human cancers, this mechanism of targeting tumors has a potential therapeutic advantage. These investigators noted that perturbations of the different components of the CDK4-cyclin D-Rb pathway, which influence E2F deregulation, are consistently affected by RXL peptides both in the cells and xenografts examined. Moreover, their results suggest that design-based peptidomimetics derived from RXL peptides could act as potentially selective antineoplastic agents *in vivo* and provide a strong rationale for intervention at this point in the cell cycle.

Using a different approach, Canela et al. prepared an all D-amino acid hexapeptide (RWIMYF-NH_2, or NBI1) that binds to the substrate-recruitment site of cyclin A [208]. This peptide has an IC_{50} value of 1.1 μM and is a steady-state non-competitive inhibitor with respect to ATP and to peptide substrates that bind to the cyclin substrate-recruitment site (Rb) or that do not bind to this site (histone H1). These investigators suggest that NBI1 causes dissociation of the CDK2-cyclin A complex by binding to a cleft on the surface of cyclin A that is important for complex formation. NBI1 exhibits selectivity for CDK2-cyclin A, but is a weak inhibitor of CDK2-cyclin E. A conjugate of the HIV transactivator of transcription (TAT) with NBI1 (TAT-NBI1) is a cell-permeable derivative that induces apoptosis and inhibits proliferation of HCT116 and HT20 human colon carcinoma cells. Although X-ray crystal structures of NBI1 with CDK2-cyclin A are not available, these investigators provided a surface representation of the hypothetical NBI1-cyclin A binding site near the interface with CDK2. These studies with protein–protein interaction inhibitors serve as a proof of concept for the effectiveness of targeting the substrate-recruitment sites of the CDK-cyclin binary complexes. However, developing drugs based upon this strategy will be problematic.

9. Epilogue

The mechanism of cell cycle progression has been under investigation for about 40 years [209]. In a pioneering study, Hartwell et al. used a genetic approach and isolated and characterized several cell division cycle (CDC) temperature-sensitive mutants of *Saccharomyces cerevisiae* whose gene function was needed at specific stages of the cell cycle [210]. Hartwell's initial collection of cell cycle mutants contained mutations in what we now recognize as key regulators of the eukaryotic cell cycle. These include CDK1 (*CDC28*), cell division control protein-4 (*CDC4*) that facilitates ubiquitylation and thereby destruction of Cdk inhibitory proteins (SIC1, CDC6) and is required at G1-S and G2-M transitions, and components of the anaphase promoting complex or cyclosome (APC/C) involved in promoting cyclin degradation [209]. Nurse also used a genetic approach and isolated temperature-sensitive mutants of *Schizosaccharomyces pompe* that produced cells of half the size of those that divided at the permissive temperature [211]. These small mutants (*wee-1*) were eventually shown to encode a protein kinase (Wee-1) that catalyzed the phosphorylation and inhibition of CDK1 (Table 1) [209].

Evans and Hunt et al. employed a biochemical approach and studied the regulation of mRNA translation in embryos of the sea urchin *Arbacia punctulata* [212]. Protein synthesis in early dividing embryos is programmed by stored maternal mRNAs, which code for a few particularly abundant proteins whose synthesis is barely, if at all, detectable in the unfertilized egg. One of these proteins, which was named cyclin, is destroyed every time that the cells divide. After fertilization cyclin was strongly labeled with [^{35}S]- methionine only to be broken down after mitosis. Moreover, the protein was again labeled during the next cycle only to be destroyed again at the end of the cycle.

Many laboratories participated in the elucidation of the regulation of the cell cycle and it was found that the process was conserved across many eukaryotic species including humans [209]. Because cancer cells exhibit dysregulated cell division along with the forma-

tion of abnormal chromosome numbers (aneuploidy) [213], it has been natural to focus on cell cycle inhibitors as potential anticancer agents [214]. Among the first publications addressing the potential of CDK antagonists as anticancer agents was that by Kaur et al. in 1992 who studied the effects of alvocidib (L86-8275 or flavopiridol) on seven breast and five lung cancer cell lines [215]. However, it was not until 2015 that one CDK6 inhibitor, palbociclib, along with letrozole was approved by the FDA as a first-line treatment for HR^+-$HER2^-$ breast cancer (www.brimr.org/PKI/PKIs.htm). Subsequently, the FDA approved the combination of palbociclib and fulvestrant as a second-line therapy in 2016 in women with disease progression following endocrine therapy. The development of a clinically approved CDK4/6 inhibitor required about two dozen years, which contrasts with the time-line for the development of an ALK antagonist (crizotinib) over four years or EGFR inhibitors (erlotinib and gefitinib) over nine years [206]. As noted in Section 8, palbociclib, abemaciclib, ribociclib, and other CDK antagonists are undergoing clinical trails for a variety of cancers as a single agent or as part of a combination of drugs.

Among the most common toxicities of the CDK antagonists is myelosuppression as indicated by neutropenia (decreased levels of neutrophils, which are important for combating infection), leukopenia (decreased levels of total white blood cells), and anemia. This is an expected side effect of such agents because these cells replicate continuously. Hyperglycemia is also a common side effect. CDK5 is found in the pancreatic β-cells that produce insulin. However, inhibition of CDK5 results in increased insulin secretion and hypoglycemia [216]. Accordingly, the mechanism responsible for producing hyperglycemia is a mystery.

Owing to the prevalence of breast cancer, it is expected that the drug will accrue nearly $5 billion annually [217] with a cost per patient in the United States of $10, 000 per month. This high fee is a major contributor to the financial toxicity of cancer drugs [218]. Owing to the high cost of co-payments in the United States, health insurance does not eliminate this financial worry among cancer patients. As a consequence of financial distress, patients become noncompliant and may take less than the prescribed amount of a medication or none at all [219]. If the patient fails to take the medication, it helps neither the patient nor the drug company. Owing to the work of thousands of investigators worldwide in developing targeted cancer therapies, more must be done to fairly distribute the fruits of this research to any patient worldwide that might benefit from the end result.

The profit margins of large pharmaceutical companies average about 21% (www.forbes.com); this calculation is based on net profit/revenues × 100% where net profit represents revenues minus cost (including research, development, and clinical trials). In contrast, the median profit margin of all large companies in the United States is about 6.5% (www.aei.org). This 300% greater profit margin of drug companies is one component that contributes to the excessive cost of many prescription drugs in the United States. The salaries of lawyers and personnel of contract research organizations that have inserted themselves as necessary brokers between pharmaceutical companies and investigators contribute to the excessive cost of drugs and drug development [218]. The salaries of pharmacy benefit managers and the fees that these profitable companies extract for services rendered are additional factors adding to the overall price of pharmaceutics to the patient. However, some executives in the nonprofit medical sector are altruistic and work voluntarily of for no or low salaries. The author had the privilege of working in the laboratory of Fritz Lipmann, MD/PhD, a 1953 Nobel laureate. Lipmann discovered coenzyme A and was the theoretician who contributed the notion of the high-energy bond to bioenergetics [220]. He was a denizen of a bygone era who said he could not imagine requesting a fee for caring for an ill person who needed medial services. Such practices are idealistic and unimaginable in today's economy and market, but charging lower prices for medicines and lower fees for medical services might decrease the incidence and severity of financial toxicity.

Conflict of interest

The author is unaware of any affiliations, memberships, or financial holdings that might be perceived as affecting the objectivity of this review.

Acknowledgment

The author thanks Laura M. Roskoski for providing editorial and bibliographic assistance.

References

[1] M.D. Malumbres, M. Barbacid, Mammalian cyclin-dependent kinases, Trends Biochem. Sci. 30 (2005) 630–641.
[2] M. Malumbres, M. Barbacid, To cycle or not to cycle: a critical decision in cancer, Nat. Rev. Cancer 1 (2001) 222–231.
[3] M. Malumbres, Cyclin-dependent kinases, Genome Biol. 15 (2014) 122.
[4] G. Manning, D.B. Whyte, R. Martinez, T. Hunter, S. Sudarsanam, The protein kinase complement of the human genome, Science 298 (2002) 1912–1934.
[5] M. Peyressatre, C. Prével, M. Pellerano, M.C. Morris, Targeting cyclin-dependent kinases in human cancers: from small molecules to peptide inhibitors, Cancers (Basel) 7 (2015) 179–237.
[6] C.J. Sherr, Cancer cell cycles, Science 274 (1996) 1672–1677.
[7] T. Arooz, C.H. Yam, W.Y. Siu, A. Lau, K.K. Li, R.Y. Poon, On the concentrations of cyclins and cyclin-dependent kinases in extracts of cultured human cells, Biochemistry 39 (2000) 9494–9501.
[8] K.I. Nakayama, K. Nakayama, Ubiquitin ligases: cell-cycle control and cancer, Nat. Rev. Cancer 6 (2006) 369–381.
[9] S. Lim, P. Kaldis, Cdks, cyclins and CKIs: roles beyond cell cycle regulation, Development 140 (2013) 3079–3093.
[10] F. Bassermann, R. Eichner, M. Pagano, The ubiquitin proteasome system — implications for cell cycle control and the targeted treatment of cancer, Biochim. Biophys. Acta 1843 (2014) 150–162.
[11] W. Kolch, M. Halasz, M. Granovskaya, B.N. Kholodenko, The dynamic control of signal transduction networks in cancer cells, Nat. Rev. Cancer 15 (2015) 515–527.
[12] M. Goldstein, M.B. Kastan, The DNA damage response: implications for tumor responses to radiation and chemotherapy, Annu. Rev. Med. 66 (2015) 129–143.
[13] A.M. Narasimha, M. Kaulich, G.S. Shapiro, Y.J. Choi, P. Sicinski, S.F. Dowdy, Cyclin D activates the Rb tumor suppressor by mono-phosphorylation, Elife (2014) 3.
[14] J.M. Trimarchi, J.A. Lees, Sibling rivalry in the E2F family, Nat. Rev. Mol. Cell Biol. 3 (2002) 11–20.
[15] L. Anders, N. Ke, P. Hydbring, Y.J. Choi, H.R. Widlund, J.M. Chick, et al., A systematic screen for CDK4/6 substrates links FOXM1 phosphorylation to senescence suppression in cancer cells, Cancer Cell 15 (20) (2011) 620–634.
[16] N.G. Starostina, E.T. Kipreos, Multiple degradation pathways regulate versatile CIP/KIP CDK inhibitors, Trends Cell Biol. 22 (2012) 33–41.
[17] K.M. LaPak, C.E. Burd, The molecular balancing act of $p16^{INK4a}$ in cancer and aging, Mol. Cancer Res. 12 (2014) 167–183.
[18] E.T. Cánepa, M.E. Scassa, J.M. Ceruti, M.C. Marazita, A.L. Carcagno, P.F. Sirkin, et al., INK4 proteins, a family of mammalian CDK inhibitors with novel biological functions, IUBMB Life 59 (2007) 419–426.
[19] F. Zindy, W. den Besten, B. Chen, J.E. Rehg, E. Latres, M. Barbacid, et al., Control of spermatogenesis in mice by the cyclin D-dependent kinase inhibitors $p18^{Ink4c}$ and $p19^{Ink4d}$, Mol. Cell. Biol. 21 (2001) 3244–3255.
[20] F. Zindy, J.J. Cunningham, C.J. Sherr, S. Jogal, R.J. Smeyne, M.F. Roussel, Postnatal neuronal proliferation in mice lacking Ink4d and Kip1 inhibitors of cyclin-dependent kinases, Proc. Natl. Acad. Sci. U. S. A. 96 (1999) 13462–13467.
[21] J. Cicenas, K. Kalyan, A. Sorokinas, A. Jatulyte, D. Valiunas, A. Kaupinis, et al., Highlights of the latest advances in research on CDK inhibitors, Cancers (Basel) 6 (2014) 2224–2242.
[22] L. Santo, K.T. Siu, N. Raje, Targeting cyclin-dependent kinases and cell cycle progression in human cancers, Semin. Oncol. 42 (2015) 788–800.
[23] E.A. Musgrove, C.E. Caldon, J. Barraclough, A. Stone, R.L. Sutherland, Cyclin D as a therapeutic target in cancer, Nat. Rev. Cancer 11 (2011) 558–572.
[24] T. Santarius, J. Shipley, D. Brewer, M.R. Stratton, C.S. Cooper, A census of amplified and overexpressed human cancer genes, Nat. Rev. Cancer 10 (2010) 59–64.
[25] M. Schwaederlé, G.A. Daniels, D.E. Piccioni, P.T. Fanta, R.B. Schwab, K.A. Shimabukuro, et al., Cyclin alterations in diverse cancers: outcome and co-amplification network, Oncotarget 6 (2015) 3033–3042.

[26] P.L. Bergsagel, W.M. Kuehl, F. Zhan, J. Sawyer, B. Barlogie, J. Shaughnessy Jr., Cyclin D dysregulation: an early and unifying pathogenic event in multiple myeloma, Blood 106 (2005) 296–303.
[27] K. Ikeda, T. Monden, M. Tsujie, H. Izawa, H. Yamamoto, T. Ohnishi, et al., Cyclin D CDK4 and p16 expression in colorectal cancer, Nihon Rinsho 54 (1996) 1054–1059.
[28] K. Lundgren, M. Brown, S. Pineda, J. Cuzick, J. Salter, L. Zabaglo, et al., Effects of cyclin D1 gene amplification and protein expression on time to recurrence in postmenopausal breast cancer patients treated with anastrozole or tamoxifen: a TransATAC study, Breast Cancer Res. 14 (2012) R57.
[29] J.H. Kim, M.J. Kang, C.U. Park, H.J. Kwak, Y. Hwang, G.Y. Koh, Amplified CDK2 and cdc2 activities in primary colorectal carcinoma, Cancer 85 (1999) 546–553.
[30] J. Seong, E.J. Chung, H. Kim, G.E. Kim, N.K. Kim, S.K. Sohn, et al., Assessment of biomarkers in paired primary and recurrent colorectal adenocarcinomas, Int. J. Radiat. Oncol. Biol. Phys. 45 (1999) 1167–1173.
[31] E.J. Belt, R.P. Brosens, P.M. Delis-van Diemen, H. Bril, M. Tijssen, D.F. van Essen, et al., Cell cycle proteins predict recurrence in stage II and III colon cancer, Ann. Surg. Oncol. 19 (2012) S682–92.
[32] S. Gansauge, F. Gansauge, M. Ramadani, H. Stobbe, B. Rau, N. Harada, et al., Overexpression of cyclin D1 in human pancreatic carcinoma is associated with poor prognosis, Cancer Res. 57 (1997) 1634–1637.
[33] Y. Dobashi, A. Goto, M. Fukayama, A. Abe, A. Ooi, Overexpression of cdk4/cyclin D1, a possible mediator of apoptosis and an indicator of prognosis in human primary lung carcinoma, Int. J. Cancer 110 (2004) 532–541.
[34] R. Li, S.J. An, Z.H. Chen, G.C. Zhang, J.Q. Zhu, Q. Nie, et al., Expression of cyclin D1 splice variants is differentially associated with outcome in non-small cell lung cancer patients, Hum. Pathol. 39 (2008) 1792–1801.
[35] G. Moreno-Bueno, S. Rodríguez-Perales, C. Sánchez-Estévez, R. Marcos, D. Hardisson, J.C. Cigudosa, et al., Molecular alterations associated with cyclin D1 overexpression in endometrial cancer, Int. J. Cancer 110 (2004) 194–200.
[36] J.A. Akervall, R.J. Michalides, H. Mineta, A. Balm, A. Borg, M.R. Dictor, et al., Amplification of cyclin D1 in squamous cell carcinoma of the head and neck and the prognostic value of chromosomal abnormalities and cyclin D1 overexpression, Cancer 79 (1997) 380–389.
[37] R.J. Michalides, N.M. van Veelen, P.M. Kristel, A.A. Hart, B.M. Loftus, F.J. Hilgers, et al., Overexpression of cyclin D1 indicates a poor prognosis in squamous cell carcinoma of the head and neck, Arch. Otolaryngol. Head Neck Surg. 123 (1997) 497–502.
[38] A. Shaye, A. Sahin, Q. Hao, K. Hunt, K. Keyomarsi, I. Bedrosian, Cyclin E deregulation is an early event in the development of breast cancer, Breast Cancer Res. Treat. 115 (2009) 651–659.
[39] A. Wang, N. Yoshimi, M. Suzui, A. Yamauchi, M. Tarao, H. Mori, Different expression patterns of cyclins A, D1 and E in human colorectal cancer, J. Cancer Res. Clin. Oncol. 122 (1996) 122–126.
[40] H. Yue, H.Y. Jiang, Expression of cell cycle regulator $p57^{kip2}$, cyclinE protein and proliferating cell nuclear antigen in human pancreatic cancer: an immunohistochemical study, World J. Gastroenterol. 11 (2005) 5057–5060.
[41] N. Nakayama, K. Nakayama, Y. Shamima, M. Ishikawa, A. Katagiri, K. Iida, et al., Gene amplification *CCNE1* is related to poor survival and potential therapeutic target in ovarian cancer, Cancer 116 (2010) 2621–2634.
[42] A.M. Karst, P.M. Jones, N. Vena, A.H. Ligon, J.F. Liu, M.S. Hirsch, et al., Cyclin E1 deregulation occurs early in secretory cell transformation to promote formation of fallopian tube-derived high-grade serous ovarian cancers, Cancer Res. 74 (2014) 1141–1152.
[43] E. Kuhn, A. Bahadirli-Talbott, Ie-M. Shih, Frequent *CCNE1* amplification in endometrial intraepithelial carcinoma and uterine serous carcinoma, Mod. Pathol. 27 (2014) 1014–1019.
[44] D. Wołowiec, M. Benchaib, P. Pernas, P. Deviller, C. Souchier, R. Rimokh, et al., Expression of cell cycle regulatory proteins in chronic lymphocytic leukemias: comparison with non-Hodgkin's lymphomas and non-neoplastic lymphoid tissue, Leukemia 9 (1995) 1382–1388.
[45] M. Erlanson, C. Portin, B. Linderholm, J. Lindh, G. Roos, G. Landberg, Expression of cyclin E and the cyclin-dependent kinase inhibitor p27 in malignant lymphomas-prognostic implications, Blood 92 (1998) 770–777.
[46] M. Furihata, T. Ishikawa, A. Inoue, C. Yoshikawa, H. Sonobe, Y. Ohtsuki, et al., Determination of the prognostic significance of unscheduled cyclin A overexpression in patients with esophageal squamous cell carcinoma, Clin. Cancer Res. 2 (1996) 1781–1785.
[47] Y. Chao, Y.L. Shih, J.H. Chiu, G.Y. Chau, W.Y. Lui, W.K. Yang, et al., Overexpression of cyclin A but not Skp 2 correlates with the tumor relapse of human hepatocellular carcinoma, Cancer Res. 58 (1998) 985–990.
[48] A. Nar, O. Ozen, N.B. Tutuncu, B. Demirhan, Cyclin A and cyclin B1 overexpression in differentiated thyroid carcinoma, Med. Oncol. 29 (2012) 294–300.
[49] S. Santala, A. Talvensaari-Mattila, Y. Soini, M. Honkavuori-Toivola, M. Santala, High expression of cyclin A is associated with poor prognosis in endometrial endometrioid adenocarcinoma, Tumour Biol. 35 (2014) 5395–5399.
[50] R.L. Huuhtanen, C.P. Blomqvist, T.O. Böhling, T.A. Wiklund, E.J. Tukiainen, M. Virolainen, et al., Expression of cyclin A in soft tissue sarcomas correlates with tumor aggressiveness, Cancer Res. 59 (1999) 2885–2890.
[51] K. Aaltonen, R.-M. Amini, P. Heikkilä, K. Aittomäki, A. Tamminen, H. Nevanlinna, et al., High cyclin B1 expression is associated with poor survival in breast cancer, Br. J. Cancer 100 (2009) 1055–1060.
[52] T. Suzuki, T. Urano, Y. Miki, T. Moriya, J. Akahira, T. Ishida, et al., Nuclear cyclin B1 in human breast carcinoma as a potent prognostic factor, Cancer Sci. 98 (2007) 644–651.
[53] J.C. Soria, S.J. Jang, F.R. Khuri, K. Hassan, D. Liu, W.K. Hong, et al., Overexpression of cyclin B1 in early-stage non-small cell lung cancer and its clinical implication, Cancer Res. 60 (2000) 4000–4004.
[54] M.D. Begnami, J.H. Fregnani, S. Nonogaki, F.A. Soares, Evaluation of cell cycle protein expression in gastric cancer: cyclin B1 expression and its prognostic implication, Hum. Pathol. 41 (2010) 1120–1127.
[55] H. Murakami, M. Furihata, Y. Ohtsuki, S. Ogoshi, Determination of the prognostic significance of cyclin B1 overexpression in patients with esophageal squamous cell carcinoma, Virchows Arch. 434 (1999) 153–158.
[56] H.G. Drexler, Review of alterations of the cyclin-dependent kinase inhibitor INK4 family genes p15, p16, p18 and p19 in human leukemia-lymphoma cells, Leukemia 12 (1998) 845–859.
[57] A. Caliò, A. Zamò, M. Ponzoni, M.E. Zanolin, A.J. Ferreri, S. Pedron, et al., Cellular senescence markers $p16^{INK4a}$ and $p21^{CIP1/WAF}$ are predictors of Hodgkin lymphoma outcome, Clin. Cancer Res. 21 (2015) 5164–5172.
[58] S. Taga, T. Osaki, A. Ohgami, H. Imoto, T. Yoshimatsu, I. Yoshino, et al., Prognostic value of the immunohistochemical detection of $p16^{INK4}$ expression in nonsmall cell lung carcinoma, Cancer 80 (1997) 389–395.
[59] J. Tsihlias, L. Kapusta, J. Slingerland, The prognostic significance of altered cyclin-dependent kinase inhibitors in human cancer, Annu. Rev. Med. 50 (1999) 401–423.
[60] R.A. Kratzke, T.M. Greatens, J.B. Rubins, M.A. Maddaus, D.E. Niewoehner, G.A. Niehans, et al., Rb and $p16^{INK4a}$ expression in resected non-small cell lung tumors, Cancer Res. 56 (1996) 3415–3420.
[61] C.J. Jennings, B. Murer, A. O'Grady, L.M. Hearn, B.J. Harvey, E.W. Kay, et al., Differential p16/INK4A cyclin-dependent kinase inhibitor expression correlates with chemotherapy efficacy in a cohort of 88 malignant pleural mesothelioma patients, Br. J. Cancer 113 (2015) 69–75.
[62] O. Straume, L.A. Akslen, Alterations and prognostic significance of p16 and p53 protein expression in subgroups of cutaneous melanoma, Int. J. Cancer 74 (1997) 535–539.
[63] Y. Liu, X. Zhong, S. Wan, W. Zhang, J. Lin, P. Zhang, Y. Li, $p16^{INK4a}$ expression in retinoblastoma: a marker of differentiation grade, Diagn. Pathol. 9 (2014) 180.
[64] J. Bu, H. Li, L.H. Liu, Y.R. Ouyang, H.B. Guo, X.Y. Li, et al., $P16^{INK4a}$ overexpression and survival in osteosarcoma patients: a meta analysis, Int. J. Clin. Exp. Pathol. 7 (2014) 6091–6096.
[65] M. Jiang, Z.M. Shao, J. Wu, J.S. Lu, L.M. Yu, J.D. Yuan, et al., p21/waf1/cip1 and mdm-2 expression in breast carcinoma patients as related to prognosis, Int. J. Cancer 74 (1997) 529–534.
[66] M. Ogawa, K. Maeda, N. Onoda, Y.S. Chung, M. Sowa, Loss of $p21^{WAF1/CIP1}$ expression correlates with disease progression in gastric carcinoma, Br. J. Cancer 75 (11) (1997) 1617–1620.
[67] Y. Gomyo, M. Ikeda, M. Osaki, S. Tatebe, S. Tsujitani, M. Ikeguchi, et al., Expression of p21 (waf1/cip1/sdi1), but not p53 protein, is a factor in the survival of patients with advanced gastric carcinoma, Cancer 79 (1997) 2067–2072.
[68] K. Aoyagi, K. Koufuji, S. Yano, N. Murakami, M. Miyagi, A. Koga, et al., The expression of p53, p21 and TGF β1 in gastric carcinoma, Kurume Med. J. 50 (2003) 1–7.
[69] T.K. Zirbes, S.E. Baldus, S.P. Moenig, S. Nolden, D. Kunze, S.T. Shafizadeh, et al., Prognostic impact of p21/waf1/cip1 in colorectal cancer, Int. J. Cancer 89 (2000) 14–18.
[70] H. Mitomi, A. Mori, H. Kanazawa, Y. Nishiyama, A. Ihara, Y. Otani, et al., Venous invasion and down-regulation of $p21^{WAF1/CIP1}$ are associated with metastasis in colorectal carcinomas, Hepatogastroenterology. 52 (2005) 1421–1426.
[71] I.K. Bukholm, J.M. Nesland, Protein expression of p53, p21 (WAF1/CIP1), bcl-2, Bax, cyclin D1 and pRb in human colon carcinomas, Virchows Arch. 436 (2000) 224–228.
[72] J. Backe, A.M. Gassel, K. Hauber, S. Krebs, J. Bartek, H. Caffier, et al., p53 protein in endometrial cancer is related to proliferative activity and prognosis but not to expression of p21 protein, Int. J. Gynecol. Pathol. 16 (1997) 361–368.
[73] K. Ito, H. Sasano, G. Matsunaga, S. Sato, A. Yajima, S. Nasim, et al., Correlations between p21 expression and clinicopathological findings, p53 gene and protein alterations, and survival in patients with endometrial carcinoma, J. Pathol. 183 (3) (1997) 318–324.
[74] P.L. Porter, K.E. Malone, P.J. Heagerty, G.M. Alexander, L.A. Gatti, E.J. Firpo, et al., Expression of cell-cycle regulators $p27^{Kip1}$ and cyclin E, alone and in combination, correlate with survival in young breast cancer patients, Nat. Med. 3 (1997) 222–225.
[75] M. Loda, B. Cukor, S.W. Tam, P. Lavin, M. Fiorentino, G.F. Draetta, et al., Increased proteasome-dependent degradation of the cyclin-dependent kinase inhibitor p27 in aggressive colorectal carcinomas, Nat. Med. 3 (1997) 231–234.
[76] X. Guan, Y. Wang, R. Xie, L. Chen, J. Bai, J. Lu, et al., $p27^{Kip1}$ as a prognostic factor in breast cancer: a systematic review and meta-analysis, J. Cell. Mol. Med. 14 (2010) 944–953.
[77] M. Mori, K. Mimori, T. Shiraishi, S. Tanaka, H. Ueo, K. Sugimachi, et al., p27 expression and gastric carcinoma, Nat. Med. 3 (1997) 593.

[78] S.P. Singh, J. Lipman, H. Goldman, F.H. Ellis Jr., L. Aizenman, M.G. Cangi, et al., Loss or altered subcellular localization of p27 in Barrett's associated adenocarcinoma, Cancer Res. 58 (1998) 1730–1735.
[79] Y. Guo, G.N. Sklar, A. Borkowski, N. Kyprianou, Loss of the cyclin-dependent kinase inhibitor $p27^{Kip1}$ protein in human prostate cancer correlates with tumor grade, Clin. Cancer Res. 3 (1997) 2269–2274.
[80] J. Tsihlias, L.R. Kapusta, G. DeBoer, I. Morava-Protzner, I. Zbieranowski, N. Bhattacharya, et al., Loss of cyclin-dependent kinase inhibitor $p27^{Kip1}$ is a novel prognostic factor in localized human prostate adenocarcinoma, Cancer Res. 58 (1998) 542–548.
[81] R.M. Yang, J. Naitoh, M. Murphy, H.J. Wang, J. Phillipson, J.B. deKernion, et al., Low p27 expression predicts poor disease-free survival in patients with prostate cancer, J. Urol. 159 (1998) 941–945.
[82] K. Li, M.K. Chen, J. Situ, W.T. Huang, Z.L. Su, D. He, et al., Role of co-expression of c-Myc, EZH2 and p27 in prognosis of prostate cancer patients after surgery, Chin. Med. J. (Engl.) 126 (2013) 82–87.
[83] V. Ananthanarayanan, R.J. Deaton, A. Amatya, V. Macias, E. Luther, A. Kajdacsy-Balla, et al., Subcellular localization of p27 and prostate cancer recurrence: automated digital microscopy analysis of tissue microarrays, Hum. Pathol. 42 (2011) 873–881.
[84] H.S. Kim, H.S. Lee, K.H. Nam, J. Choi, W.H. Kim, p27 Loss is associated with poor prognosis in gastroenteropancreatic neuroendocrine tumors, Cancer Res. Treat. 46 (2014) 383–392.
[85] M. Oya, W.A. Schulz, Decreased expression of $p57^{KIP2}$ mRNA in human bladder cancer, Br. J. Cancer 83 (2000) 626–631.
[86] S. Noura, H. Yamamoto, M. Sekimoto, I. Takemasa, Y. Miyake, M. Ikenaga, et al., Expression of second class of KIP protein $p57^{KIP2}$ in human colorectal carcinoma, Int. J. Oncol. 19 (2001) 39–47.
[87] H. Guo, K. Nan, T. Hu, J. Meng, W. Hui, X. Zhang, et al., Prognostic significance of co-expression of nm23 and p57 protein in hepatocellular carcinoma, Hepatol Res. 40 (2010) 1107–1116.
[88] Y. Ito, T. Takeda, K. Wakasa, M. Tsujimoto, N. Matsuura, Expression of p57/Kip2 protein in pancreatic adenocarcinoma, Pancreas 23 (2001) 246–250.
[89] L. Sui, Y. Dong, M. Ohno, Y. Watanabe, K. Sugimoto, M. Tokuda, Expression of $p57^{kip2}$ and its clinical relevance in epithelial ovarian tumors, Anticancer Res. 22 (2002) 3191–3196.
[90] M.H. Khouja, M. Baekelandt, J.M. Nesland, R. Holm, The clinical importance of Ki-67, p16, p14, and p57 expression in patients with advanced ovarian carcinoma, Int. J. Gynecol. Pathol. 26 (2007) 418–425.
[91] M.I. Gutiérrez, A.K. Siraj, M.M. Ibrahim, A. Hussain, K. Bhatia, Childhood and adult ALL: differences in epigenetic lesions associated with cell cycle genes, Am. J. Hematol. 80 (2005) 158–160.
[92] L. Shen, M. Toyota, Y. Kondo, T. Obata, S. Daniel, S. Pierce, et al., Aberrant DNA methylation of p57KIP2 identifies a cell-cycle regulatory pathway with prognostic impact in adult acute lymphocytic leukemia, Blood 101 (2003) 4131–4136.
[93] C. Abdullah, X. Wang, D. Becker, Expression analysis and molecular targeting of cyclin-dependent kinases in advanced melanoma, Cell Cycle 10 (2011) 977–988.
[94] M.Y. Zhao, A. Auerbach, A.M. D'Costa, A.P. Rapoport, A.M. Burger, E.A. Sausville, et al., Phospho-p70S6K/p85S6K and cdc2/cdk1 are novel targets for diffuse large B-cell lymphoma combination therapy, Clin. Cancer Res. 15 (2009) 1708–1720.
[95] J. Georgieva, P. Sinha, D. Schadendorf, Expression of cyclins and cyclin dependent kinases in human benign and malignant melanocytic lesions, J. Clin. Pathol. 54 (2001) 229–235.
[96] D. Zheng, Y.Y. Cho, A.T. Lau, J. Zhang, W.Y. Ma, A.M. Bode, et al., Cyclin-dependent kinase 3-mediated activating transcription factor 1 phosphorylation enhances cell transformation, Cancer Res. 68 (18) (2008) 7650–7660.
[97] T.H. Cheung, M.M. Yu, K.W. Lo, S.F. Yim, T.K. Chung, Y.F. Wong, Alteration of cyclin D1 and CDK4 gene in carcinoma of uterine cervix, Cancer Lett. 166 (2001) 199–206.
[98] K.S. Smalley, R. Contractor, T.K. Nguyen, M. Xiao, R. Edwards, V. Muthusamy, et al., Identification of a novel subgroup of melanomas with KIT/cyclin-dependent kinase-4 overexpression, Cancer Res. 68 (2008) 5743–5752.
[99] E.E. Schmidt, K. Ichimura, G. Reifenberger, V.P. Collins, *CDKN2 (p16/MTS1)* gene deletion or *CDK4* amplification occurs in the majority of glioblastomas, Cancer Res. 54 (1994) 6321–6324.
[100] G. Wei, F. Lonardo, T. Ueda, T. Kim, A.G. Huvos, J.H. Healey, et al., *CDK4* gene amplification in osteosarcoma: reciprocal relationship with *INK4A* gene alterations and mapping of 12q13 amplicons, Int. J. Cancer 80 (1999) 199–204.
[101] J.S. Wunder, K. Eppert, S.R. Burrow, N. Gokgoz, R.S. Bell, I.L. Andrulis, Co-amplification and overexpression of CDK4, SAS and MDM2 occurs frequently in human parosteal osteosarcomas, Oncogene 18 (1999) 783–788 (Erratum in: Oncogene 2000;19:1734).
[102] S. Lee, H. Park, S.Y. Ha, K.Y. Paik, S.E. Lee, J.M. Kim, et al., *CDK4* amplification predicts recurrence of well-differentiated liposarcoma of the abdomen, PLoS One 9 (2014) e99452.
[103] S. Park, J. Lee, I.G. Do, J. Jang, K. Rho, S. Ahn, et al., Aberrant CDK4 amplification in refractory rhabdomyosarcoma as identified by genomic profiling, Sci. Rep. 4 (2014) 3623.
[104] Q. Liang, L. Li, J. Zhang, Y. Lei, L. Wang, D.X. Liu, et al., CDK5 is essential for TGF-β1-induced epithelial-mesenchymal transition and breast cancer progression, Sci. Rep. 3 (2013) 2932.
[105] J.P. Eggers, P.M. Grandgenett, E.C. Collisson, M.E. Lewallen, J. Tremayne, P.K. Singh, et al., Cyclin-dependent kinase 5 is amplified and overexpressed in pancreatic cancer and activated by mutant K-Ras, Clin. Cancer Res. 17 (2011) 6140–6150.
[106] Z. Levacque, J.L. Rosales, K.Y. Lee, Level of cdk5 expression predicts the survival of relapsed multiple myeloma patients, Cell Cycle 11 (2012) 4093–4095.
[107] J.F. Costello, C. Plass, W. Arap, V.M. Chapman, W.A. Held, M.S. Berger, et al., Cyclin-dependent kinase 6 (CDK6) amplification in human gliomas identified using two-dimensional separation of genomic DNA, Cancer Res. 57 (1997) 1250–1254.
[108] J. Easton, T. Wei, J.M. Lahti, V.J. Kidd, Disruption of the cyclin D/cyclin-dependent kinase/INK4/retinoblastoma protein regulatory pathway in human neuroblastoma, Cancer Res. 58 (1998) 2624–2632.
[109] M. Chilosi, C. Doglioni, Z. Yan, M. Lestani, F. Menestrina, C. Sorio, et al., Differential expression of cyclin-dependent kinase 6 in cortical thymocytes and T-cell lymphoblastic lymphoma/leukemia, Am. J. Pathol. 152 (1998) 209–217.
[110] M.Y. Kim, S.I. Han, S.C. Lim, Roles of cyclin-dependent kinase 8 and β-catenin in the oncogenesis and progression of gastric adenocarcinoma, Int. J. Oncol. 38 (2011) 1375–1383.
[111] A.S. Adler, M.L. McCleland, T. Truong, S. Lau, Z. Modrusan, T.M. Soukup, et al., CDK8 maintains tumor dedifferentiation and embryonic stem cell pluripotency, Cancer Res. 72 (2012) 2129–2139.
[112] R. Firestein, A.J. Bass, S.Y. Kim, I.F. Dunn, S.J. Silver, I. Guney, et al., CDK8 is a colorectal cancer oncogene that regulates β-catenin activity, Nature 455 (2008) 547–551.
[113] R. Firestein, K. Shima, K. Nosho, N. Irahara, Y. Baba, E. Bojarski, et al., CDK8 expression in 470 colorectal cancers in relation to β-catenin activation, other molecular alterations and patient survival, Int. J. Cancer 126 (2010) 2863–2873.
[114] J.O. Seo, S.I. Han, S.C. Lim, Role of CDK8 and β-catenin in colorectal adenocarcinoma, Oncol. Rep. 24 (2010) 285–291.
[115] G. De Falco, C. Bellan, A. D'Amuri, G. Angeloni, E. Leucci, A. Giordano, et al., Cdk9 regulates neural differentiation and its expression correlates with the differentiation grade of neuroblastoma and PNET tumors, Cancer Biol. Ther. 4 (2005) 277–281.
[116] Z. Duan, J. Zhang, E. Choy, D. Harmon, X. Liu, P. Nielsen, et al., Systematic kinome shRNA screening identifies CDK11 (PITSLRE) kinase expression is critical for osteosarcoma cell growth and proliferation, Clin. Cancer Res. 18 (2012) 4580–4588.
[117] H. Miyagaki, M. Yamasaki, H. Miyata, T. Takahashi, Y. Kurokawa, K. Nakajima, et al., Overexpression of PFTK1 predicts resistance to chemotherapy in patients with oesophageal squamous cell carcinoma, Br. J. Cancer 106 (2012) 947–954.
[118] F. Mendrzyk, B. Radlwimmer, S. Joos, F. Kokocinski, A. Benner, D.E. Stange, et al., Genomic and protein expression profiling identifies CDK6 as novel independent prognostic marker in medulloblastoma, J. Clin. Oncol. 23 (2005) 8853–8862.
[119] U. Asghar, A.K. Witkiewicz, N.C. Turner, E.S. Knudsen, The history and future of targeting cyclin-dependent kinases in cancer therapy, Nat. Rev. Drug Discov. 14 (2015) 130–146.
[120] R. Roskoski Jr., ERK1/2 MAP kinases: structure, function, and regulation, Pharmacol. Res. 66 (2012) 105–143.
[121] N.R. Brown, M.E. Noble, J.A. Endicott, L.N. Johnson, The structural basis for specificity of substrate and recruitment peptides for cyclin-dependent kinases, Nat. Cell Biol. 1 (1999) 438–443.
[122] N.R. Brown, S. Korolchuk, M.P. Martin, W.A. Stanley, R. Moukhametzianov, M.E. Noble, et al., CDK1 structures reveal conserved and unique features of the essential cell cycle CDK, Nat. Commun. 6 (2015) 6769.
[123] S.S. Taylor, E. Radzio-Andzelm, T. Hunter, How do protein kinases discriminate between serine/threonine and tyrosine?: Structural insights from the insulin receptor protein-tyrosine kinase, FASEB J. 9 (1995) 1255–1266.
[124] S.K. Hanks, A.M. Quinn, T. Hunter, The protein kinase family: conserved features and deduced phylogeny of the catalytic domains, Science 241 (1988) 42–52.
[125] S.K. Hanks, T. Hunter, Protein kinases 6: The eukaryotic protein kinase superfamily: kinase (catalytic) domain structure and classification, FASEB J. 9 (1995) 576–596.
[126] D.R. Knighton, J.H. Zheng, L.F. Ten Eyck, V.A. Ashford, N.H. Xuong, S.S. Taylor, et al., Crystal structure of the catalytic subunit of cyclic adenosine monophosphate-dependent protein kinase, Science 253 (1991) 407–414.
[127] D.R. Knighton, J.H. Zheng, L.F. Ten Eyck, N.H. Xuong, S.S. Taylor, J.M. Sowadski, Structure of a peptide inhibitor bound to the catalytic subunit of cyclic adenosine monophosphate-dependent protein kinase, Science 253 (1991) 414–420.
[128] S.S. Taylor, A.P. Kornev, Protein kinases: evolution of dynamic regulatory proteins, Trends Biochem. Sci. 36 (2011) 65–77.
[129] R. Roskoski Jr., A historical overview of protein kinases and their targeted small molecule inhibitors, Pharmacol. Res. 100 (2015) 1–23.
[130] D.M. Jacobsen, Z.Q. Bao, P. O'Brien, C.L. Brooks 3rd, M.A. Young, Price to be paid for two-metal catalysis: magnesium ions that accelerate chemistry

unavoidably limit product release from a protein kinase, J. Am. Chem. Soc. 134 (2012) 15357–15370.
[131] R. Roskoski Jr., Src protein-tyrosine kinase structure, mechanism, and small molecule inhibitors, Pharmacol. Res. 94 (2015) 9–25.
[132] K.Y. Cheng, M.E. Noble, V. Skamnaki, N.R. Brown, E.D. Lowe, L. Kontogiannis, et al., The role of the phospho-CDK2/cyclin A recruitment site in substrate recognition, J. Biol. Chem. 281 (2006) 23167–23179.
[133] A.C. Hengge, Mechanistic studies on enzyme-catalyzed phosphoryl transfer, Adv. Phys. Org. Chem. 40 (2005) 49–108.
[134] V.L. Schramm, Enzymatic transition states and transition state analog design, Annu. Rev. Biochem 67 (1998) 693–720.
[135] V.L. Schramm, Transition States, analogues, and drug development, ACS Chem. Biol. 8 (2013) 71–81.
[136] M. Valiev, J. Yang, J.A. Adams, S.S. Taylor, J.H. Weare, Phosphorylation reaction in cAPK protein kinase-free energy quantum mechanical/molecular mechanics simulations, J. Phys. Chem. 111 (2007) 13455–13464 (Erratum in: J. Phys. Chem. 2010;114:6763).
[137] Y. Cheng, Y. Zhang, J.A. McCammon, How does the cAMP-dependent protein kinase catalyze the phosphorylation reaction: an ab initio QM/MM study, J. Am. Chem. Soc. 127 (2005) 1553–1562.
[138] Z.Q. Bao, D.M. Jacobsen, M.A. Young, Briefly bound to activate: transient binding of a second catalytic magnesium activates the structure and dynamics of CDK2 kinase for catalysis, Structure 19 (2011) 675–690.
[139] A. Cook, E.D. Lowe, E.D. Chrysina, V.T. Skamnaki, N.G. Oikonomakos, L.N. Johnson, Structural studies on phospho-CDK2/cyclin A bound to nitrate, a transition state analogue: implications for the protein kinase mechanism, Biochemistry 41 (2002) 7301–7311.
[140] L. Pauling, Chemical achievement and hope for the future, Am. Sci. 36 (1948) 51–58.
[141] T.L. Amyes, J.P. Richard, Specificity in transition state binding: the Pauling model revisited, Biochemistry 52 (2013) 2021–2035.
[142] A.P. Kornev, N.M. Haste, S.S. Taylor, L.F. Ten Eyck, Surface comparison of active and inactive protein kinases identifies a conserved activation mechanism, Proc. Natl. Acad. Sci. U. S. A. 103 (2006) 17783–17788.
[143] A.P. Kornev, S.S. Taylor, L.F. Ten Eyck, A helix scaffold for the assembly of active protein kinases, Proc. Natl. Acad. Sci. U. S. A. 105 (2008) 14377–14382.
[144] H.S. Meharena, P. Chang, M.M. Keshwani, K. Oruganty, A.K. Nene, N. Kannan, et al., Deciphering the structural basis of eukaryotic protein kinase regulation, PLoS Biol. 11 (2013) e1001680.
[145] R. Roskoski Jr., Classification of small molecule protein kinase inhibitors based upon the structures of their drug-enzyme complexes, Pharmacol. Res. 103 (2016) 26–48.
[146] K. Shah, Y. Liu, C. Deirmengian, K.M. Shokat, Engineering unnatural nucleotide specificity for Rous sarcoma virus tyrosine kinase to uniquely label its direct substrates, Proc. Natl. Acad. Sci. U. S. A. 94 (1997) 3565–3570.
[147] Y. Liu, K. Shah, F. Yang, L. Witucki, K.M. Shokat, A molecular gate which controls unnatural ATP analogue recognition by the tyrosine kinase v-Src, Bioorg. Med.Chem. 6 (1998) 1219–1226.
[148] U. Schulze-Gahmen, H.L. De Bondt, S.H. Kim, High-resolution crystal structures of human cyclin-dependent kinase 2 with and without ATP: bound waters and natural ligand as guides for inhibitor design, J. Med. Chem. 39 (1996) 4540–4546.
[149] P.D. Jeffrey, A.A. Russo, K. Polyak, E. Gibbs, J. Hurwitz, J. Massagué, et al., Mechanism of CDK activation revealed by the structure of a cyclinA-CDK2 complex, Nature 376 (1995) 313–320.
[150] A.A. Russo, P.D. Jeffrey, N.P. Pavletich, Structural basis of cyclin-dependent kinase activation by phosphorylation, Nat. Struct. Biol. 3 (1996) 696–700.
[151] H. Higashi, I. Suzuki-Takahashi, S. Saitoh, K. Segawa, Y. Taya, A. Okuyama, et al., Cyclin-dependent kinase-2 (Cdk2) forms an inactive complex with cyclin D1 since Cdk2 associated with cyclin D1 is not phosphorylated by Cdk7-cyclin-H, Eur. J. Biochem. 237 (1996) 460–467.
[152] N.R. Brown, M.E. Noble, A.M. Lawrie, M.C. Morris, P. Tunnah, G. Divita, et al., Effects of phosphorylation of threonine 160 on cyclin-dependent kinase 2 structure and activity, J. Biol. Chem. 274 (1999) 8746–8756.
[153] A.A. Russo, P.D. Jeffrey, A.K. Patten, J. Massagué, N.P. Pavletich, Crystal structure of the $p27^{Kip1}$ cyclin-dependent-kinase inhibitor bound to the cyclin A-Cdk2 complex, Nature 382 (1996) 325–331.
[154] J.W. Harper, S.J. Elledge, K. Keyomarsi, B. Dynlacht, L.H. Tsai, P. Zhang, et al., Inhibition of cyclin-dependent kinases by p21, Mol. Biol. Cell 6 (1995) 387–400.
[155] P.D. Jeffrey, L. Tong, N.P. Pavletich, Structural basis of inhibition of CDK-cyclin complexes by INK4 inhibitors, Genes Dev. 14 (2000) 3115–3125.
[156] A.A. Russo, L. Tong, J.O. Lee, P.D. Jeffrey, N.P. Pavletich, Structural basis for inhibition of the cyclin-dependent kinase Cdk6 by the tumour suppressor $p16^{INK4a}$, Nature 395 (1998) 237–243.
[157] A. Plückthun, Designed ankyrin repeat proteins (DARPins): binding proteins for research, diagnostics, and therapy, Annu. Rev. Pharmacol. Toxicol. 55 (2015) 489–511.
[158] Q. Zhou, T. Li, D.H. Price, RNA polymerase II elongation control, Annu. Rev. Biochem. 81 (2012) 119–143.
[159] J. Kohoutek, P-TEFb- the final frontier, Cell Div. 4 (2009) 19.
[160] J.E. Karp, B.D. Smith, L.S. Resar, J.M. Greer, A. Blackford, M. Zhao, et al., Phase 1 and pharmacokinetic study of bolus-infusion flavopiridol followed by cytosine arabinoside and mitoxantrone for acute leukemias, Blood 117 (12) (2011) 3302–3310.
[161] J.F. Zeidner, M.C. Foster, A.L. Blackford, M.R. Litzow, L.E. Morris, S.A. Strickland, et al., Randomized multicenter phase II study of flavopiridol (alvocidib), cytarabine, and mitoxantrone (FLAM) versus cytarabine/daunorubicin (7 + 3) in newly diagnosed acute myeloid leukemia, Haematologica 100 (2015) 1172–1179.
[162] B.A. Christian, M.R. Grever, J.C. Byrd, T.S. Lin, Flavopiridol in the treatment of chronic lymphocytic leukemia, Curr. Opin. Oncol. 19 (2007) 573–578.
[163] T.S. Lin, A.S. Ruppert, A.J. Johnson, B. Fischer, N.A. Heerema, L.A. Andritsos, et al., Phase II study of flavopiridol in relapsed chronic lymphocytic leukemia demonstrating high response rates in genetically high-risk disease, J. Clin. Oncol. 27 (2009) 6012–6018.
[164] S. George, B.S. Kasimis, J. Cogswell, P. Schwarzenberger, G.I. Shapiro, P. Fidias, et al., Phase I study of flavopiridol in combination with paclitaxel and carboplatin in patients with non-small-cell lung cancer, Clin. Lung Cancer 9 (2008) 160–165.
[165] M.C. Lanasa, L. Andritsos, J.R. Brown, J. Gabrilove, F. Caligaris-Cappio, P. Ghia, et al., Final results of EFC6663: a multicenter, international, phase 2 study of alvocidib for patients with fludarabine-refractory chronic lymphocytic leukemia, Leuk. Res. 39 (2015) 495–500.
[166] O.P. van Linden, A.J. Kooistra, R. Leurs, I.J. de Esch, C. de Graaf, KLIFS: a knowledge-based structural database to navigate kinase-ligand interaction space, J. Med. Chem. 57 (2014) 249–277.
[167] M.W. Karaman, S. Herrgard, D.K. Treiber, P. Gallant, C.E. Atteridge, B.T. Campbell, et al., A quantitative analysis of kinase inhibitor selectivity, Nat. Biotechnol. 26 (2008) 127–132.
[168] P.M. Fracasso, K.J. Williams, R.C. Chen, J. Picus, C.X. Ma, M.J. Ellis, et al., A Phase 1 study of UCN-01 in combination with irinotecan in patients with resistant solid tumor malignancies, Cancer Chemother. Pharmacol. 67 (2011) 1225–1237.
[169] J. Kortmansky, M.A. Shah, A. Kaubisch, A. Weyerbacher, S. Yi, W. Tong, et al., Phase I trial of the cyclin-dependent kinase inhibitor and protein kinase C inhibitor 7-hydroxystaurosporine in combination with fluorouracil in patients with advanced solid tumors, J. Clin. Oncol. 23 (2005) 1875–1884.
[170] S.J. Hotte, A. Oza, E.W. Winquist, M. Moore, E.X. Chen, S. Brown, et al., Phase I trial of UCN-01 in combination with topotecan in patients with advanced solid cancers: a Princess Margaret Hospital Phase II Consortium study, Ann. Oncol. 17 (2006) 334–340.
[171] I. Gojo, A. Perl, S. Luger, M.R. Baer, K.J. Norsworthy, K.S. Bauer, et al., Phase I study of UCN-01 and perifosine in patients with relapsed and refractory acute leukemias and high-risk myelodysplastic syndrome, Invest. New Drugs 31 (2013) 1217–1227.
[172] S.R. Whittaker, M.I. Walton, M.D. Garrett, P. Workman, The cyclin-dependent kinase inhibitor CYC202 (R-roscovitine) inhibits retinoblastoma protein phosphorylation, causes loss of cyclin D1, and activates the mitogen-activated protein kinase pathway, Cancer Res. 64 (2004) 262–272.
[173] W.S. Hsieh, R. Soo, B.K. Peh, T. Loh, D. Dong, D. Soh, et al., Pharmacodynamic effects of seliciclib, an orally administered cell cycle modulator, in undifferentiated nasopharyngeal cancer, Clin. Cancer Res. 15 (2009) 1435–1442.
[174] C. Le Tourneau, S. Faivre, V. Laurence, C. Delbaldo, K. Vera, V. Girre, et al., Phase I evaluation of seliciclib (R-roscovitine), a novel oral cyclin-dependent kinase inhibitor, in patients with advanced malignancies, Eur. J. Cancer 46 (2010) 3243–3250.
[175] L.M. Gelbert, S. Cai, X. Lin, C. Sanchez-Martinez, M. Del Prado, M.J. Lallena, et al., Preclinical characterization of the CDK4/6 inhibitor LY2835219: in-vivo cell cycle-dependent/independent antitumor activities alone/in combination with gemcitabine, Invest. New Drugs 32 (2014) 825–837.
[176] N. Vidula, H.S. Rugo, Cyclin-dependent kinase 4/6 inhibitors for the treatment of breast cancer: a review of preclinical and clinical data, Clin. Breast Cancer 16 (2016) 8–17.
[177] L. Santo, S. Vallet, T. Hideshima, D. Cirstea, H. Ikeda, S. Pozzi, et al., AT7519, A novel small molecule multi-cyclin-dependent kinase inhibitor, induces apoptosis in multiple myeloma via GSK-3β activation and RNA polymerase II inhibition, Oncogene 2 (9) (2010) 2325–2336.
[178] D. Mahadevan, R. Plummer, M.S. Squires, D. Rensvold, S. Kurtin, C. Pretzinger, et al., A phase I pharmacokinetic and pharmacodynamic study of AT7519, a cyclin-dependent kinase inhibitor in patients with refractory solid tumors, Ann. Oncol. 22 (2011) 2137–2143.
[179] E.X. Chen, S. Hotte, H. Hirte, L.L. Siu, J. Lyons, M. Squires, et al., A phase I study of cyclin-dependent kinase inhibitor, AT7519, in patients with advanced cancer: NCIC clinical trials group IND 177, Br. J. Cancer 111 (2014) 2262–2267.
[180] R.N. Misra, H.Y. Xiao, K.S. Kim, S. Lu, W.C. Han, S.A. Barbosa, et al., *N*-(cycloalkylamino) acyl-2-aminothiazole inhibitors of cyclin-dependent kinase 2. *N*-[5-[[[5-(1,1-dimethylethyl)-2-oxazolyl]methyl]thio]-2-thiazolyl]-4-piperidinecarboxamide (BMS-387032), a highly efficacious and selective antitumor agent, J. Med. Chem. 47 (2004) 1719–1728 (Erratum in: J Med Chem 2015;58:7609).
[181] E.I. Heath, K. Bible, R.E. Martell, D.C. Adelman, P.M. Lorusso, A phase 1 study of SNS-032 (formerly BMS-387032), a potent inhibitor of cyclin-dependent kinases 2, 7 and 9 administered as a single oral dose and weekly infusion in patients with metastatic refractory solid tumors, Invest. New Drugs 26 (2008) 59–65.
[182] W.G. Tong, R. Chen, W. Plunkett, D. Siegel, R. Sinha, R.D. Harvey, et al., Phase I and pharmacologic study of SNS-032, a potent and selective Cdk2, 7, and 9

inhibitor, in patients with advanced chronic lymphocytic leukemia and multiple myeloma, J. Clin. Oncol. 28 (2010) 3015–3022.
[183] D. Parry, T. Guzi, F. Shanahan, N. Davis, D. Prabhavalkar, D. Wiswell, et al., Dinaciclib (SCH 727965), a novel and potent cyclin-dependent kinase inhibitor, Mol. Cancer Ther. 9 (2010) 2344–2353.
[184] K. Paruch, M.P. Dwyer, C. Alvarez, C. Brown, T.Y. Chan, R.J. Doll, et al., Discovery of dinaciclib (SCH 727965): a potent and selective inhibitor of cyclin-dependent kinases, ACS Med Chem Lett 1 (2010) 204–208.
[185] J.J. Nemunaitis, K.A. Small, P. Kirschmeier, D. Zhang, Y. Zhu, Y.M. Jou, et al., A first-in-human, phase 1, dose-escalation study of dinaciclib, a novel cyclin-dependent kinase inhibitor, administered weekly in subjects with advanced malignancies, J. Transl. Med. 11 (2013) 259.
[186] J.J. Stephenson, J. Nemunaitis, A.A. Joy, J.C. Martin, Y.M. Jou, D. Zhang, et al., Randomized phase 2 study of the cyclin-dependent kinase inhibitor dinaciclib (MK-7965) versus erlotinib in patients with non-small cell lung cancer, Lung Cancer 83 (2014) 219–223.
[187] M.M. Mita, A.A. Joy, A. Mita, K. Sankhala, Y.M. Jou, D. Zhang, et al., Randomized phase II trial of the cyclin-dependent kinase inhibitor dinaciclib (MK-7965) versus capecitabine in patients with advanced breast cancer, Clin. Breast Cancer 14 (2014) 169–176.
[188] J. Flynn, J. Jones, A.J. Johnson, L. Andritsos, K. Maddocks, S. Jaglowski, et al., Dinaciclib is a novel cyclin-dependent kinase inhibitor with significant clinical activity in relapsed and refractory chronic lymphocytic leukemia, Leukemia 29 (2015) 1524–1529.
[189] Z. Mitri, C. Karakas, C. Wei, B. Briones, H. Simmons, N. Ibrahim, et al., A phase 1 study with dose expansion of the CDK inhibitor dinaciclib (SCH 727965) in combination with epirubicin in patients with metastatic triple negative breast cancer, Invest. New Drugs 33 (2015) 890–894.
[190] C.J. Sherr, D. Beach, G.I. Shapiro, Targeting CDK4 and CDK6: from discovery to therapy, Cancer Discov. (2015) (Epub ahead of print).
[191] J. Rader, M.R. Russell, L.S. Hart, M.S. Nakazawa, L.T. Belcastro, D. Martinez, et al., Dual CDK4/CDK6 inhibition induces cell-cycle arrest and senescence in neuroblastoma, Clin. Cancer Res. 19 (2013) 6173–6182.
[192] K.S. Joshi, M.J. Rathos, R.D. Joshi, M. Sivakumar, M. Mascarenhas, S. Kamble, et al., *In vitro* antitumor properties of a novel cyclin-dependent kinase inhibitor, P 276-00, Mol. Cancer Ther. 6 (2007) 918–925.
[193] S.M. Manohar, M.J. Rathos, V. Sonawane, S.V. Rao, K.S. Joshi, Cyclin-dependent kinase inhibitor, P 276-00 induces apoptosis in multiple myeloma cells by inhibition of Cdk9-T1 and RNA polymerase II-dependent transcription, Leuk. Res. 35 (2011) 821–830.
[194] K.S. Joshi, M.J. Rathos, P. Mahajan, V. Wagh, S. Shenoy, D. Bhatia, et al., P 276-00, a novel cyclin-dependent inhibitor induces G1-G2 arrest, shows antitumor activity on cisplatin-resistant cells and significant *in vivo* efficacy in tumor models, Mol. Cancer Ther. 6 (2007) 926–934.
[195] R.D. Cassaday, A. Goy, S. Advani, P. Chawla, R. Nachankar, M. Gandhi, et al., A phase II, single-arm, open-label, multicenter study to evaluate the efficacy and safety of P 276-00, a cyclin-dependent kinase inhibitor, in patients with relapsed or refractory mantle cell lymphoma, Clin. Lymphoma Myeloma Leuk. 15 (2015) 392–397.
[196] D.W. Fry, P.J. Harvey, P.R. Keller, W.L. Elliott, M. Meade, E. Trachet, et al., Specific inhibition of cyclin-dependent kinase 4/6 by PD 0332991 and associated antitumor activity in human tumor xenografts, Mol. Cancer Ther. 3 (2004) 1427–1438.
[197] S.N. VanderWel, P.J. Harvey, D.J. McNamara, J.T. Repine, P.R. Keller, J. Quin 3rd, et al., Pyrido[2,3-*d*]pyrimidin-7-ones as specific inhibitors of cyclin-dependent kinase 4, J. Med. Chem. 48 (2005) 2371–2387.
[198] P.L. Toogood, P.J. Harvey, J.T. Repine, D.J. Sheehan, S.N. VanderWel, H. Zhou, et al., Discovery of a potent and selective inhibitor of cyclin-dependent kinase 4/6, J. Med. Chem. 48 (2005) 2388–2406.
[199] R.S. Finn, J. Dering, D. Conklin, O. Kalous, D.J. Cohen, A.J. Desai, et al., PD 0332991, a selective cyclin D kinase 4/6 inhibitor, preferentially inhibits proliferation of luminal estrogen receptor-positive human breast cancer cell lines *in vitro*, Breast Cancer Res. 11 (2009) R77.
[200] T.W. Miller, J.M. Balko, E.M. Fox, Z. Ghazoui, A. Dunbier, H. Anderson, et al., ERα-dependent E2F transcription can mediate resistance to estrogen deprivation in human breast cancer, Cancer Discov. 1 (2011) 338–351.
[201] R.S. Finn, J.P. Crown, I. Lang, K. Boer, I.M. Bondarenko, S.O. Kulyk, et al., The cyclin-dependent kinase 4/6 inhibitor palbociclib in combination with letrozole versus letrozole alone as first-line treatment of oestrogen receptor-positive, HER2-negative, advanced breast cancer (PALOMA-1/TRIO-18): a randomised phase 2 study, Lancet Oncol. 16 (2015) 25–35.
[202] N.C. Turner, J. Ro, F. André, S. Loi, S. Verma, H. Iwata, et al., Palbociclib in hormone-receptor-positive advanced breast cancer, N. Engl. J. Med. 373 (2015) 209–219.
[203] T.L. Nero, C.J. Morton, J.K. Holien, J. Wielens, M.W. Parker, Oncogenic protein interfaces: small molecules, big challenges, Nat. Rev. Cancer 14 (2014) 248–262.
[204] L. Jin, W. Wang, G. Fang, Targeting protein–protein interaction by small molecules, Annu. Rev. Pharmacol. Toxicol. 54 (2014) 435–456.
[205] M.R. Arkin, Y. Tang, J.A. Wells, Small-molecule inhibitors of protein–protein interactions: progressing toward the reality, Chem. Biol. 21 (2014) 1102–1114.
[206] R. Roskoski Jr., Anaplastic lymphoma kinase (ALK): structure, oncogenic activation, and pharmacological inhibition, Pharmacol. Res. 68 (2013) 68–94.
[207] N. Mendoza, S. Fong, J. Marsters, H. Koeppen, R. Schwall, D. Wickramasinghe, Selective cyclin-dependent kinase 2/cyclin A antagonists that differ from ATP site inhibitors block tumor growth, Cancer Res. 63 (2003) 1020–1024.
[208] N. Canela, M. Orzáez, R. Fucho, F. Mateo, R. Gutierrez, A. Pineda-Lucena, et al., Identification of an hexapeptide that binds to a surface pocket in cyclin A and inhibits the catalytic activity of the complex cyclin-dependent kinase 2-cyclin A, J. Biol. Chem. 281 (2006) 35942–35953.
[209] K. Nasmyth, A prize for proliferation, Cell 107 (2001) 689–701.
[210] L.H. Hartwell, J. Culotti, B. Reid, Genetic control of the cell-division cycle in yeast. I. Detection of mutants, Proc. Natl. Acad. Sci. U. S. A. 66 (1970) 352–359.
[211] P. Nurse, Genetic control of cell size at cell division in yeast, Nature 256 (1975) 547–551.
[212] T. Evans, E.T. Rosenthal, J. Youngblom, D. Distel, Hunt T. Cyclin, a protein specified by maternal mRNA in sea urchin eggs that is destroyed at each cleavage division, Cell 33 (1983) 389–396.
[213] H. Rajagopalan, C. Lengauer, Aneuploidy and cancer, Nature 432 (2004) 338–341.
[214] A.M. Senderowicz, E.A. Sausville, Preclinical and clinical development of cyclin-dependent kinase modulators, J. Natl. Cancer Inst. 92 (2000) 376–387.
[215] G. Kaur, M. Stetler-Stevenson, S. Sebers, P. Worland, H. Sedlacek, C. Myers, et al., Growth inhibition with reversible cell cycle arrest of carcinoma cells by flavone L86-8275, J. Natl. Cancer Inst. 84 (1992) 1736–1740.
[216] F.Y. Wei, K. Nagashima, T. Ohshima, Y. Saheki, Y.F. Lu, M. Matsushita, et al., Cdk5-dependent regulation of glucose-stimulated insulin secretion, Nat. Med. 11 (2005) 1104–1108.
[217] A. Mullard, 2015 FDA drug approvals, Nat. Rev. Drug Discov. 15 (2016) 73–76.
[218] H.M. Kantarjian, T. Fojo, M. Mathisen, L.A. Zwelling, Cancer drugs in the United States: *justum pretium*–the just price, J. Clin. Oncol. 31 (2013) 3600–3604.
[219] S.Y. Zafar, J.M. Peppercorn, D. Schrag, D.H. Taylor, A.M. Goetzinger, X. Zhong, et al., The financial toxicity of cancer treatment: a pilot study assessing out-of-pocket expenses and the insured cancer patient's experience, Oncologist 18 (2013) 381–390.
[220] R. Roskoski Jr., Fritz lipmann (1899–1986): an appreciation, Trends Biochem. Sci. 12 (1987) 136–138.